

**SAFETY AND CONVERGENCE ANALYSIS OF  
INTERSECTING AIRCRAFT FLOWS UNDER  
DECENTRALIZED COLLISION AVOIDANCE**

by

**Ahmed H. Dallal**

B.S. in Biomedical Engineering, Cairo University, 2009

M.S. in Biomedical Engineering, Cairo University, 2013

Submitted to the Graduate Faculty of  
Swanson School of Engineering in partial fulfillment  
of the requirements for the degree of

**Doctor of Philosophy**

University of Pittsburgh

2017

UNIVERSITY OF PITTSBURGH  
SWANSON SCHOOL OF ENGINEERING

This dissertation was presented

by

Ahmed H. Dallal

It was defended on

July 13, 2017

and approved by

Zhi-Hong Mao, Ph.D., Associate Professor  
Department of Electrical and Computer Engineering

Yiran Chen, Ph.D., Associate Professor  
Department of Electrical and Computer Engineering

Murat Akcakaya, Ph.D., Assistant Professor  
Department of Electrical and Computer Engineering

Amro El-Jaroudi, Ph.D., Associate Professor  
Department of Electrical and Computer Engineering

Natasa Miskov-Zivanov, Ph.D., Assistant Professor  
Department of Electrical and Computer Engineering

Mingui Sun, Ph.D., Professor  
Department of Neurology

Dissertation Advisors: Zhi-Hong Mao, Ph.D., Associate Professor,

Yiran Chen, Ph.D., Associate Professor

Copyright © by Ahmed H. Dallal  
2017

# SAFETY AND CONVERGENCE ANALYSIS OF INTERSECTING AIRCRAFT FLOWS UNDER DECENTRALIZED COLLISION AVOIDANCE

Ahmed H. Dallal, PhD

University of Pittsburgh, 2017

Safety is an essential requirement for air traffic management and control systems. Aircraft are not allowed to get closer to each other than a specified safety distance, to avoid any conflicts and collisions between aircraft. Forecast analysis predicts a tremendous increase in the number of flights. Subsequently, automated tools are needed to help air traffic controllers resolve air born conflicts. In this dissertation, we consider the problem of conflict resolution of aircraft flows with the assumption that aircraft are flowing through a fixed specified control volume at a constant speed. In this regard, several centralized and decentralized resolution rules have been proposed for path planning and conflict avoidance. For the case of two intersecting flows, we introduce the concept of conflict touches, and a collaborative decentralized conflict resolution rule is then proposed and analyzed for two intersecting flows. The proposed rule is also able to resolved airborne conflicts that resulted from resolving another conflict via the domino effect. We study the safety conditions under the proposed conflict resolution and collision avoidance rule. Then, we use Lyapunov analysis to analytically prove the convergence of conflict resolution dynamics under the proposed rule. The analysis show that, under the proposed conflict resolution rule, the system of intersecting aircraft flows is guaranteed to converge to safe, conflict free, trajectories within a bounded time. Simulations are provided to verify the analytically derived conclusions and study the convergence of the conflict resolution dynamics at different encounter angles. Simulation results show that lateral deviations taken by aircraft in each flow, to resolve conflicts, are bounded, and aircraft converged to safe and conflict free trajectories, within a finite time.

The proposed rule is powerful when the pilots of the collaborating aircraft, resolving a potential conflict, are either humans or robots. However, when a human pilot is collaborating with a robot pilot for the first time, the robot control should optimize its control criteria to collaborate well with the human. Basically, the robot must adapt its output as it learns from the human. We study the situation of the Human-in-the-Loop, assuming that human will follow lateral maneuvers for conflict resolution. We model the human as an optimal controller that minimizes the risk of collision. Based on that model, we use differential game analysis to get an accurate estimate for the human control criteria. We propose a new algorithm, based on least square minimization, to estimate the Kalman gain of the human's model, and therefore accurately estimate his optimal control criteria. Simulations of this learned rule show that robot pilot can successfully learn from the human pilot actions, and both can cooperate successfully to resolve any conflicts between their aircraft.

## TABLE OF CONTENTS

<b>PREFACE</b> . . . . .	xiii
<b>1.0 INTRODUCTION</b> . . . . .	1
1.1 Conflict detection and Resolution Process . . . . .	2
1.1.1 National Airspace System . . . . .	2
1.1.2 Air Traffic Management . . . . .	4
1.1.3 ATC based Conflict Avoidance . . . . .	6
1.1.4 Airspace Redesign . . . . .	10
1.1.5 Advisory Decision-Support Tools . . . . .	13
1.1.6 Mixed Automation for Conflict Resolution . . . . .	14
1.1.7 Automated Conflict Resolution . . . . .	15
1.2 Previous Work . . . . .	16
1.3 Introduction to The Proposed Work . . . . .	20
1.4 Organization of The Dissertation . . . . .	22
<b>2.0 CONFLICT RESOLUTION MODEL</b> . . . . .	23
2.1 Basic Assumptions and Maneuver Model . . . . .	23
2.2 Aircraft Flow and Conflict Geometry . . . . .	27
2.3 Conflict Resolution Rule . . . . .	30
<b>3.0 AIRCRAFT FLOW SAFETY AND CONFLICT RESOLUTION CON- VERGENCE</b> . . . . .	32
3.1 Safety Under Conflict Resolution Rule . . . . .	33
3.2 Convergence of Conflict Resolution Dynamics . . . . .	35
3.3 Summary . . . . .	40

<b>4.0 SIMULATION OF AUTOMATIC CONFLICT RESOLUTION . . . . .</b>	<b>41</b>
4.1 Convergence to Safe Trajectories . . . . .	41
4.2 Magnitude of Lateral Deviations . . . . .	50
4.3 Convergence of The Lyapunov Function . . . . .	53
4.4 Summary . . . . .	56
<b>5.0 HUMAN-MACHINE CO-LEARNING FOR CONFLICT RESOLUTION</b>	<b>62</b>
5.1 Introduction . . . . .	62
5.2 Modeling of Human-Robot Interactions for Aircraft Conflict Avoidance . . . . .	65
5.3 Estimation of Human Control Criteria . . . . .	68
5.3.1 The Inverse LQR Problem . . . . .	70
5.3.2 Least-Squares Estimation of Human Feedback Gain . . . . .	71
5.4 Experimental Results . . . . .	72
5.4.1 Experimental Setup . . . . .	73
5.4.2 Results . . . . .	74
5.5 Summary . . . . .	76
<b>6.0 CONCLUSIONS . . . . .</b>	<b>80</b>
<b>APPENDIX A. ACRONYMS . . . . .</b>	<b>82</b>
<b>APPENDIX B. NOTATION . . . . .</b>	<b>84</b>
<b>APPENDIX C. LYAPUNOV THEORY AND LASALLE’S STABILITY</b>	
<b>PRINCIPLE . . . . .</b>	<b>87</b>
<b>BIBLIOGRAPHY . . . . .</b>	<b>90</b>

## LIST OF TABLES

1	Advantages and disadvantages of using simulation tools for ATC training and experiments . . . . .	7
2	Average convergence time. ( $\Delta t \equiv$ sampling time) . . . . .	52

## LIST OF FIGURES

1	Map of the 20 Air Route Traffic Control Centers covering the continental United States. (figure adopted from [1]) . . . . .	3
2	Center map for Minneapolis Center (ZMP) with high-altitude sector boundaries. (figure adopted from [1]) . . . . .	4
3	Structure of ATC operator training. . . . .	5
4	Components of conflict detection and resolution. (figure adopted from [2]) . .	8
5	Each aircraft is protected by a safety zone. Whenever the safety zones of two aircraft overlap, a conflict is detected. . . . .	8
6	Conflict detection and resolution phases. (figure adopted from [2]) . . . . .	11
7	In traditional systems, ATC operators use radar and vocal communication systems to monitor and issue commands to aircraft. . . . .	12
8	Conflict detection and resolution decision-support tools aid ATC operators by providing them with possible resolution solutions. . . . .	13
9	Aircraft flow in and out a defined control volume. (figure adopted from [3]) .	24
10	Heading change model vs. offset model. Left: The aircraft maneuver is a heading change. Middle: The aircraft maneuver is a heading change followed by a second heading change. Right: The aircraft maneuver is a relative position change. (figure adopted from [3]) . . . . .	25
11	Aircraft deviation amplitudes under heading change and offset maneuvers. (figure adopted from [3]) . . . . .	26
12	Aircraft fly on two flows, moving in and out a control volume. Shaded areas define a shadow in which a conflict may occur. . . . .	27

13	Two aircraft in conflict with (a) left touch, and (b) right touch. Solid line (blue) corridors are associated with eastbound aircraft, and dashed line (red) corridors are associated with southbound aircraft. Dashed arrows represent the direction of lateral maneuver taken by each aircraft to collaboratively resolve the conflict. . . . .	28
14	Conflict resolution for four intersecting flows of aircraft. The control space is divide into multiple conflict zones including pairs of intersecting flows. The conflict zone area should be designed to guarantee that aircraft approaching the point of conflict can resolve such conflict entirely, without straying outside the area. . . . .	29
15	Safe control volume, where $\dot{L} = 0$ for all aircraft within it. . . . .	34
16	Conflicting aircraft with $\dot{L} = 0$ (a), and their conflict graph representation (b). . . . .	34
17	Conflict graph representation for the case of two intersecting aircraft flows. . . . .	35
18	Conflict resolution maneuver sequence with lateral maneuvers ( $\theta = 90^\circ$ ), at the 1st (a) – 4th (d) time steps. Solid (blue) lines represent the shadows of eastbound aircraft, and dashed (red) lines represent the shadows of southbound aircraft. . . . .	43
18	(cont.) Conflict resolution maneuver sequence with lateral maneuvers ( $\theta = 90^\circ$ ), at the 5th (e) – 8th (h) time steps. Solid (blue) lines represent the shadows of eastbound aircraft, and dashed (red) lines represent the shadows of southbound aircraft. . . . .	44
18	(cont.) Conflict resolution maneuver sequence with lateral maneuvers ( $\theta = 90^\circ$ ), at the 9th (i) – 12th (l) time steps. Solid (blue) lines represent the shadows of eastbound aircraft, and dashed (red) lines represent the shadows of southbound aircraft. . . . .	45
19	Conflict resolution maneuver sequence with lateral maneuvers ( $\theta = 60^\circ$ ), at the 1st (a) – 4th (d) time steps. Solid (blue) lines represent the shadows of flow 1 aircraft, and dashed (red) lines represent the shadows of flow 2 aircraft. . . . .	46

19	(cont.) Conflict resolution maneuver sequence with lateral maneuvers ( $\theta = 60^\circ$ ), at the 5th (e) – 8th (h) time steps. Solid (blue) lines represent the shadows of flow 1 aircraft, and dashed (red) lines represent the shadows of flow 2 aircraft. . . . .	47
20	Conflict resolution maneuver sequence with lateral maneuvers ( $\theta = 45^\circ$ ), at the 1st (a) – 4th (d) time steps. Solid (blue) lines represent the shadows of flow 1 aircraft, and dashed (red) lines represent the shadows of flow 2 aircraft. . . . .	48
20	(cont.) Conflict resolution maneuver sequence with lateral maneuvers ( $\theta = 45^\circ$ ), at the 5th (e) – 8th (h) time steps. Solid (blue) lines represent the shadows of flow 1 aircraft, and dashed (red) lines represent the shadows of flow 2 aircraft. . . . .	49
20	(cont.) Conflict resolution maneuver sequence with lateral maneuvers ( $\theta = 45^\circ$ ), at the 9th (i) and 10th (j) time steps. Solid (blue) lines represent the shadows of flow 1 aircraft, and dashed (red) lines represents the shadows of flow 2 aircraft. . . . .	50
21	Summation of the magnitude of $\dot{L}$ for all the aircraft in the control volume flying in flows with encounter angle is (a) $90^\circ$ , (b) $60^\circ$ , and (c) $45^\circ$ , $c = 1$ . . . . .	51
21	(cont.) Summation of the magnitude of $\dot{L}$ for all the aircraft in the control volume flying in flows with encounter angle is (a) $90^\circ$ , (b) $60^\circ$ , and (c) $45^\circ$ , $c = 1$ . . . . .	52
22	Example of aircraft lateral deviations for two perpendicular flows, eastbound (solid) and southbound (dashed). . . . .	54
23	Magnitude of lateral deviation with time for two intersecting flows, $\theta = 60^\circ$ . . . . .	55
24	Magnitude of lateral deviation with time for two intersecting flows, $\theta = 45^\circ$ . . . . .	55
25	Net magnitude of lateral deviations of the aircraft forming flows with an encounter angle $\theta = 90^\circ$ . . . . .	56
26	Net magnitude of lateral deviations of the aircraft forming flows with an encounter angle $\theta = 60^\circ$ . . . . .	57
27	Net magnitude of lateral deviations of the aircraft forming flows with an encounter angle $\theta = 45^\circ$ . . . . .	58
28	Histogram of lateral deviations for 100 aircraft. . . . .	58

29	Lyapunov function $V$ for two intersecting flows at $\theta = 90^\circ$ . . . . .	59
30	Lyapunov function $V$ for two intersecting flows at $\theta = 60^\circ$ . . . . .	60
31	Lyapunov function $V$ for two intersecting flows at $\theta = 45^\circ$ . . . . .	61
32	Robot mechanisms leading to joint action. (figure adopted from [4]) . . . . .	64
33	Computer simulation framework for aircraft conflict resolution HRC system. Human can cooperate with the computer controller by using joystick to control the acceleration of the lateral maneuver. . . . .	73
34	Human participant control criteria (right) and his estimated criteria (left), measured for the error function $e(t)$ (top), and the acceleration control input $u(t)$ (bottom). . . . .	75
35	Human-Robot collaboration to resolve a complete overlap of aircraft shadows, at equal contribution level. (top) The error function in nm, (bottom) each agent control input. . . . .	77
36	Human-Robot collaboration to resolve a complete overlap of aircraft shadows, with the robot seeking to minimize the human input. (top) The error function in nm, (bottom) each agent control input. . . . .	78
37	LaSalle's Invariance Principle. Every solution starting in $\Omega$ approaches $M$ as $t \rightarrow \infty$ . . . . .	89

## PREFACE

This research work was motivated by the increased complexity of the air traffic management and by the desire of automating the process of conflict detection and resolution. The dissertation aims to propose automatic solutions for the air traffic management that reduce that complexity and help the air traffic controllers with their workload. Beside proposing decentralized collision avoidance control rules, this work provides a mathematical framework to analyze the safety and the converge of the conflict resolution dynamics using Lyapunov analysis.

This dissertation can be divided into three parts. The first part (Chapter 1) introduces the existing air traffic management systems and efforts for collision avoidance and aircraft conflict resolution. Chapter 2–4 constitute the second part of this dissertation. In this part, the conflict resolution geometry is defined, followed by proposing an automatic collaborative decentralized conflict resolution rule. Then, mathematical and numerical analysis was conducted was derived to prove the safety and convergence of the conflict resolution dynamics under the proposed automatic rule. This mathematical framework is based on Lyapunov analysis of dynamical systems. The third part of this dissertation studies human-robot collaboration for aircraft conflict resolution in Chapter 5. The work proposes a model to estimate human control action to train a robot pilot that work collaboratively with human pilot to resolve an existing conflict.

The work in this dissertation can be extended to build a framework to study multi-agent networks. Therefore, this dissertation should be of interest to scholars working on air traffic management systems, decentralized and networked control, human-robot interactions and collaboration, and Lyapunov analysis.

## ACKNOWLEDGMENT

I owe my deepest gratitude to my PhD adviser, Professor Zhi-Hong Mao, for his guidance and support throughout all the phases of my doctoral study. His continuous help and support was of valuable contribution towards finishing my PhD program and so much more. Beside that, his pleasant and respectful personality has made collaborating with him an enjoyable experience. Professor Mao is a caring mentor, devoted instructor, and role model to all of his students. I learned from him much more than scientific knowledge. I will always be grateful to him for everything he has taught me.

I would like to express my gratitude to Professor Mahmoud El-Nokali and Professor Amro El-Jaroudi for their continued help, support, and care. I would like to thank them for devoting parts of their valuable time to discuss my research projects and my plans, and for providing their wise advice. Each has taught me to push the boundaries of research and to never be apprehensive about exploration. Moreover, both professors are amazing instructors, and I have learned a lot from them.

During my course of study, I had the opportunity to collaborate with several extraordinary professors and colleagues, who influenced my work and provided me with invaluable pieces of advice in my research. In particular, I would like to thank Professor Murat Akcakaya for giving me the opportunity to work closely with him, providing me with his thoughtful opinions, and supporting me in my research. I would also like to thank all my committee members for their valuable comments that helped me to write a better dissertation.

It has been an honor for me to have worked in such a great environment at our department. An environment created by remarkable people including professors, staff, and graduate students. I would like to thank all of them for creating this amazing environment. For the administrative part, I would like to thank Sandy Weisberg for her efforts on managing the graduate program, and for providing me with help.

This work was supported by the National Science Foundation under grant CNS-1544578.

Finally, I would like to thank my family for their unconditional endless love and support.

This dissertation is dedicated to them.

*To Mom, Dad, Safaa, Mohamed, and my little son Hassan.*

## 1.0 INTRODUCTION

Supported by decades of operation, the conventional geographical network based air traffic control system, in which aircraft fly along fixed routes, is proven to be safe. However, the continuous increase in number of daily flights, bring the entire system to a congested state; and this triggered the evolution of new air traffic control rules. On the other hand, motivated by the desire for more efficient handling of airborne traffic, Free Flight operations [5] depend on navigation and surveillance technologies to increase the freedom of route planning. Free Flight thus enables flexible routing systems and can replace the fixed routing structure, especially with the increasing growth in air transportation. The concept of Free Flight was enabled by the advent of global navigation satellite systems, e.g. GPS, that facilitated precise positioning of aircraft and thus eliminated the routing constraints imposed by the conventional fixed-route system. Under Free Flight, aircraft are able to optimize their own trajectories according to some certain criteria, such as weather, safety, time of flight, and cost of operation [6, 7]. It also enables larger traffic volume; potentially, airspace capacity may be increased by at least a factor of three [8]. This confines with the Joint Planning and Development Office stated goal of tripling the available capacity of the National Airspace System by 2025 [9]. Free Flight motivates distributing the traffic control decisions based on information available locally to potential sites of air traffic conflict, and emphasizes on the possibility of using decentralized control strategies. This may lead to dismantling of most of the current structure of the air traffic management system in favor of a seemingly chaotic but more efficient management system. However, with this approach, Free Flight may increase the complexity of conflict detection and resolution process on the air traffic controllers, since distributed control may result in a lack of predictability of potential conflicts [10], and more complex conflict scenarios may arise because of the unstructured trajectories resulted

from pilot-preferred routing [11]. Moreover, ensuring safe separation has now become the responsibility of each individual aircraft [12]. To be able to take this responsibility, individual aircraft should have the capability of monitoring, detecting, and resolving any potential air-born conflicts efficiently and without the intervention of the ground air traffic controllers. Therefore, the effect of any Free Flight based approach on system efficiency and safety needs to be proven by simulating the automated and optimal conflict detection and resolution algorithms [3,13]. Examples of Free Flight systems that are introduced to overcome air traffic complexity are the American Next Generation Air Transportation System (NextGen) [12], and its European equivalent Single European Sky Air traffic management Research program (SESAR) [14]. Both systems aim to automate the air traffic control operation and allow a higher level of decision making by the pilots in response to changing flight conditions. Hence, rather than depending on experience with reliable operation, such as the network based system, new traffic management schemes should provide appropriate analysis and mathematical modeling to verify its efficiency and safety.

## 1.1 CONFLICT DETECTION AND RESOLUTION PROCESS

### 1.1.1 National Airspace System

In order to understand air traffic management systems and the conflict resolution process, it is important to learn about the composition of the National Airspace System (NAS). The NAS, as operated by the Aviation Administration (FAA), enables the safe and efficient transportation of aircraft [1]. It consists of a heterogeneous set of interacting units that includes human operators, airspace, technologies, practices, procedures, and policies. Air Route Traffic Control Centers (ARTCC) are essential functional components of the NAS structure. There are 22 (20 in the continental US) ARTCC centers responsible for managing en route aircraft, and controlling an airspace of up to 60,000 feet [15]. Figure 1 shows a map of the 20 centers spanning the continental United States. Each center is structured into multiple layers (low-altitude, high-altitude, and super-high-altitude), which are further

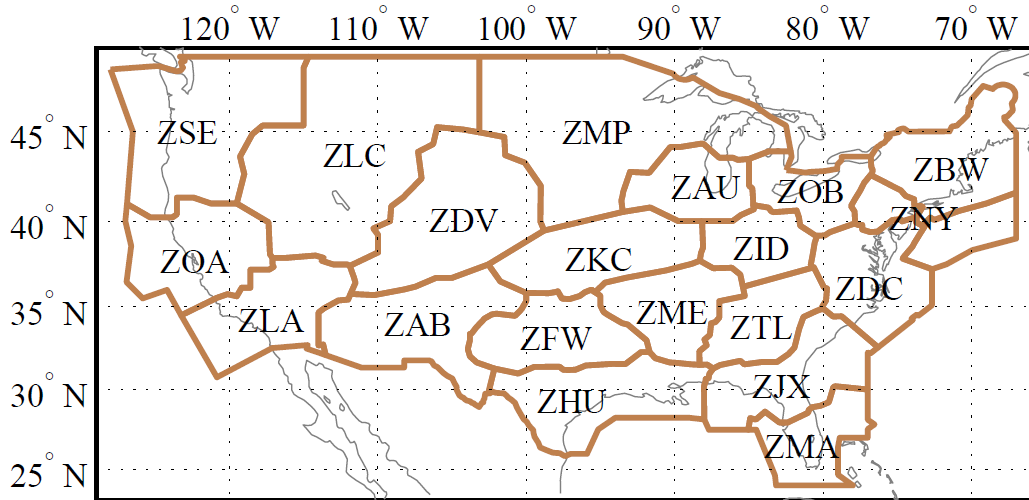


Figure 1: Map of the 20 Air Route Traffic Control Centers covering the continental United States. (figure adopted from [1])

subdivided into en route sectors. For example, the map of the high-altitude sector boundaries for Minneapolis Center (ZMP) is shown in Figure 2. Depending on traffic conditions, one or two air traffic controllers are responsible for managing aircraft traffic in one sector. Within each sector, navigation infrastructure (e.g., waypoints, jetways and navigation aids) is used to help with the traffic flow management. As will be extensively described below, The primary task of the air traffic controller working an en route sector is to ensure the proper separation of aircraft all the time. For the operations near airports, air traffic control is managed by control tower that handles arriving and departing flights at airports [16]. Towers are equipped with tools and devices that enable human operators to perform efficiently. For example, towers have radars that covers ground activities, air activity, radio communication, meteorological surveillance and light control for taxi-ways and run-aways [17]. Therefore, serving as a complementary element, Airport towers along side ARTCCs are used to control the airspace within a specified range (e.g., sector) and ensure that safe and efficient traffic flow is maintained.

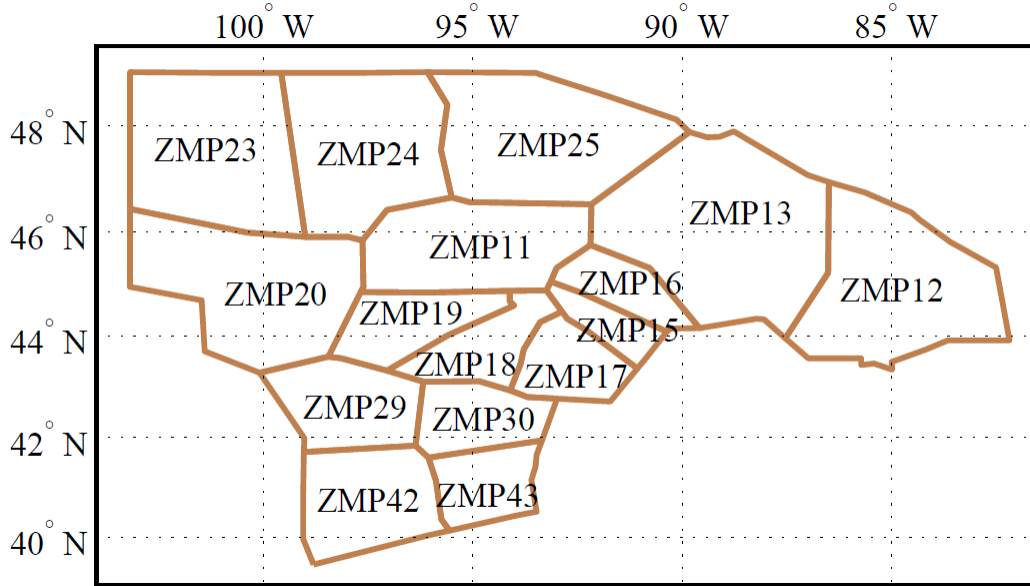


Figure 2: Center map for Minneapolis Center (ZMP) with high-altitude sector boundaries. (figure adopted from [1])

### 1.1.2 Air Traffic Management

Aircraft conflict resolution is an important aspect in air traffic management (ATM) and safety. ATM aims to provide safe, orderly, and efficient operation of both civilian and unmanned aircraft by imposing certain requirements on aircraft control [18, 19]. With the increased demand of air traffic, avoidance of airborne collisions that may occur in a congested network is a necessary requirement. Two main components constitute the ATM system, namely the Traffic Flow Management (TFM) and Air Traffic Control (ATC). The TFM role is to organize the flow patterns of aircraft to ensure efficient operation. In other words, TFM manages the air traffic in the NAS based on system capacity and demand [15]. TFM deals with demand management and typically deals with traffic at the ARTCC level. On the other hand, the ATC ensures separation of aircraft as a means to avoid aircraft conflict or collision [16, 17]. ATM process conflict detection and resolution at three different levels:

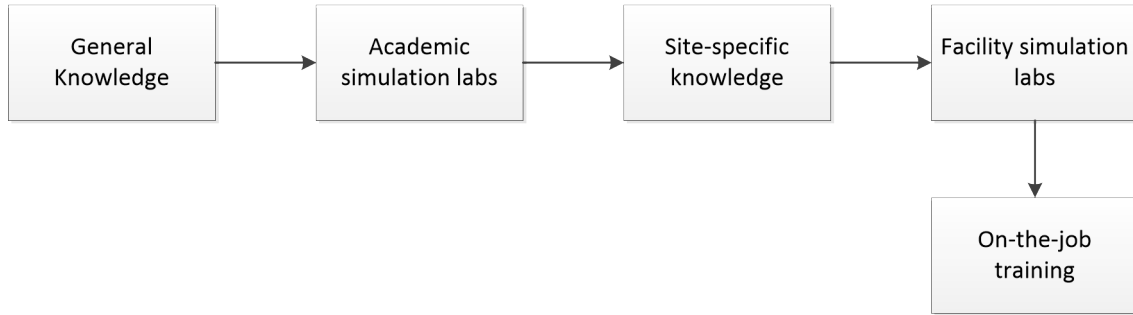


Figure 3: Structure of ATC operator training.

1. *Long Range*: At this level, conflict detection and resolution are performed at the level of the entire national airspace system, over a relatively long time horizon that extends for several hours [20, 21]. This process involves using large-scale integer and linear programming techniques to predetermine flight trajectories and airlines schedules. This guarantees that airports and air sectors capacities are not exceeded.
2. *Mid-Range*: Conflict detection and resolution are managed by the ATCs, over a time horizon of the order of tens of minutes. Deviations from the originally planned trajectories are instructed to each aircraft to ensure safe separation between aircraft.
3. *Short Range*: Conflict detection and resolution are performed in a decentralized fashion. The detection and resolution are performed on board the aircraft by the flight management systems, over a short time horizon of the order of seconds to few minutes.

For most of the operations, conflict detection and resolution are managed by trained ATC operators. ATC operators must be trained before dealing with real conflict situations. Figure 3 shows the structure of a typical training program. The training is conducted using simulation tools for learning both general knowledge and site-specific knowledge. Simulation tools are used, along with the theoretical framework, throughout the training course to train operators on new equipment and new routines.

Simulation has proven to be an adaptable tool that is useful for many situations where real life training might be risky or too expensive. Simulation tools are commonly used for ATC operator because of their valuable features. By using simulators, ATCs have the ability freeze

scenarios and directly evaluate other solutions. Also, simulators can record the whole training session that can be replayed at a later time for further evaluation. However, simulators cannot train the ATC operators under the stressful environment of real scenarios, where they cannot compensate of fatal mistakes. Table 1 lists the advantages and disadvantages associated with the use of simulation tools in ATC training and as an experimental tool.

### 1.1.3 ATC based Conflict Avoidance

Technically, ATC operators monitor flights in real time to ensure safe flight operations. Therefore, ATC operators constitute an essential element for the ATM process due to their ability to observe, integrate information, and make guided decisions. Figure 4 shows the components of conflict detection and resolution system. A conflict occurs when two or more aircraft are close to each other, i.e., a loss of separation (c.f. Figure 5). The International Civil Aviation Organization defines and enforces a safe separation zone for each aircraft. The safety distance is defined by means of a minimum allowed horizontal separation and a minimum vertical separation. Current en-route airspace regulations set the minimum horizontal separation to 5 nautical miles (nm), while inside the terminal radar approach control (TRACON) area it is reduced to 3 nm. The minimum vertical separation is 2000 ft above the altitude of 29000 ft (FL290), and 1000 ft below FL290. Thus, aircraft are in conflict if their separation zones intersect (Figure 5).

Conflict avoidance is a two stage process. First, aircraft trajectories are continuously monitored by air traffic control operators who handle detection and resolution of any possible conflicts. The future positions of the aircraft are predicted based on their current trajectories and flying conditions. A potential conflict is detected if the predicted positions of any pair of aircraft violate the safe separation requirements at any time in the future. Second, to avoid any possible collisions, the trajectories of the aircraft involved in each of the detected conflicts are replanned to resolve that conflict. Conflict resolutions are performed through conservative maneuvers, mainly a combination of speed and heading changes, and flight level reassignment, to ensure aircraft separation rather than to reduce operations costs [22, 23]. However, the altitude changes are not common for many reasons such as fuel consumption,

Table 1: Advantages and disadvantages of using simulation tools for ATC training and experiments

	Advantages	Disadvantages
Software and Hardware	(a) test new tools and their compatibility (b) reveal bugs and technical issues	
Training	(a) low cost (b) risk free (c) easy to develop (d) mimic real scenarios at variety of conditions (e) ability to freeze any given scenarios	no feeling of real stress or responsibility
Scenarios	(a) excellent for emergency training (b) ability to repeat scenarios	trainers could learn the traffic pattern
Experiment	(a) ability to save data for future analysis (b) high accuracy and reliability due to controlled environment (c) ability to control every variable during the experiment.	(a) need a detailed plan for which data to be collected (b) too much control might not reveal unexpected results
Fidelity	(a) good for specific training (b) ability to conduct experiments and simulations using high and low fidelity.	

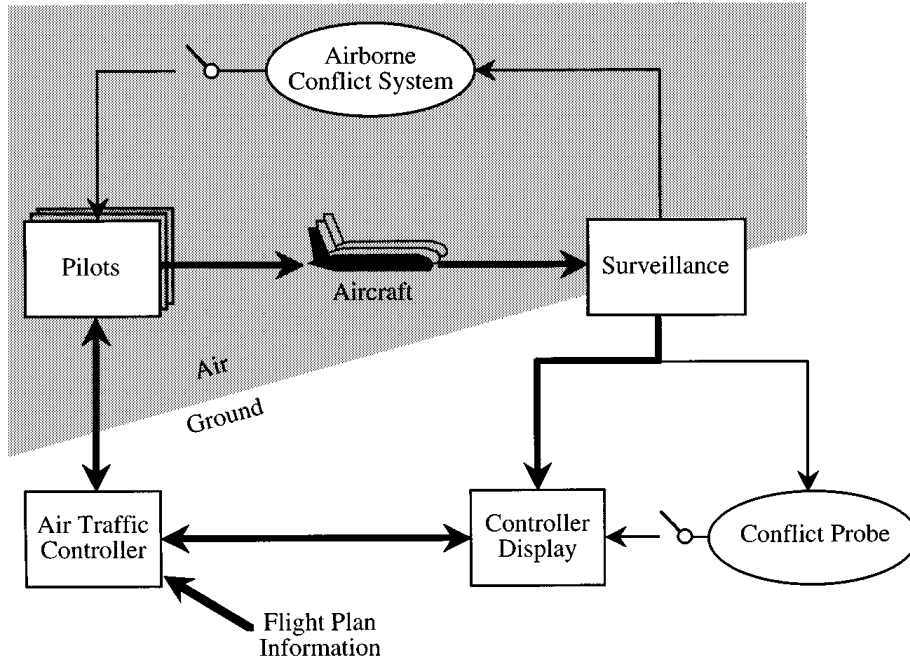


Figure 4: Components of conflict detection and resolution. (figure adopted from [2])

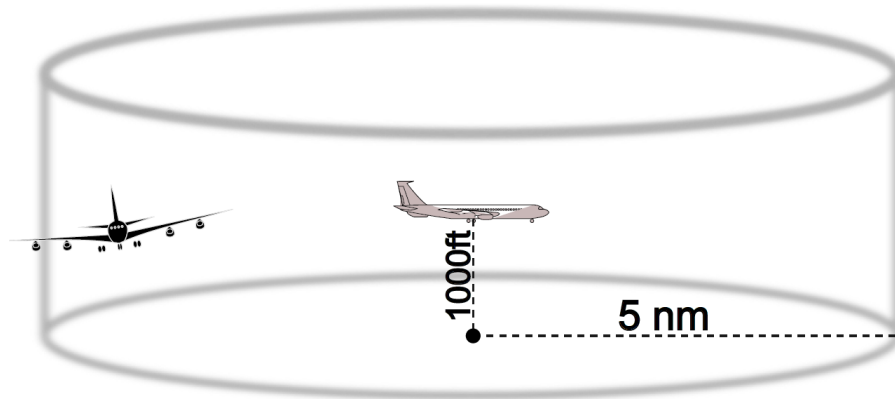


Figure 5: Each aircraft is protected by a safety zone. Whenever the safety zones of two aircraft overlap, a conflict is detected.

passengers discomfort, and ease of monitoring. Air traffic control is thus a crucial stage in the overall air traffic management, since it constrains the airspace structure and traffic flow.

Eurocontrol estimated a 50% increase in air traffic density by 2035 [24]. Consequently, the FAA (Federal Aviation Administration) is making several efforts to improve the capacity and throughput of existing airspaces by means of airspace redesign, trajectory based operations, new traffic flow management tools, and automated data communication and navigation systems. Also, the increase of air traffic would continuously increase the complexity of the conflict detection and resolution process. Air traffic control complexity refers to a set of descriptions of the prevailing air traffic patterns and sector characteristics that aid or hinder in the management of aircraft conflict detection and resolution. This increasing complexity adds intensive workloads to the ground controllers [25].

ATC operator workload associated with air traffic control corresponds to the stress, or “...the amount of effort, both physical and psychological, expended in response to system demands (task load) and also in accordance with the operators internal standard of performance” [26]. Beside air traffic control complexity, there are three other mediating factors that influence the ATC operators workload: quality of equipment, individual differences, and operator cognitive strategies [27, 28]. Quality of equipment considers, for example, the accuracy of tracking systems and (or) the usability of user interfaces for computer-assist tools [1]. Individual differences, such as personality, age, and experience, have shown correlation with ATC operators workload. The last actor, cognitive strategies, assimilates how operators adapt their strategies in managing traffic according to pressures from increasing traffic density. For example, at low traffic densities operators use a wide variety of information and options in managing traffic, while at high traffic densities, operators limit the amount of information they use and adapt their management strategies based on economical constraints, including strategies for resolving potential conflicts.

Although, as previously discussed, human performance and human factors have been considered to be of great importance to, and directly affect, air traffic system performance; the increased work load would probably lead to failures and operational errors [2, 29]. Subsequently, automated reliable tools will be needed to help ATC in accommodating this traffic increase and the associated complexities and to facilitate air traffic management. Together,

these automated tools would provide a safety net when normal procedures, and controller and pilot actions fail to keep aircraft separated beyond established minimum safety distance. One goal for these automated systems is to predict a conflict that is going to occur, convey the detected conflict to an ATC operator, and assist in the resolution of the detected conflict situation [2]. This process can be organized into modular phases as shown in figure. 6. The system will be able to detect possible conflicts by first monitoring and (or) estimating the current state of traffic situation. The traffic state is then used to project the states into the future, by using the dynamic trajectory model, in order to predict the existence of possible conflicts. If a conflict is detected and an action is considered necessary, the conflict resolution phase may be initiated. Without the automated systems, conflict detection and resolution would be manually handled through procedures. For example, visual flight rules place the responsibility for collision avoidance on the pilot, who must visually scan for traffic (conflict detection) and if a conflict is perceived, take appropriate action according to a predefined set of rules (conflict resolution). Under instrument flight rules, an ATC operator monitors traffic using radar and issues resolving maneuvers to pilots when a conflict is estimated to occur (Figure. 7). However, as previously discussed, the use of automated systems would be helpful in reducing the workload experienced by the ATC operators by aiding them, and would be helpful in increasing the efficiency of the conflict detection and resolution process.

#### **1.1.4   Airspace Redesign**

In the face of the increasing traffic demand and as a means to reduce the workload on ATCs, airspaces have been redesigned into smaller and more specialized sectors for ATC operators to manage. Such division allows ATC controllers to monitor a smaller set of aircraft, while decreasing variance in traffic patterns. Examples of such airspace redesign include sectors ZMP15 and ZMP16 in Minneapolis center (Figure 2). Both are dominated by aircraft arrivals into Minneapolis - St. Paul International Airport (MSP) and are significantly smaller than other sectors in that center. However, there is a certain limit after which sectorization will no longer be an efficient strategy for reducing ATC controller workload. Dividing the ARTCC

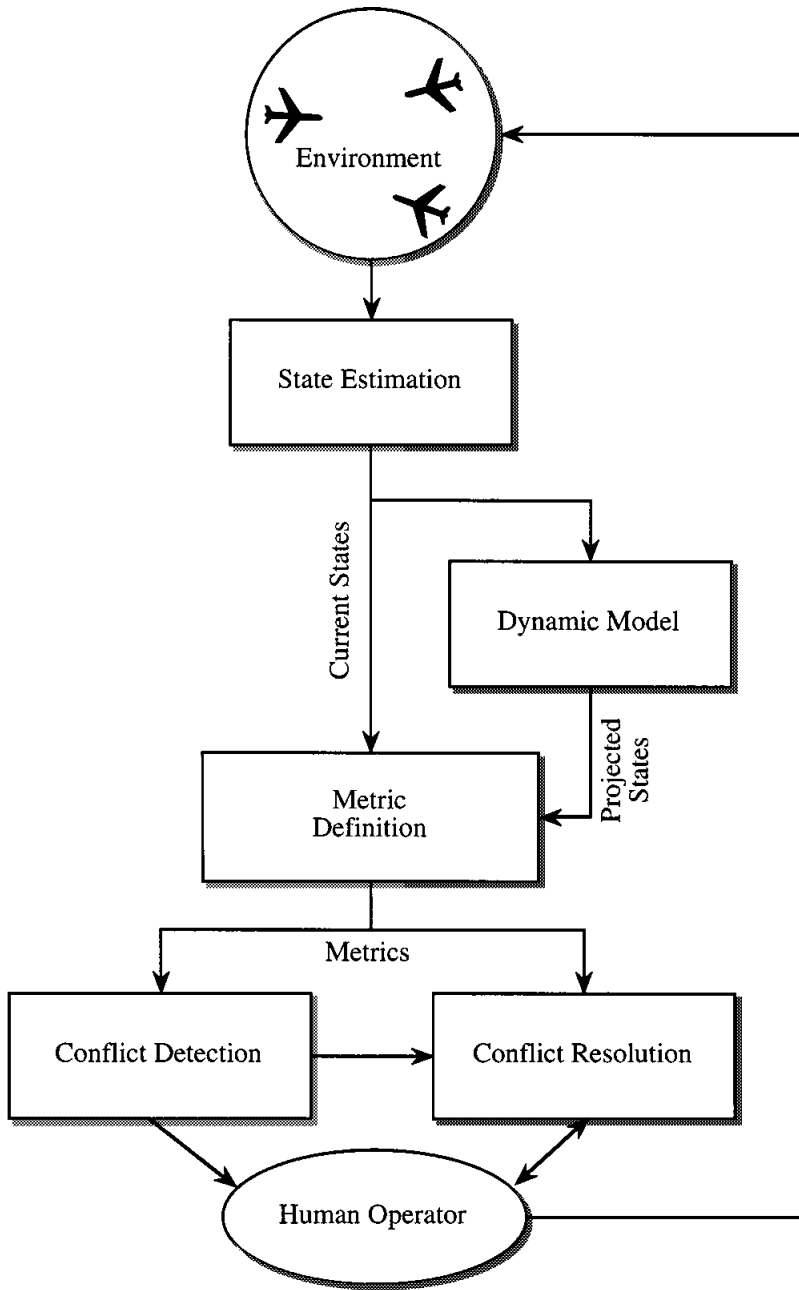


Figure 6: Conflict detection and resolution phases. (figure adopted from [2])

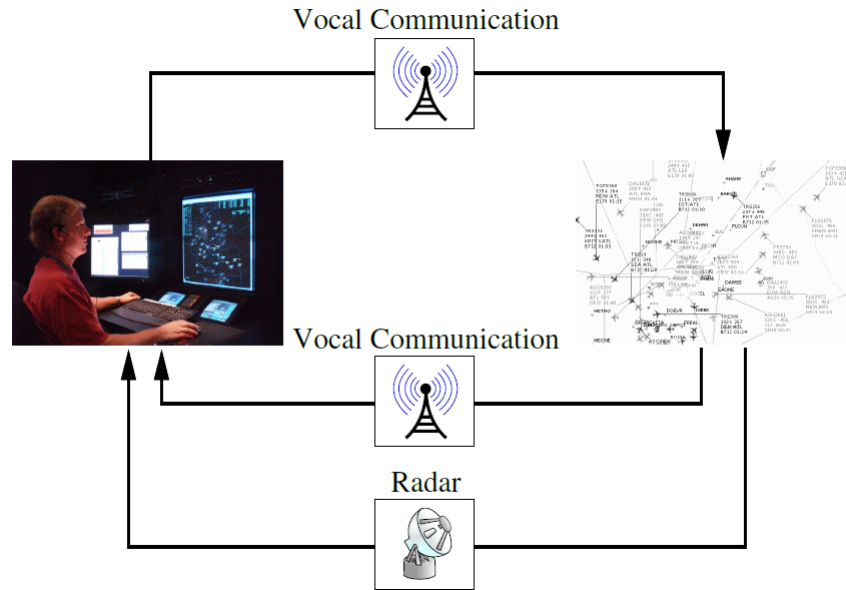


Figure 7: In traditional systems, ATC operators use radar and vocal communication systems to monitor and issue commands to aircraft.

centers into smaller sectors basically reduces the amount of traffic that any single sector can accommodate, and places restrictions on the types of conflict resolution maneuvers available to ATC operators. Additionally, increasing the number of small sectors requires larger number of ATC staff and higher level coordination between adjacent sectors. The advantage of smaller sectors in terms of managing ATC operators workload and traffic complexity is reaching its limits. Hence, while airspace redesign, along with the introduction of tighter navigation standards, will result in further gains in capacity, these changes alone are not sufficient to accommodate the anticipated growth in air traffic density. Therefore, the use of advisory decision-support tools and automated conflict detection and resolution tools and became a necessity.

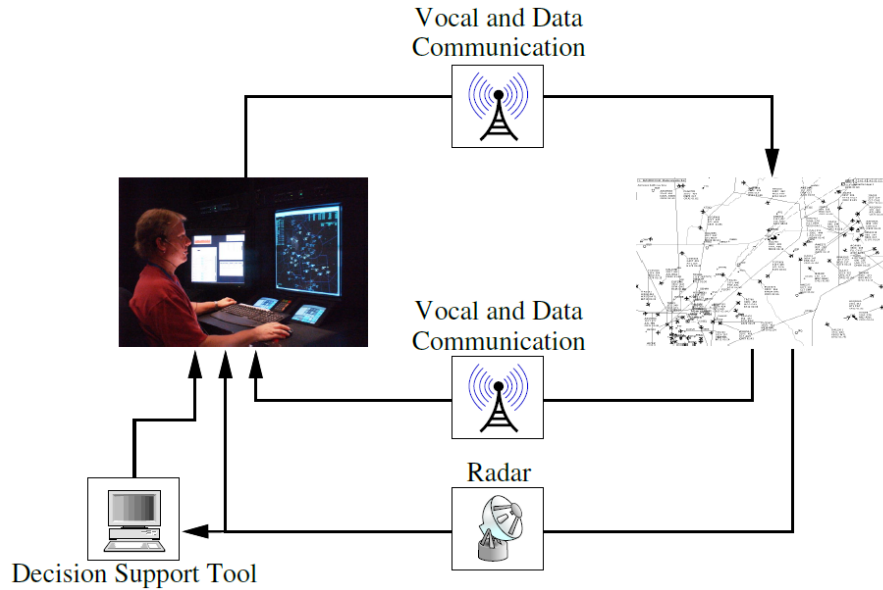


Figure 8: Conflict detection and resolution decision-support tools aid ATC operators by providing them with possible resolution solutions.

### 1.1.5 Advisory Decision-Support Tools

Advisory conflict detection and resolution decision-support tools are used to aid ATC operators, without replacing them. Advisory decision-support tools provide conflict resolution options to ATC operators, and can be used as an alternative to fully- or semi-automated systems that require advanced data communication and navigation sub-systems. Figure 8 shows a diagram of the control structure for human-in-the-loop (ATC operator in this case) control with conflict detection and resolution decision-support tools. The conflict detection and resolution decision-support tools detect potential conflicts and propose resolution maneuver commands for the ATC operators to review and issue to aircraft. If ATC approved the resolution strategy, the new trajectories are uploaded to the aircraft via data link for pilot approval.

One advantage with use of the decision-support tools is the ability to design these tools to handle large and complex traffic loads, and provide real time solutions. Moreover, there exist a safety net associated with these tools, because these tools does not exclude the human ATC

operator out of the loop, and (s)he can accept or reject the suggested solution. However, there still some concerns about degraded performance of ATC operators and the proper design of the decision-support tools. For example, conflict detection and resolution systems should be designed appropriately such that human controllers neither overly depend on the support tool nor lack faith in the tool and disregard it [1, 30, 31].

The design and implementation of conflict detection and resolution algorithms for decision-support tools in human-based air traffic control operations should take a different approach, because the existence of the human in the loop would require additional design specifications. In other words, the method by which conflict detection and resolution algorithms identify and resolve conflicts is critical to the function of a decision-support tool. For example, the algorithms must explicitly acknowledge the role of the ATC human operators and accommodate their abilities. There is a need to ensure that the inclusion of conflict-resolution decision-support tools will reduce, or at the very least not worsen ATC operator workload, while improving service.

#### **1.1.6 Mixed Automation for Conflict Resolution**

Some research efforts, that are more consistent with human-factors constraints, was directed toward mixed levels of automation of the conflict detection and resolution process. For example, the En Route Air Traffic Soft Management Ultimate System (ERASMUS) project [32] was funded by EUROCONTROL to study approaches that effectively integrate advanced automation concepts consistent with controllers human factors issues. This project introduced the concept of “subliminal control” [32, 33]. Under this concept, significant portions of traffic are deconflicted or further spaced with minor automated speed control commands within  $\pm 6\%$ . The magnitude of this change is not perceptible to ATC operators or pilots. Thus, the use of this minor change of speed to force separation of aircraft reduces both the total number of aircraft that ATC operators actively monitor for potential conflicts and the number of resolution commands that operators issue. Some simulation studies suggest that controller workload is reduced using this approach [1].

Although it may enhance the system performance, there are some concerns about the subliminal control. The concerns address the applicability, practicality and ability to implement the subliminal control based systems in the real world. For example, subliminal control systems require very advanced data communication and navigation systems to control aircraft directly away from the pilot and the ATC operator. Moreover, mixed-modes of operation that include dynamic allocation of separation tasks would lead to ambiguity about who is in control and who is responsible for recovery in the case of system failure (pilots or ATC operators). Also the use of mixed-automation systems may lead to loss of motivation for the ATC operator, since most of the process is allocated to automation systems [34].

### 1.1.7 Automated Conflict Resolution

Automated conflict detection and resolution systems aim to increase the air traffic capacity while reducing the ATC workload and system complexity, by automatically detecting conflicts and generating conflict free trajectories as a solution to the detected conflicts. The resuction in ATC operators workload is achieved by decreasing the amount of time and mental effort ATC controllers spend detecting and resolving potential conflicts [35]. On average, ATC operator takes around 27.6 seconds to resolve a potential conflict between two aircraft [36]. However, the impact of the automated tools on the system performance should be studied alongside investigating the practical implementation of these methods. Practical implementations are topic of concern, because automated systems need advanced digital communication and navigation systems to directly communicate with, and control, aircraft. Also, an automatic conflict detection and resolution system should provide provably safe solutions while attempting to satisfy aircraft dynamic limitations [37,38]. In Section 1.2, we review some of the recently proposed automatic conflict detection and resolution algorithms.

## 1.2 PREVIOUS WORK

Trajectory prediction and conflict detection approaches can be categorized into three classes: nominal, worst case, and probabilistic [2]. The nominal predictors project the current state along a single trajectory into the future. Although being simple and straightforward, this approach does not account for uncertainties that may lead to deviations in aircraft routes. Worst case predictors (for example, [39] and [40]) are more conservative, since they assume that the aircraft can perform any of a range of maneuvers, and report a conflict alarm if any of these maneuvers could result in a conflict. In dense traffic situations, this approach could cause high false alarm rate. The probabilistic approaches consider uncertainties in the predicted aircraft trajectories. Probabilistic methods consider use an ensemble of sample paths and compute the probability of projected conflicts. Thus, aircraft trajectories are modeled as a probability density function, from which a probability of conflict is estimated. This avoids the conservativeness of the worst case approach, but is still robust with respect to uncertainty. Hence, for situations with a high density traffic and uncertainties, these methods are useful in evaluating air traffic safety. However, it is difficult to build a simple but realistic model the perturbations that affect aircraft trajectories. Wind and errors in tracking, control, and navigation are the common sources of uncertainty that are taken into consideration when designing a probabilistic model. Usually, the deviations from nominal trajectories are modeled as the sum of independent random variables, each corresponds to one source of uncertainty, acting in disjoint time periods [41]. Paielli and Erzberger [42] modeled tracking errors by zero-mean Gaussian random variables. They proposed a closed form analytic expression for the probability of conflict for level flight, assuming that the two aircraft fly along straight lines with constant tracking errors over the whole time horizon. To get rid of the errors that may be introduced if the simplifying assumptions in [42] are not satisfied, Monte Carlo simulation, incorporating aircraft intent information, was used to estimate the probability of conflict in [43]. This method can be applied under different scenarios and does not require particular assumptions. It is not computationally efficient though. Prandini et al. [41] have used a stochastic kinematic model in which uncertainties for short-term trajectory prediction were modeled as a two-dimensional Brownian motion. This method

does not require of flight plan, but its prediction error tends to grow quadratically with time. Thus, this method is usually used for short-term trajectory and conflict predictions of up to 5 min into the future. In [44], the heading change of an aircraft was modeled with a Poisson distribution derived based on empirical data. This method does not explicitly assume any intent information. NextGen [12] incorporates aircraft intent information into a probabilistic framework by using both an aircraft dynamics model for short-term prediction and an aircraft navigation model for long-term prediction. Irrespective of the approach used to detect conflicts, once a conflict detected, a conflict resolution procedure must be initiated.

Since conflict resolution is the most important challenge to ATC, several centralized and decentralized approaches have been proposed, in the last few years, to solve air conflicts with dense traffic involved (e.g., [2, 3, 10, 13, 45–56]). For example, Bicchi and Pallottino [45] introduced a heuristic heading change decentralized collaborative approach, i.e., all aircraft involved in a conflict collaborate to its resolution, while Pallottino *et al.* [13] proposed a centralized collaborative conflict resolution approach based on mixed integer linear programming (MILP) optimization for an optimal path planning considering two cases: instantaneous velocity change and heading angle change. However, the velocity change approach cannot be applied to every conflict situation, e.g., head-to-head conflict. Yoo and Devasia [46] studied the effect of turn dynamics by bounding the heading change rate on the space needed for a safe conflict resolution procedure. Christodoulou and Kodaxakis [47] solved the conflicts in three dimensions with only velocity changes by minimizing the total flight time using mixed-integer nonlinear programming. However, this approach suffers from a high computational time. Alonso-Ayuso *et al.* [48] combined velocity and altitude changes to develop a MILP method. They showed interesting results in the perspectives of computational time and the efficiency of resolution in situations with large number of conflicts. However, altitude changes are not acceptable by airlines because of the high fuel cost and passengers discomfort associated with altitude change maneuvers. Alejo *et al.* [49] considered real time decentralized change of the velocity profile in three dimensions to maintain the safety distance separation. On the other hand, Bilimoria [50] proposed a geometric approach designed to minimize the deviation from a nominal velocity vector. The model sequentially solve conflicts involving multiple aircraft, consequently, the model cannot con-

verge to a global optimal solutions. Rey *et al.* [51] introduced a subliminal speed control model designed to reduce the impact of conflict onto air traffic controllers workload. Cafieri and Durand [52] proposed nonlinear formulation to separate aircraft while minimizing the deviation to aircraft nominal trajectories. Their model depends on velocity regulation using mixed integer optimization. Omer [53] proposed a MILP based space-discretized model that allows both velocity and heading maneuvers. These maneuvers are restricted to trapezoidal patterns and aim to minimize fuel consumption while resolving existing conflicts. Compared to a non linear hybrid time-discretized model [54], this method performed faster but with a higher fuel consumption. Durand and Alliot [55] modeled aircraft trajectories as a path in a graph and used ant colony optimization for conflict free path planning. However, this method is restricted to piecewise-linear trajectories. Mao *et al.* [3] introduced a sequential decentralized control rule to resolve conflicts in a specified control volume. Their model considers only a one time bounded lateral maneuver for each aircraft entering the control volume. The model was proven to be stable, and the lateral deviation has the same effect in resolving conflicts as heading change procedure in [57]. In [56], Frazzoli *et al.* introduced a hybrid method that combines decentralized aircraft speed vector preferences with centralized conflict resolution rule that minimizes aircraft deviations from the desired trajectories. Their centralized conflict resolution approach is based on formulating a nonconvex quadratic cost function and its solution using semidefinite programming with a randomization scheme to obtain conflict free rectilinear trajectories. In [10], it has been proven that certain periodic planar partitions of space are able to provide conflict resolution for any distribution of aircraft in the flows. Space partitioning is an offline optimization approach provides a priori geometrical configuration for conflict avoidance. Mao *et al.* [10] studied space partitions conflict avoidance for two and three intersecting flows. The idea is to generate a space partition using appropriately constructed aisles aligned along relative velocity vectors. This space partition will consequently create a collection of protected quadrilaterals for each flow such that an aircraft may avoid conflict from the other flows whenever its circular protected zone is located in a protected quadrilateral of the same flow. Using the aisles convention, the conflict resolution is equivalent to finding a feasible partition of the planar space such that the aisles are distributed in a way where aisles of one flow will not overlap aisles of

the other flows. Feasible solutions are obtained if the airspace is partitioned and structured with different aisle width patterns for each of the four aircraft flow pairs. Mao *et al.* [10] defined the requirements for a feasible space partition as: (1) all aircraft can find safe locations in some protected quadrilaterals via lateral deviations and (2) the magnitude of lateral deviation required of any aircraft is bounded. Barnier and Allignol [35] used constraint programming model with ground holding approach to solve all potential conflicts occurring above a given flight level. However, their approach is computationally expensive, especially for busy flight schedules. In the approaches proposed in [58–60], arriving aircraft are guaranteed safe trajectories to choose from. Therefore, the available airspace and arrivals runway capacities can be efficiently utilized. Resmerita et al. [60] proposed a two-phase (conflict resolution phase followed by an agent-accommodation phase) decentralized multi-agent framework for conflict free navigation in a discrete environment. Beside the aforementioned methods, effects of weather uncertainties [61], perturbations, navigational errors [62], and airspace disturbances [63] on conflict resolution procedures were studied as well. A review of some other conflict detection and resolution methods can be found in [2], [11], and [64].

Generally speaking, optimization approaches require a proper definition of the cost function. Usually, aircraft separation, fuel consumption, and (or) time delays are used to formulate the cost function. Typically, optimization approaches combine a kinematic model with a set of cost measures. An optimal resolution strategy is then determined by solving for the trajectories that minimize the cost [2]. TCAS (Traffic Alert and Collision Avoidance System), for example, searches through a set of possible climb or descent maneuvers and chooses the least-aggressive maneuver that still ensures adequate protection [65]. One issue with the optimization based method is the complexity of the models. These models can be complex and would require a large computational time to converge to a feasible optimum trajectories. On the other hand, decentralized approaches are more simpler than the optimization approaches and do not require large computation time.

### 1.3 INTRODUCTION TO THE PROPOSED WORK

This dissertation focuses on air traffic scenarios with intersecting aircraft flows. Intersecting aircraft flows are considered for two main reasons. First, rearranging air traffic into standard flows can reduce the traffic complexity [66, 67], and the conflict resolution of two intersecting flows can be used to build an efficient global conflict resolution system by resolving local conflicts between every pair of intersecting aircraft flows [25, 68, 69]. Devasia *et al.* defined the necessary and sufficient conditions to decouple conflicts within intersecting flows, and they proved the existence of decentralized conflict resolution rules that satisfy the decoupling conditions and ensure global conflict resolution. Second, in conflict management of intersecting flows, some difficult problems, such as the domino effect, may arise and affect the efficiency of the global system [3, 22, 68]. In realistic traffic situations, it is indispensable that a conflict resolution system be able to manage encounters involving more than two aircraft. For example, in a pairwise approach, if one conflict resolution maneuver induces a new conflict (the domino effect), the initial solution may be modified until a conflict-free trajectory is obtained. Thus, extra care should be given to the stability and design of conflict resolution procedures to overcome the associated problems that may arise. Conditions for conflict resolution rules stability under intersecting flows were studied in [10], and it was proven that a centralized solution is needed. In contrast to that, this work seeks a decentralized procedure that guarantees safe conflict resolution of the intersecting flows.

The approach proposed here use flow shadows for conflict detection and is based on decentralized collaborative conflict resolution rule for aircraft flowing through a finite control volume of the airspace. In this collaborative resolution scheme, every aircraft involved in the conflict makes a horizontal lateral maneuver to resolve this conflict. This resolution rule also takes care of conflicts that may result via the domino effect, where one conflict resolution maneuver creates new conflicts. Collaborative conflict resolution between aircraft has two major benefits. First, the required magnitude of maneuvering for each aircraft involved in a conflict situation may be reduced when the aircraft maneuver collaboratively when compared against a case in which only one aircraft maneuvers. Second, collaboration helps ensure that aircraft do not maneuver in a direction that could intensify or prolong the conflict [2].

The main concern of this research is the aircraft flow safety and convergence of conflict resolution dynamics under the proposed decentralized conflict resolution rule. Traditionally, the convergence of control systems is related to the behavior of the dynamical system with time, and whether it converges to a desired state or not. We focus on both analytical approaches and simulations to study the evolution of system dynamics and aircraft trajectories within a control volume. Although many efforts have been used toward designing conflict resolution systems, comparatively fewer efforts have been spent on analyzing these systems. Although simulation provides a fast and efficient means to build intuition about the efficiency and safety of the conflict avoidance systems, we believe that analytical arguments can also provide important conclusions about the system dynamics. However, analytical approaches usually require simplified assumptions and scenarios, because it sometimes can be an overwhelming task to prove even the simplest statements about traffic flow properties. Therefore, simulations and analytical approaches must be considered as complementary tools. We use Lyapunov theory to analytically study the system dynamics behavior as time evolves, and to prove the convergence of the system to conflict free trajectories under the proposed conflict resolution control rule. Under air traffic management regulations, the aircraft safety can be related to the requirement that aircraft attains safe operation, and be adequately separated on conflict free trajectories, while being close enough to a pre-specified position. We define the safety requirements of our model in Section 2.3. To confirm our analytically obtained conclusions, we then simulate the two intersecting flows system at different scenarios in Chapter 4.

Another concern of this dissertation is the human-machine collaboration. We study the collaboration between human and robot pilots in resolving an existing conflict between their aircraft. Both agents are assumed to follow lateral maneuvers to avoid the potential collision, the maneuver rate is not known in prior though. We build a robot model that learn from the human pilot actions to efficiently collaborate with the human partner. In order to achieve that goal and train the robot, we first have to estimate the human control behavior. Therefore, we assume the human as a human controller and we propose a model to estimate the human control actions by estimating the human feedback gain given his previous actions and observations of the surrounding environment, the output of this model can then be used

to train the robot pilot. This assumption of an optimal controller is matching the human nature for decision making, and is in agreement with the neurological studies. This human model is proposed in Chapter 5 along with simulations of the human-robot collaboration behavior based on the output of that model.

## 1.4 ORGANIZATION OF THE DISSERTATION

The proposal is organized as follows. In Chapter 2 the basic assumptions, and aircraft flow model and geometry introduced. The proposed automatic conflict resolution rule is presented and discussed in Section 2.3, followed by conditions to ensure safe navigation trajectories for the flying aircraft. In Chapter 3, we study the necessary conditions for safety under the proposed conflict resolution rule, and we mathematically prove the safety and convergence of the conflict resolution dynamics using Lyapunov analysis. In Chapter 4, convergence results are discussed along with numerical simulations. In Chapter 5, we propose a human-machine co-learning based conflict resolution rule. The chapter presents a human controller model, followed by an algorithm to train a robot-pilot, based on human actions, to collaborate with a human pilot in resolving an existing conflict between their aircraft. Finally, the dissertation concludes in Chapter 6.

## 2.0 CONFLICT RESOLUTION MODEL

In this chapter, we describe the intersecting airflow model under consideration, and the assumptions used in our analysis. Then, we review the possible maneuver models that can be used in conflict resolution. The geometry of the conflict resolution problem is illustrated, followed by proposing a continuous time collaborative conflict resolution control rule. The chapter ends with defining the safety requirements to allow further analysis of system safety and efficiency.

Section 2.3 presents the main contribution for this dissertation. In this section a decentralized, collaborative, conflict resolution rule is proposed; where aircraft involved in a conflict situation make lateral maneuvers towards the least congested direction. We introduce the concept of conflict touch, and the rate of the resolution maneuver taken by an aircraft action depends on the number of touches on that aircraft.

### 2.1 BASIC ASSUMPTIONS AND MANEUVER MODEL

Defining an appropriate model is a significant challenge when considering problems in air transportation. The study focuses on a system model that consists of a given volume of airspace and a set of aircraft moving in and out of it (Figure 9). In our model, aircraft are assumed to fly at a fixed altitude layer, i.e., a horizontal plane, through a finite portion of the airspace. Thus, aircraft kinematics can thus be simplified as a point in a plane associated with velocity vector, that defines the direction of motion, and a safety zone radius. Hence, within the airspace volume under study, the dynamics of the system are determined by aircraft position, speed, rate at which aircraft enter the volume, and their individual behaviors

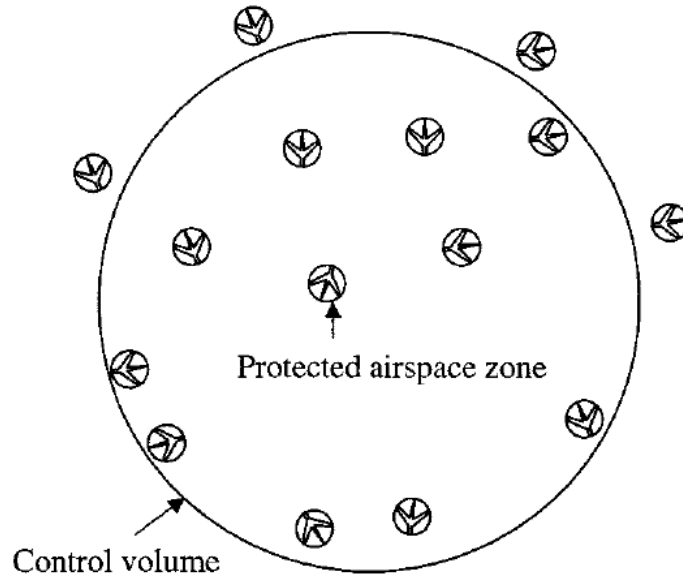


Figure 9: Aircraft flow in and out a defined control volume. (figure adopted from [3])

while they navigate within the airspace. The planar horizontal maneuvers seems to be more strategic in conflict resolution than the tactical vertical maneuvers [3]. Beside that, horizontal maneuvers induce less discomfort for passengers, and does not require flight level changes and thus does not perturb the vertical traffic structure that exists in the enroute airspace.

Aircraft are also assumed to fly with a constant absolute speed, and they are able to communicate with each other and can share information about their status, e.g. position. The aircraft continuously attempt to maneuver and avoid conflicts at minimum effort using lateral offset.

Two maneuver models for conflict resolution exist: (i) heading change model and (ii) offset model. Figure. 10 illustrates both models. In the heading change model, aircraft make a single heading change, while maintaining its speed constant, to modify its trajectory and avoid conflict with other aircraft. These changes are assumed to occur instantaneously when the aircraft makes the avoidance decision [3, 13].

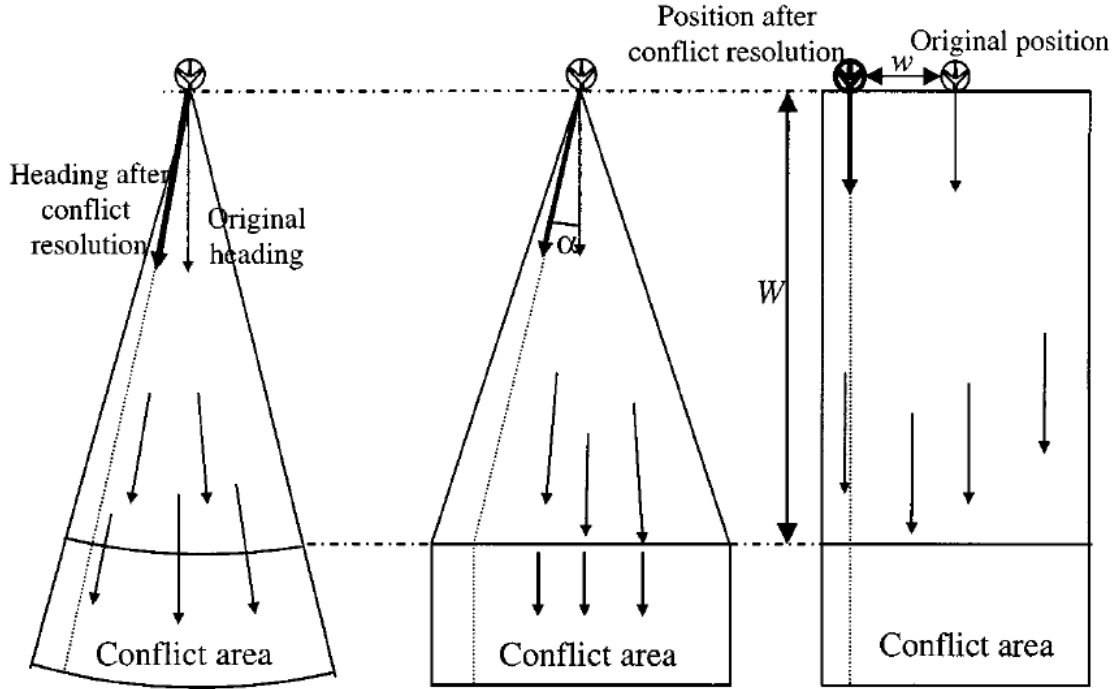


Figure 10: Heading change model vs. offset model. Left: The aircraft maneuver is a heading change. Middle: The aircraft maneuver is a heading change followed by a second heading change. Right: The aircraft maneuver is a relative position change. (figure adopted from [3])

In the lateral offset model, aircraft maneuvers change the trajectory by a lateral position change, while keeping both heading angle and speed unchanged. Although it seems unrealistic, this model is simple for analysis and simulation purposes, and it has been proven to closely approximate the heading change (fig. 10–left) and the two-stage maneuver (fig. 10–middle) models [3]. If the distance to the conflict  $W$  is much larger than the offset lateral displacement  $w$ , then  $w$  is equivalent to a heading change  $\alpha = \tan^{-1}(w/W) \approx w/W$ ; and the difference in longitudinal displacement between these two maneuver models is on the order of  $w^2/W$ , which is considered to be small. An experiment was done in [3] to study the effect of both heading change and offset models on the deviations taken by each aircraft in a conflict situation. Figure. 11 shows the comparison result of this experiment. There is

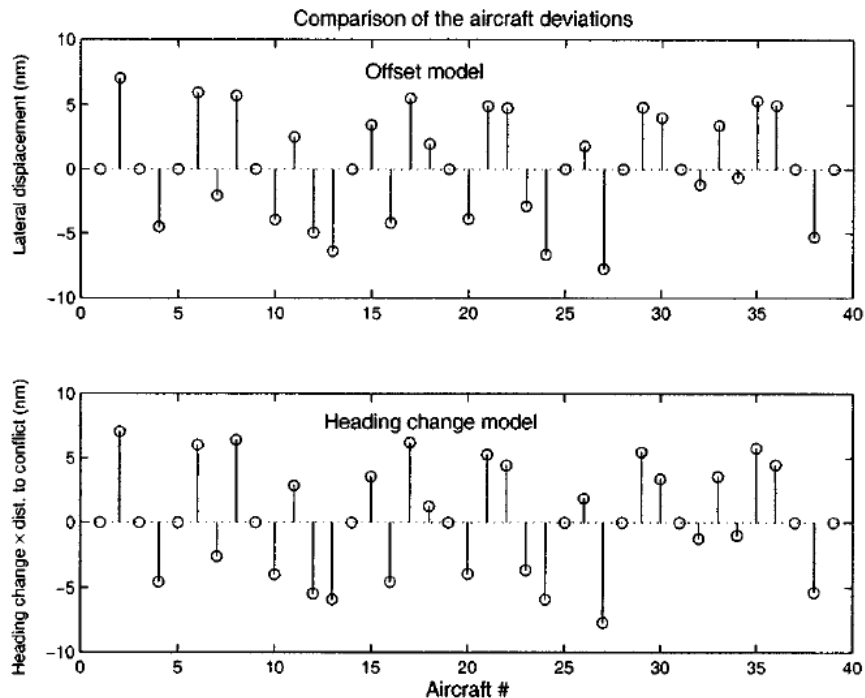


Figure 11: Aircraft deviation amplitudes under heading change and offset maneuvers. (figure adopted from [3])

no significant difference between the resulting aircraft deviation amplitudes, this proves that the lateral displacement offset model is a valid approximation to the more realistic heading model.

In this dissertation, we use the lateral displacement offset model to resolve conflicts arising from intersecting aircraft flows in a specified control volume. A similar problem was considered in [3]. However, the approach followed there allows each aircraft to make only one lateral maneuver when it enters the control volume, and these one time maneuvers are done sequentially. On the contrary, the approach presented here allows continuous time conflict detection and resolution. Two aircraft can simultaneously do a lateral maneuver to collaboratively resolve a conflict between both of them. New conflicts may hence be introduced to the system as a result of the domino effect, but the proposed rule deals with it in the same manner, until each aircraft reaches a safe path within the control volume.

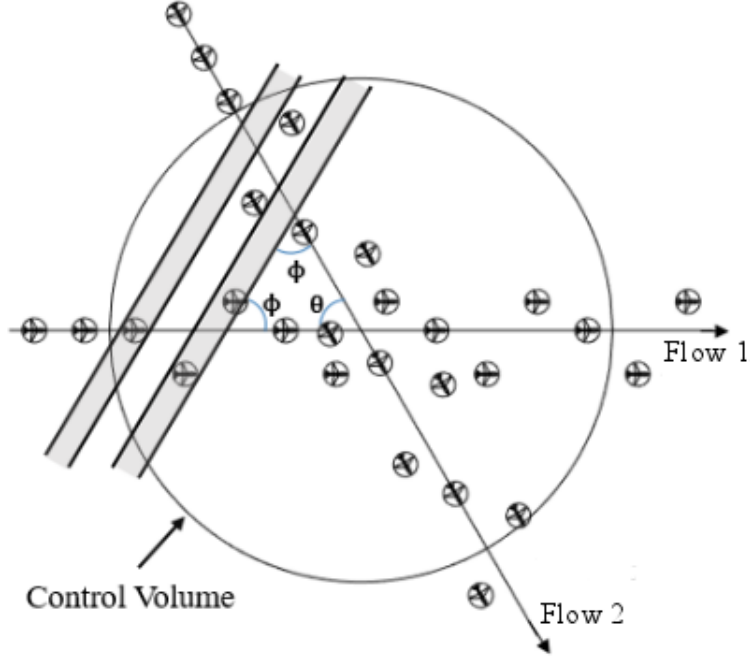


Figure 12: Aircraft fly on two flows, moving in and out a control volume. Shaded areas define a shadow in which a conflict may occur.

## 2.2 AIRCRAFT FLOW AND CONFLICT GEOMETRY

In this work, we consider the case of two aircraft flows, oriented at angle  $\theta \in (0, \pi)$  relative to each other, entering a circular volume, both flows intersect at the center of the control volume. The configuration is shown in Fig. 12, and was first introduced in [70]. Let  $\mathbf{v}_1$  be the velocity vector of aircraft in flow 1, and  $\mathbf{v}_2$  be the velocity vector of aircraft in flow 2. With the assumption that all aircraft fly at a constant speed (i.e.,  $\|\mathbf{v}_1\| = \|\mathbf{v}_2\|$ ), then, for two aircraft, one from each flow, entering the control volume at the same time instant, a conflict will occur at the center of the control volume if no avoidance maneuver has been made. Each aircraft is surrounded by a safety zone circular envelope, and the initial spacing between successive aircraft could be arbitrary but must be larger than the safety distance  $d_s$  (current enroute air traffic control rules consider  $d_s = 5$  nautical miles (nm)). Each aircraft

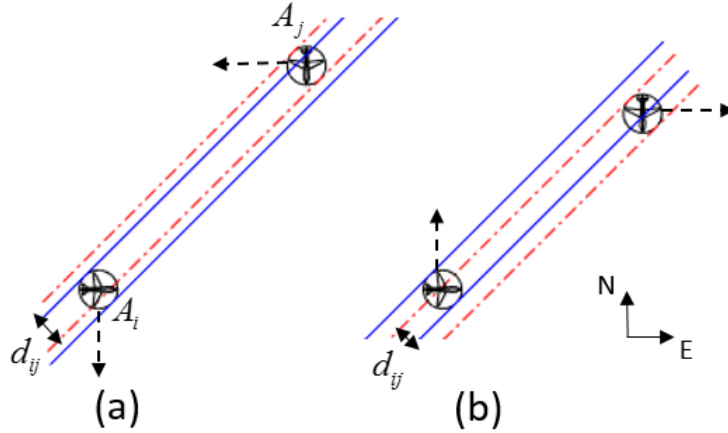


Figure 13: Two aircraft in conflict with (a) left touch, and (b) right touch. Solid line (blue) corridors are associated with eastbound aircraft, and dashed line (red) corridors are associated with southbound aircraft. Dashed arrows represent the direction of lateral maneuver taken by each aircraft to collaboratively resolve the conflict.

in the control volume has a shadow oriented at angle  $\phi = \pi/2 - \theta/2$ , the angle between the relative velocity vector  $\mathbf{v}_1 - \mathbf{v}_2$  and the velocity vector  $\mathbf{v}_1$ . The shadows are considered here facilitate the detection of future conflicts and collisions. Therefore, the shadow associated with each aircraft must confine with the safety zone and its width should equal to  $d_s$ .

A conflict is detected whenever the projected straight paths of any aircraft pair, from two different streams, lead them to a miss distance that is strictly less than  $d_s$ . In other words, whenever shadow of aircraft  $i$  from flow 1 overlaps with shadow of aircraft  $j$  from flow 2, both aircraft will be in conflict and need to take a collaborative maneuver to resolve this conflict. We define the notion of left and right touch, by which define the direction of collision will occur from aircraft left side or right side. Fig. 13 illustrates the left and right touch conflicts, and we consider a complete overlap of the flow shadows as a right touch. This notion is used in defining the conflict resolution rule, in the following section.

The particular case of two intersecting flows is considered here because the analysis for more than three intersecting flows tends to be very complicated. However, two intersecting

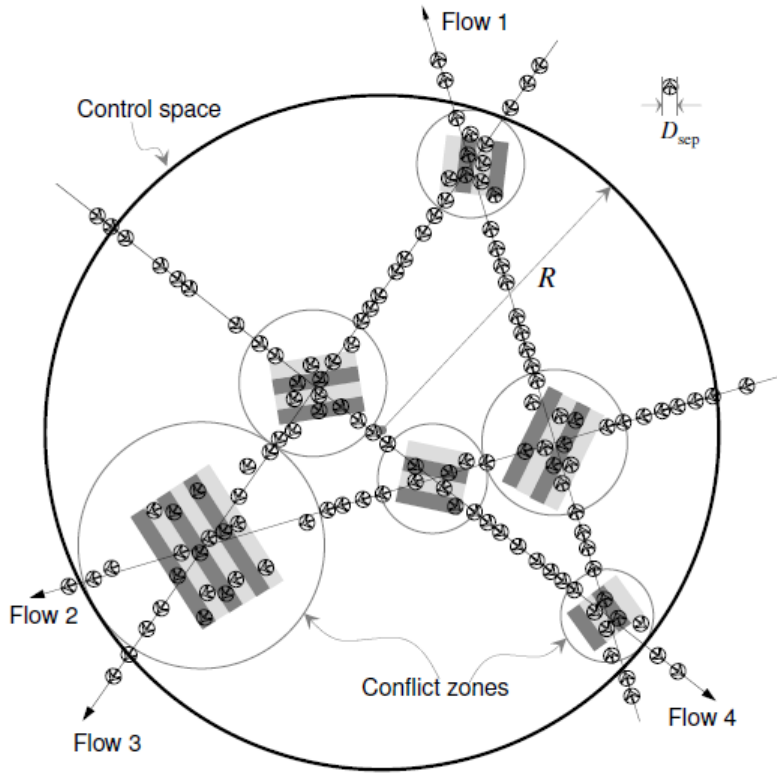


Figure 14: Conflict resolution for four intersecting flows of aircraft. The control space is divide into multiple conflict zones including pairs of intersecting flows. The conflict zone area should be designed to guarantee that aircraft approaching the point of conflict can resolve such conflict entirely, without straying outside the area.

flows can be used to build an efficient global conflict resolution system by resolving local conflicts between every pair of intersecting aircraft flows. Basically, the multi-flows conflict resolution problem can be divided into a sequence of sub-problems each involving only two intersecting flows of aircraft. Then, by using the analytically obtained results for two intersecting flows, we can obtain safe trajectories and estimate the performance for cases including more than three intersecting flows. This situation is described in figure. 14, where a control volume with four intersecting flow streams is decomposed into smaller non-overlapping

conflict zones such that the flows intersect in pairs within each zone. According to [25], a conflict zone surrounding a pair of intersecting aircraft flows is defined as the minimum area that guarantees resolving all the conflicts among the approaching pair of aircraft streams without the necessity of straying any of the aircraft outside that area. At this point we assume no parallel or anti-parallel flows, such that all flow pairs have a single intersection in the finite horizon. Thus, for  $n$  mutually non-parallel flows converging on a control volume, we have  $n - 1$  points of potential conflict along a single flow stream line, or  $n(n - 1)/2$  intersections in total. The decomposition of multiple flows is beyond the scope of this dissertation. The dissertation focuses on implementing and analyzing a new conflict resolution rule considering two intersecting aircraft flows. The following section presents the proposed collaborative decentralized conflict resolution rule. Safety and analytical convergence analysis of the proposed model are discussed in Chapter. 3.

### 2.3 CONFLICT RESOLUTION RULE

The conflict resolution scheme presented in this dissertation follows a collaborative decentralized approach, whereby all aircraft involved in the conflict do lateral maneuver in the opposite direction to the conflict touch such that the overlap in the flow shadow is reduced, and thus the conflict is resolved. For example, if two aircraft are in a left touch conflict, both aircraft make a right lateral maneuver to change their lateral position in a way that decreases the flow shadow overlapping area (fig. 13(a)), and increases the miss distance, while the nominal speed remains constant; whereas aircraft involved in a right touch conflict do left lateral maneuvers (fig. 13(b)).

Generally, an aircraft may be in conflict with more than one aircraft at a given time instance, and it may encounter both left and right touches at the same time. In this case, the offset maneuver should be toward the direction that minimizes the total number of touches experienced by this aircraft. We propose the following resolution rule for the rate of change of lateral maneuver,  $L$ , of an aircraft  $A_i$ :

$$\dot{L}_i = -c(N_{Ri} - N_{Li}) \mathbf{u}_i^\perp, \quad (2.1)$$

where  $c$  is a positive constant,  $N_{Ri}$  and  $N_{Li}$  are the number of right and left touches experienced by aircraft  $i$  respectively, and  $\mathbf{u}_i^\perp$  is a unit vector normal (clockwise direction) to the direction of flow of  $A_i$ . The rate of lateral maneuver depends on the number of collision threats on each side of the aircraft. However, if the detected touches from each side are equal, the aircraft will not take any lateral maneuvers. Every aircraft involved in the conflict will make a lateral maneuver in a direction opposing the highly congested touch direction to minimize the total number of conflicts and hereby resolve this conflict situation, where the projected aircraft shadows do not overlap. If a new conflict is created as a result of the previous maneuver (domino effect), the aircraft will follow the same rule until it reaches a safe conflict free path. We later prove that if  $\dot{L}_i = 0$  for all aircraft in the control volume, then the aircraft flow becomes safe with no further conflicts.

The following requirements must be met to ensure safe and efficient traffic management: (i) all conflicts within the control volume are resolved, whether they are direct or as a result of domino effect, and (ii) deviation of aircraft from their original trajectories, as a result of conflict resolution maneuver remains bounded. The first point ensures that all aircraft within the control volume have safe path to proceed flying without any further conflicts, and the second point is considered about the maximum deviations taken, due to resolution of detected conflicts, from the originally planned path. We use this set of conditions to prove safety and efficiency of the proposed continuous time conflict resolution procedure (2.1) in the next chapter.

### 3.0 AIRCRAFT FLOW SAFETY AND CONFLICT RESOLUTION CONVERGENCE

In this chapter, we provide the analysis of two intersecting aircraft flows system under the flow geometry and conflict resolution rule described in section 2.3. The main goal here is to prove that the proposed conflict resolution rule (2.1) will converge to a safe system of aircraft flows within a finite time. First, we study the safety of the system under the proposed conflict resolution rule and provide the conditions upon which the aircraft with the control volume converge to safe trajectories. Second, we use Lyapunov stability theorem to analytically prove the convergence of the system dynamics and define an upper bound for the convergence time.

The main focus in this chapter is given to analytical approaches to evaluate the evolution of aircraft within a control volume, defined in section 2.1. Despite the extensive work on designing conflict avoidance systems (for example, [2, 3, 13, 45–55]), only few studies have been focusing on analyzing these systems. Although simulations provide fast and efficient means to build intuition about the efficiency and safety of the conflict management systems, we believe that analytical arguments can also provide useful information about the system dynamics. However, analytical analysis usually requires simplified scenarios and assumptions. Therefore, simulations and analytical approaches must be considered as complementary tools. We use simulations in Chapter 4 to complement our analytical analysis in this chapter.

To simplify the mathematical analysis in this dissertation, we only consider two perpendicular flows, i.e.,  $\theta = \pi/2$ . Let flow 1 be an eastbound flow with  $N_e$  aircraft in the control

volume, and flow 2 be a southbound flow with  $N_s$  aircraft in the control volume. Hence, the unit vector  $\mathbf{u}_e^\perp$  for the eastbound flow will be pointing toward south, and the unit vector  $\mathbf{u}_s^\perp$  for the southbound flow will be pointing toward west.

### 3.1 SAFETY UNDER CONFLICT RESOLUTION RULE

Safety is a crucial requirement for air traffic management. In this section, we study the safety of the proposed conflict resolution resolution, and conclude the necessary conditions that guarantee convergence of the system of aircraft to safe, conflict free, trajectories.

When an eastbound aircraft  $A_{ei}$  is in conflict with a southbound aircraft  $A_{sj}$ , both aircraft follow the rules  $\dot{L}_{ei}$  and  $\dot{L}_{sj}$  respectively. If the conflict resolution rule converged to zero, such that  $\dot{L}_{ei} = \dot{L}_{sj} = 0$ , for all aircraft flying within the control volume ( $i = 1, \dots, N_e$  and  $j = 1, \dots, N_s$ ), then all aircraft will be safe and no further conflicts will occur. To prove this, consider the situation in figure. 15. Without loss of generality, assume that the right most corridor covering the control volume is occupied by an eastbound aircraft  $A_{ek}$ . Then, with  $\dot{L} = 0$  for all aircraft within the control volume, and since  $A_{ek}$  can proceed to exit the control volume from right,  $A_{ek}$  does not experience any left touches. Hence,  $A_{ek}$  will be safe, and can proceed moving without creating any conflicts. Now consider the southbound aircraft  $A_{sl}$  in the corridor on the immediate left of that for  $A_{ek}$ . Given that  $\dot{L}_{sl} = 0$  and  $A_{ek}$  does not conflict with  $A_{sl}$  (i.e.,  $N_{Lsl} = N_{Lek} = 0$ ), this implies that  $N_{Rsl} = 0$ . Therefore,  $A_{sl}$  has to be safe if  $\dot{L} = 0$  for all other aircraft. Similarly, we can iterate through all other aircraft and prove that they must be safe, as long as  $\dot{L} = 0$  for all aircraft contained within the control volume.

The previous proof can be generalized for aircraft flows oriented to each other at any relative angle,  $\theta$ , and the safety condition for the proposed collision avoidance rule (2.1) can be summarized in Lemma 3.1.1. It is also worth to mention that overlapping shadows of aircraft belonging to the same flow stream does not imply a conflict in this particular case. This is because aircraft in one flow stream are guaranteed to be separated by a distance greater than or equal to  $d_s$ , as described in Section 2.2.

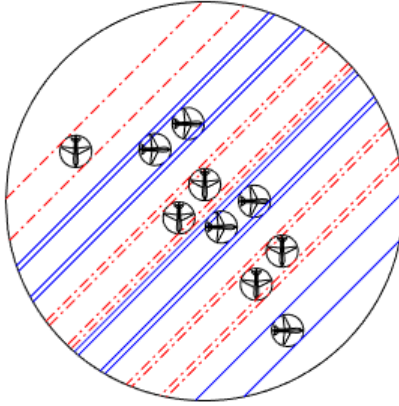


Figure 15: Safe control volume, where  $\dot{L} = 0$  for all aircraft within it.

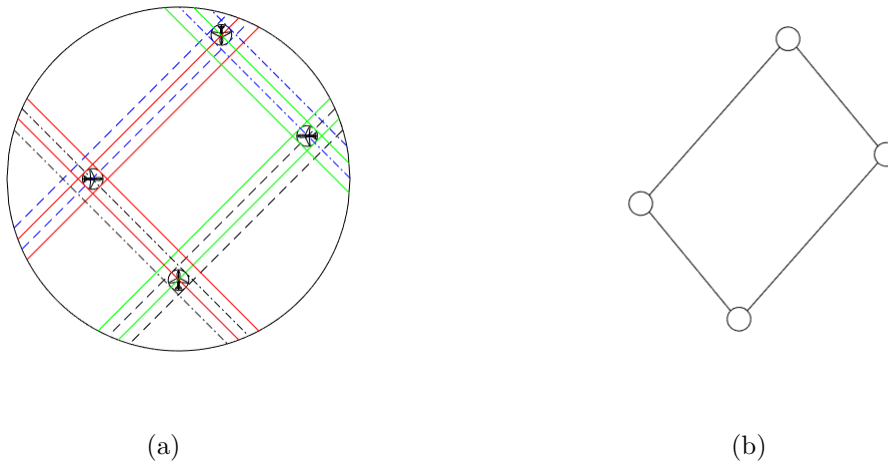


Figure 16: Conflicting aircraft with  $\dot{L} = 0$  (a), and their conflict graph representation (b).

**Lemma 3.1.1.** *For the case of intersecting aircraft flows within a specified control volume, no matter what the value of the encounter angle is, if the conflict resolution rule (2.1) converged to zero, such that  $\dot{L} = 0$ , for all aircraft flying within the control volume, then all aircraft will be safe and no further conflicts will occur, i.e., all aircraft have converged to safe trajectories.*

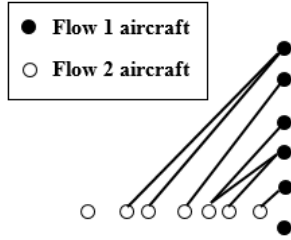


Figure 17: Conflict graph representation for the case of two intersecting aircraft flows.

One remark here is that without the constraint of aircraft flying on intersecting flows, the convergence of  $\dot{L}$  to zero does not necessarily mean convergence of aircraft to safe routes. For example, consider the situation shown in Figure. 16(a), all aircraft within that control volume have their lateral offset rate  $\dot{L}$  equal to zero, but none of them can fly safely under this configuration. The conflict graph for this situation, Figure. 16(b), shows that any path taken would lead to unresolved conflict, since none of the aircraft within the control volume belong to one group. However, under the aircraft flows configuration, no conflict can occur between pair of aircraft belonging to the same flow since they are guaranteed to be separated by at least  $d_s$  nm. Hence, an aircraft in a conflict can do a lateral maneuver and find a safe path through an unoccupied shadow corridor within the control volume or maneuver to hide in the shadow of an aircraft from the same flow in front of it (e.g., Figure. 15). A conflict graph example of two aircraft flows case is shown in Figure. 17, an aircraft can hide in the shadow of another aircraft from the same flow, thus, if  $\dot{L}$  converged to zero, this means that all aircraft have a feasible safe path.

### 3.2 CONVERGENCE OF CONFLICT RESOLUTION DYNAMICS

Systems with flying aircraft agents must be able to resolve conflicts to guarantee safety for each individual agent. Conflict resolution not only deals with finding maneuvers for each

aircraft to avoid potential collisions at any time instant, but also concerns with maintaining the whole system stability as the system evolves over time, i.e., to ensure that all aircraft will always be able to converge to feasible conflict free trajectories. This convergence aspect of conflict resolution becomes critical, particularly for large-scale systems, where the interactions among agents may be complicated, and the conflict resolution has to take care of emergent issues such as the domino effect.

Safety of aircraft flows is guaranteed when  $\dot{L}_{ei}$  and  $\dot{L}_{sj}$  converge to zero for all aircraft in the control volume, as proven in the previous section. Here, we study the convergence of system dynamics under the proposed conflict resolution rule (2.1) for two intersecting flows using Lyapunov stability theory (Appendix C).

Let  $V$  be the Lyapunov function associated with the system:

$$V \equiv \sum_{i=1}^{N_e} \sum_{j=1}^{N_s} \max \{d_s - d_{e_i s_j}, 0\} \quad (3.1)$$

where  $d_s$  is the safety distance and  $d_{e_i s_j}$  is the miss distance between aircraft  $A_{ei}$  and  $A_{sj}$ .  $V$  will be greater than zero whenever there is a conflict, and it will converge to zero when all aircraft converge to safe, conflict free, trajectories.

Lyapunov stability is determined based on conditions imposed on the values of Lyapunov function,  $V$ , and its derivative,  $\dot{V}$ . In order to derive an expression for  $\dot{V}$ , we need to obtain the derivative of  $d_{e_i s_j}$  at the first place. The miss distance changes with the change in lateral position of aircraft, and it should be increasing in response to the efforts that resolve the existing conflict. Thus, the rate of change of  $d_{e_i s_j}$  when performing a lateral maneuver (i.e.,  $\dot{d}_{e_i s_j}$ ) can be computed as:

$$\dot{d}_{e_i s_j} = \frac{1}{\sqrt{2}} \left( -\dot{L}_{ei} - \dot{L}_{sj} \right) \quad (3.2)$$

for right touch conflicts, and as:

$$\dot{d}_{e_i s_j} = \frac{1}{\sqrt{2}} \left( \dot{L}_{ei} + \dot{L}_{sj} \right) \quad (3.3)$$

for left touch conflicts. To combine the expressions in (3.2) and (3.3) into one formula, we introduce a definition for the touch function,  $\delta_{ij}$ , to describe the “direction of touch” between aircraft  $A_{ei}$  and  $A_{sj}$ :

$$\delta_{ij} = \begin{cases} 1 & \text{if right touch conflict} \\ 0 & \text{if no conflict} \\ -1 & \text{if left touch conflict.} \end{cases} \quad (3.4)$$

With the definition in (3.4), the expression for  $\dot{d}_{e_i s_j}$  in (3.2) and (3.3) can be reformulated as

$$\dot{d}_{e_i s_j} = -\frac{1}{\sqrt{2}}\delta_{ij} (\dot{L}_{ei} + \dot{L}_{sj}) \quad (3.5)$$

and the lateral maneuver rule (2.1) can be rewritten using the touch function as:

$$\begin{aligned} \dot{L}_{ei} &= -c \sum_{j=1}^{N_s} \delta_{ij} \\ \dot{L}_{sj} &= -c \sum_{i=1}^{N_e} \delta_{ij}. \end{aligned} \quad (3.6)$$

for eastbound ( $A_{ei}$ ) and southbound ( $A_{sj}$ ) aircraft respectively. Substituting (3.6) into (3.5), the rate of change of the lateral distance,  $\dot{d}_{e_i s_j}$ , can then be given by

$$\sqrt{2}\dot{d}_{e_i s_j} = -\dot{L}_{ei}\delta_{ij} - \dot{L}_{sj}\delta_{ij} \quad (3.7)$$

$$= c\delta_{ij} \left( \sum_{k=1}^{N_s} \delta_{ik} + \sum_{k=1}^{N_e} \delta_{kj} \right). \quad (3.8)$$

We use the above definitions to compute the derivative of the Lyapunov function,  $\dot{V}$ , to prove the convergence of system dynamics:

$$\begin{aligned}
\frac{\sqrt{2}}{c}\dot{V} &= -\frac{\sqrt{2}}{c}\sum_{i=1}^{N_e}\sum_{j=1}^{N_s}\delta_{ij}^2\cdot\dot{d}_{e_i s_j} \\
&= -\sum_{i=1}^{N_e}\sum_{j=1}^{N_s}\delta_{ij}^2\delta_{ij}\left(\sum_{k=1}^{N_s}\delta_{ik}+\sum_{k=1}^{N_e}\delta_{kj}\right) \\
&= -\sum_{i=1}^{N_e}\sum_{j=1}^{N_s}\delta_{ij}\left(\sum_{k=1}^{N_s}\delta_{ik}+\sum_{k=1}^{N_e}\delta_{kj}\right) \\
&= -\sum_{i=1}^{N_e}\left(\sum_{j=1}^{N_s}\sum_{k=1}^{N_s}\delta_{ij}\delta_{ik}\right)-\sum_{j=1}^{N_s}\left(\sum_{i=1}^{N_e}\sum_{k=1}^{N_e}\delta_{ij}\delta_{kj}\right) \\
&= -\sum_{i=1}^{N_e}\left(\sum_{j=1}^{N_s}\delta_{ij}\sum_{k=1}^{N_s}\delta_{ik}\right)-\sum_{j=1}^{N_s}\left(\sum_{i=1}^{N_e}\delta_{ij}\sum_{k=1}^{N_e}\delta_{kj}\right) \\
&= -\sum_{i=1}^{N_e}\left(\sum_{j=1}^{N_s}\delta_{ij}\right)^2-\sum_{j=1}^{N_s}\left(\sum_{i=1}^{N_e}\delta_{ij}\right)^2. \tag{3.9}
\end{aligned}$$

The right-hand side of (3.9) is always less than or equal to zero. Hence,  $\dot{V} \leq 0$ , and therefore,  $V$  is strictly decreasing with time when  $\dot{V} \neq 0$ . According to Lasalle's invariance principle [71],  $\dot{V}$  will converge to zero. In order that  $\dot{V} = 0$ ,  $\sum_{j=1}^{N_s}\delta_{ij}$  has to be zero for all  $i = 1, \dots, N_e$  and  $\sum_{i=1}^{N_e}\delta_{ij}$  has to be zero for all  $j = 1, \dots, N_s$ ; that is  $\dot{L}_{ei} = \dot{L}_{sj} = 0$ , for all the eastbound and southbound aircraft in the control volume ( $i = 1, \dots, N_e$  and  $j = 1, \dots, N_s$ ). Hence, according to Lemma 3.1.1, with the conflict resolution maneuver rule (2.1) and with the assumption that all aircraft within the control volume are flying as intersecting flows, all the aircraft in the control volume will find safe trajectories, and no collision will occur during their navigation, as discussed in the previous subsection.

The analysis of the Lyapunov function, can be further extended to show that the convergence time of the conflict resolution dynamics is bounded under the proposed rule. Theorem 3.2.1 defines an upper bound for the time of convergence to safe trajectories.

**Theorem 3.2.1.** *For two intersecting flows within a specified control volume, the conflicting aircraft following the collision avoidance maneuvers in (2.1) are guaranteed to converge to*

safe trajectories within a finite period of time. The convergence time,  $t_{conv}$ , of conflict resolution dynamics has an upper bound given by:

$$t_{conv} \leq \frac{\sqrt{2}N_c d_s}{c} \quad (3.10)$$

where  $N_c$  is the initial number of conflicts within the control volume before any lateral maneuver is taken,  $d_s$  is the safety distance, and  $c$  is a positive constant.

*Proof:* Since the Lyapunov function reaches its maximum value when the shadows of all the pairs of intersecting aircraft completely overlaps (i.e.,  $d_{e_i s_j} = 0$ ), then for  $N_c$  conflicts, the Lyapunov function is bounded by  $V \leq 2N_c d_s$ . In addition, from (3.9), if  $\dot{V} \neq 0$ , this means that  $\sum_{i=1}^{N_e} \left( \sum_{j=1}^{N_s} \delta_{ij} \right)^2 \neq 0$  and  $\sum_{j=1}^{N_s} \left( \sum_{i=1}^{N_e} \delta_{ij} \right)^2 \neq 0$ . Moreover, since  $\delta_{ij} \in \{-1, 0, 1\}$  is an integer, both  $\sum_{i=1}^{N_e} \left( \sum_{j=1}^{N_s} \delta_{ij} \right)^2$  and  $\sum_{j=1}^{N_s} \left( \sum_{i=1}^{N_e} \delta_{ij} \right)^2$  have to be greater than or equal to 1, and therefore  $\frac{\sqrt{2}}{c} \dot{V} \leq -2$  when  $\dot{V} \neq 0$ . Subsequently, the derivative of Lyapunov function satisfies this inequality,  $\dot{V} \leq -2c/\sqrt{2} = -\sqrt{2}c$  when  $\dot{V} \neq 0$ . Hence, based on the bounds imposed on  $V$  and  $\dot{V}$ , and according to the definition of convergence time from Lyapunov theory,  $t_{conv}$  is bounded by the expression given in (3.10). ■

This section focused on an analytical proof of convergence of system dynamics, under the proposed conflict resolution and collision avoidance rule, based on the Lyapunov theory and Lasalle's stability principle (Appendix C). The analysis conducted in this section have shown that the derivative of Lyapunov function is always less than or equal to zero and it will eventually converge to zero, according to Lasalle's invariance principle. Therefore, the value of the Lyapunov function is always positive and is strictly decreasing with time. Subsequently, it will converge to zero at equilibrium, within a finite time ( $t_{conv}$ ), when all conflicts are resolved and all aircraft converged to safe trajectories. This satisfies the Lyapunov theory stability conditions, and the system of two intersecting flows is stable in the sense of Lyapunov under the proposed conflict resolution rule in (2.1).

### 3.3 SUMMARY

This chapter focused on the mathematical analysis of the proposed automatic decentralized conflict resolution rule (2.1). The chapter started by studying the necessary conditions for safety of the intersecting aircraft flows under the proposed rule. Then, we defined a Lyapunov function to study the convergence of the conflict resolution dynamics under the proposed rule. The analysis showed that, according to Lyapunov theory and LaSalle's invariance principle, the system will converge to safe trajectories following the proposed conflict resolution rule. Moreover, we were able to find an upper bound for the convergence time, based on the Lyapunov analysis.

## 4.0 SIMULATION OF AUTOMATIC CONFLICT RESOLUTION

Simulations provide fast and efficient means to build intuition about the efficiency and safety of the conflict management systems. In this chapter, we use numerical simulations of aircraft traffic under the prescribed conditions in Chapter 2.1 to gain more insight about flow structure after resolution maneuvers, and to numerically verify the convergence and safety of the conflict resolution rule (2.1). Also, the simulation results will allow us to complement our analytical conclusions obtained in Chapter 3 by considering different scenarios.

In the simulations presented in this chapter, we consider a circular control volume of radius ranging between 30 nm and 36 nm, and aircraft safety separation distance ( $d_s$ ) of 5 nm. We consider three different simulations with aircraft flows that have different encounter angles ( $\theta = 90^\circ, 60^\circ$ , and  $45^\circ$ , respectively). For each case, we study the convergence of aircraft to safe trajectories, net magnitude of performed lateral deviations, and the behavior of Lyapunov function and its derivative over time.

### 4.1 CONVERGENCE TO SAFE TRAJECTORIES

Figure. 18 shows simulation of two aircraft flows that are orthogonal to each other ( $\theta = \pi/2$ ). The figure shows the sequence of lateral conflict resolution maneuvers for eastbound and southbound aircraft. Figures. 19 and 20 show the maneuvers sequence for two flows whose encounter angle equals to  $60^\circ$ , and  $45^\circ$  respectively. Through Figures 18–20, it is shown that every aircraft involved in a conflict (overlapping of two flow shadows) takes a lateral maneuver to resolve this conflict. This collaborative action may cause other conflicts (the domino effect), for example, the transition from figure. 18(d)–(e)–(f). These newly born

conflicts will be resolved in the same collaborative manner, until all aircraft converge to safe trajectories without any future conflicts that may appear later as they proceed flying with their nominal speed, e.g., figure. 18(l). Note that, aircraft with the same direction of flow can safely have overlapping shadows since they are strictly separated by a distance that is larger than or equal to  $d_s$ .

It can be seen that, when aircraft converge to safe trajectories (Figure. 18(l), 19(h), and 20(j)),  $\dot{L} = 0$  for aircraft in the control volume, this verifies the analytical results in Section 3.1. Figure. 21 shows the summation of the magnitude of  $\dot{L}$  for all the aircraft,  $\sum_{i,j} \|\dot{L}\| \forall i \in \text{flow 1, and } j \in \text{flow 2}$ , in the control volumes studied in Figures. 18, 19, and 20. It is shown that conflict avoidance procedure at one time instance may introduce more other conflicts due to the domino effect, reflected as an increase in the value of  $\sum_{i,j} \|\dot{L}\|$ . However, the conflict resolution procedure continues to solve the newly born conflicts until no further lateral maneuver is needed, i.e.,  $\dot{L}_{1i} = \dot{L}_{2j} = 0$  for all aircraft ( $i \in \text{flow 1, and } j \in \text{flow 2}$ ) within the control volume. Thus a safe trajectory is achieved for all the aircraft. Also, it is worth noting that finding a safe and bounded solution (i.e.,  $\dot{L} = 0$  for all aircraft flying within the control volume) was done within a finite bounded time.

We studied the convergence time of 100 simulation sequence instances for each of the simulated flows, where each sequence instance has a different set of initial conditions (position, separation between aircraft, and number of conflicts). Table 2 shows the average convergence time for  $\theta = 90^\circ, 60^\circ$ , and  $45^\circ$  at two different values of the constant  $c$ . It can be noted that the convergence time decreases with increasing the value of  $c$ . This is in agreement with the definition of the time of convergence in theorem 3.2.1. The results also show that the convergence time is bounded and is relatively short compared to the nominal speed of flow. Hence, the system is guaranteed to converge to safe trajectories without imposing any of the aircraft within the control volume to the risk of collision.

The simulations in this section have proved the convergence of the proposed conflict resolution rule to safe trajectories within a finite period of time. Basically, whenever a conflict situation is detected, all of the involved aircraft start to maneuver collaboratively towards the direction that minimize the number of touches/conflicts. As a result of these collaborative maneuvers new conflicts may emerge, but as the system evolves with time,

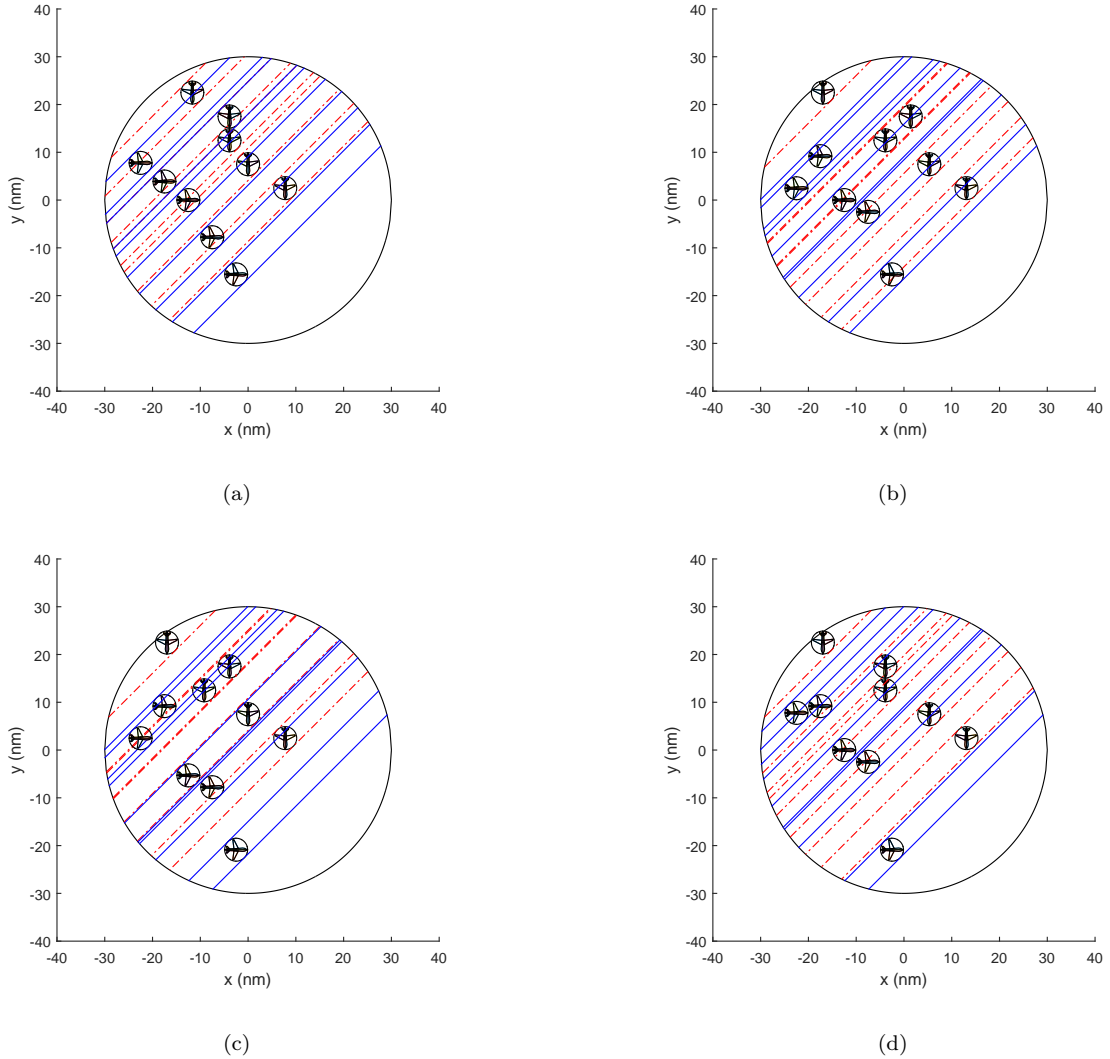
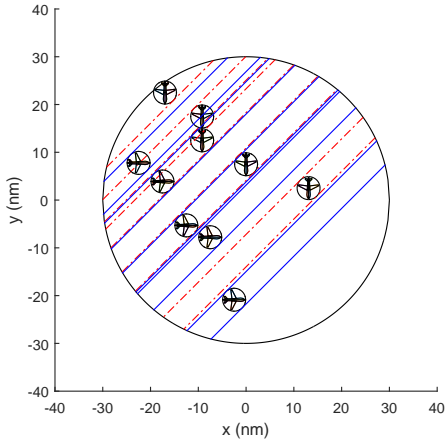
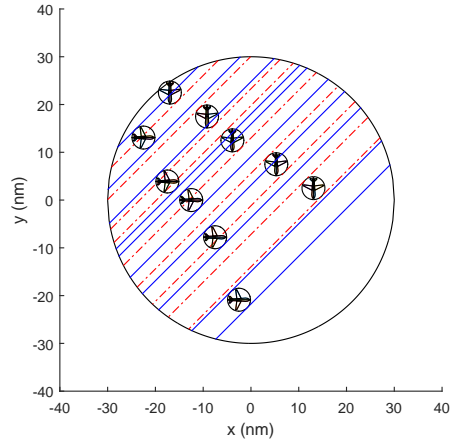


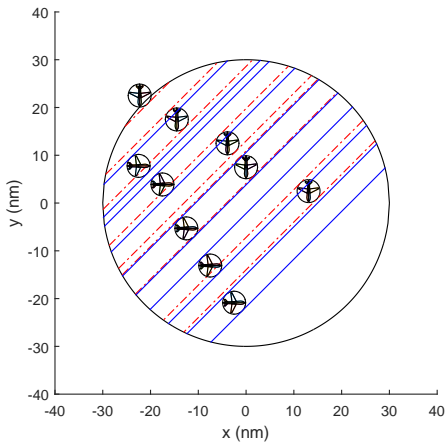
Figure 18: Conflict resolution maneuver sequence with lateral maneuvers ( $\theta = 90^\circ$ ), at the 1st (a) – 4th (d) time steps. Solid (blue) lines represent the shadows of eastbound aircraft, and dashed (red) lines represent the shadows of southbound aircraft.



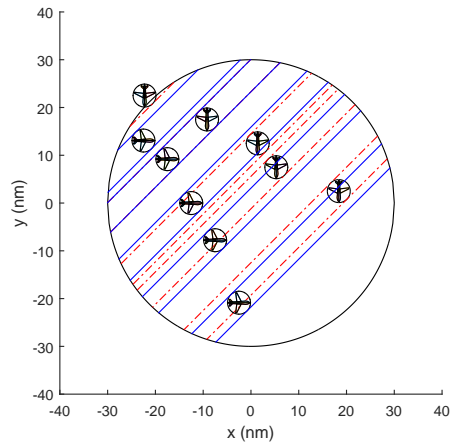
(e)



(f)

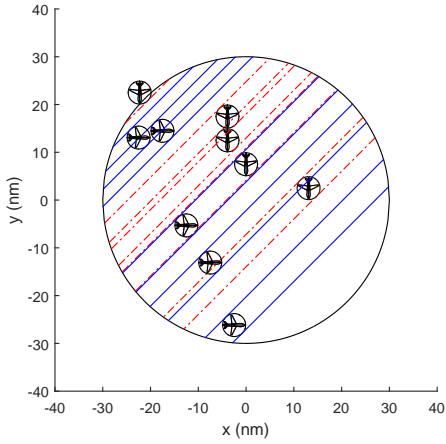


(g)

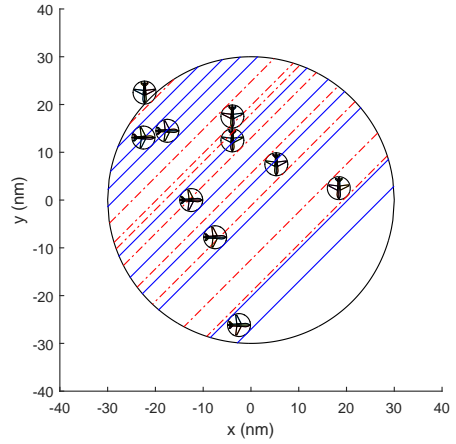


(h)

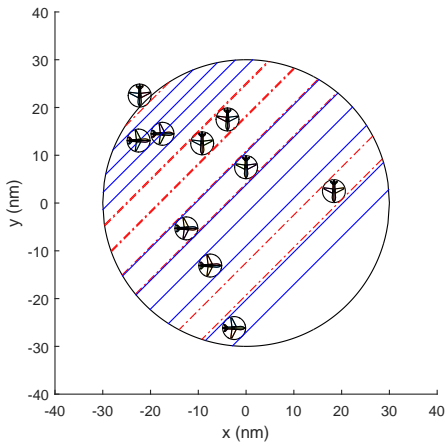
Figure 18: (cont.) Conflict resolution maneuver sequence with lateral maneuvers ( $\theta = 90^\circ$ ), at the 5th (e) – 8th (h) time steps. Solid (blue) lines represent the shadows of eastbound aircraft, and dashed (red) lines represent the shadows of southbound aircraft.



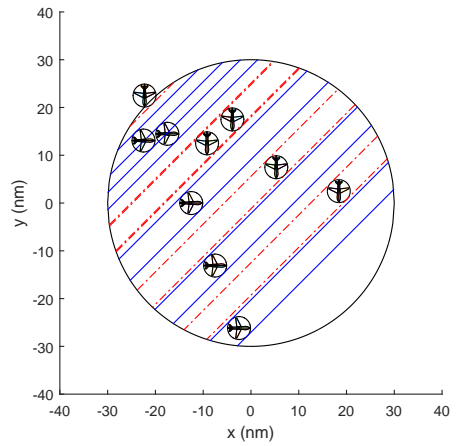
(i)



(j)

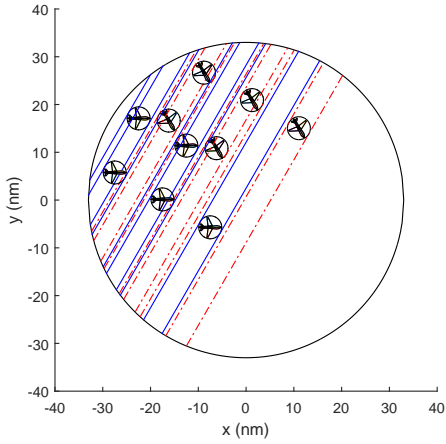


(k)

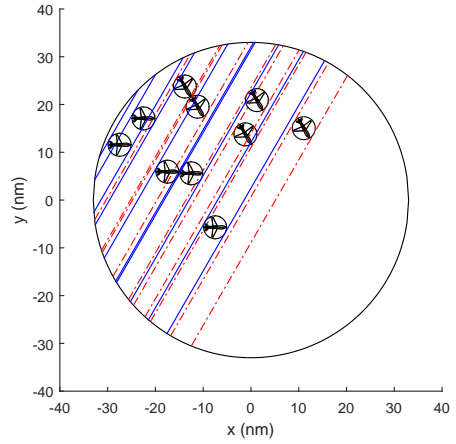


(l)

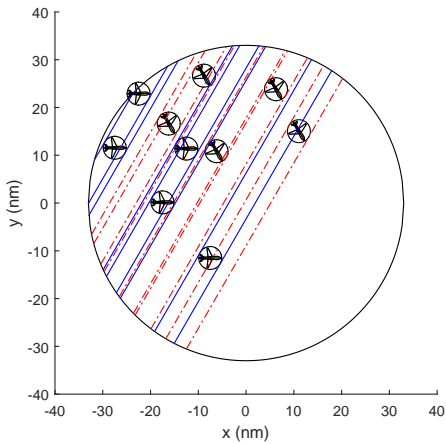
Figure 18: (cont.) Conflict resolution maneuver sequence with lateral maneuvers ( $\theta = 90^\circ$ ), at the 9th (i) – 12th (l) time steps. Solid (blue) lines represent the shadows of eastbound aircraft, and dashed (red) lines represent the shadows of southbound aircraft.



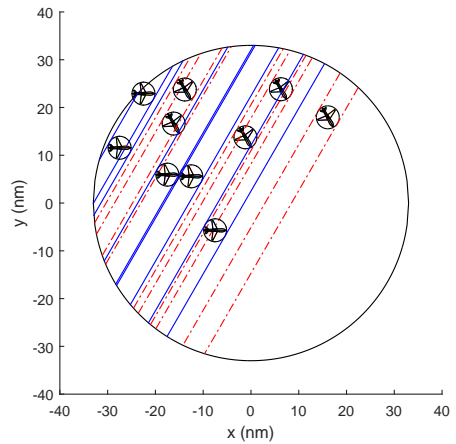
(a)



(b)

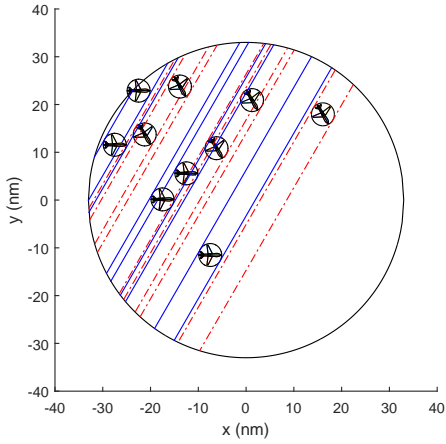


(c)

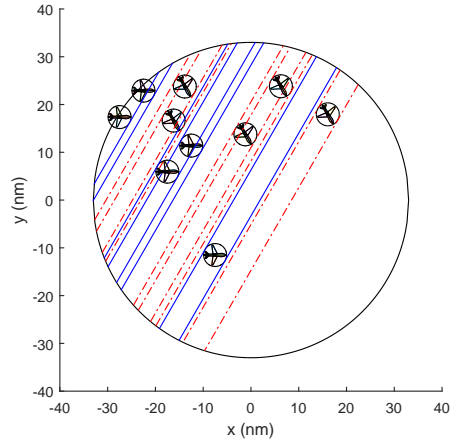


(d)

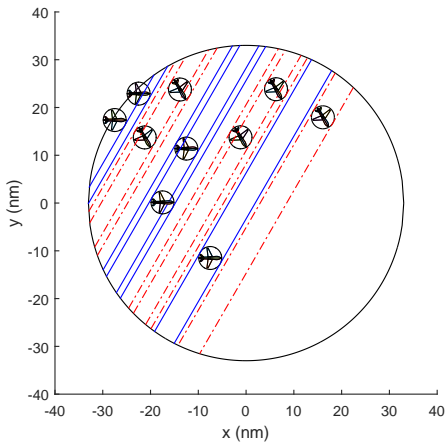
Figure 19: Conflict resolution maneuver sequence with lateral maneuvers ( $\theta = 60^\circ$ ), at the 1st (a) – 4th (d) time steps. Solid (blue) lines represent the shadows of flow 1 aircraft, and dashed (red) lines represent the shadows of flow 2 aircraft.



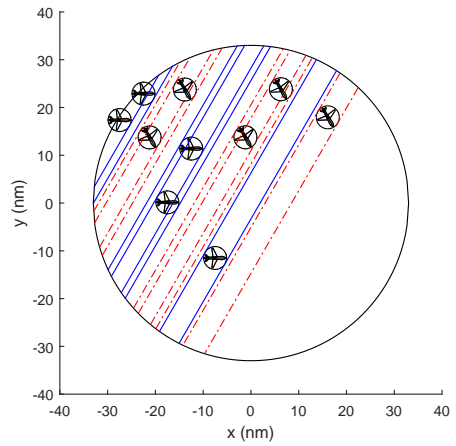
(e)



(f)

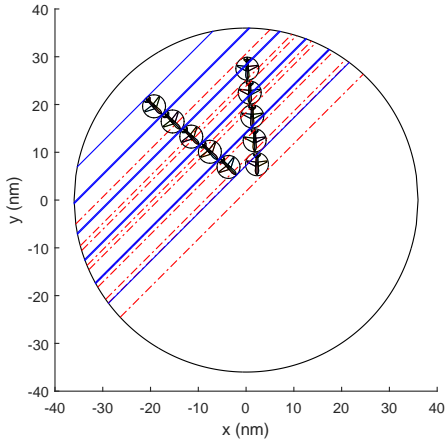


(g)

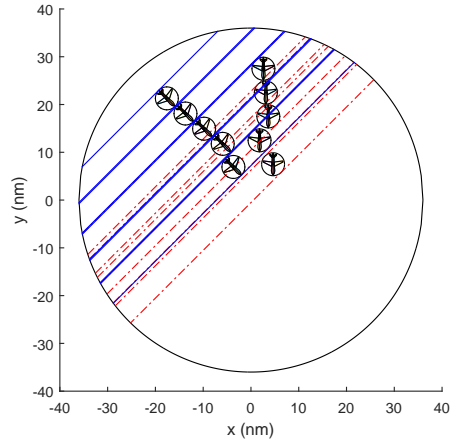


(h)

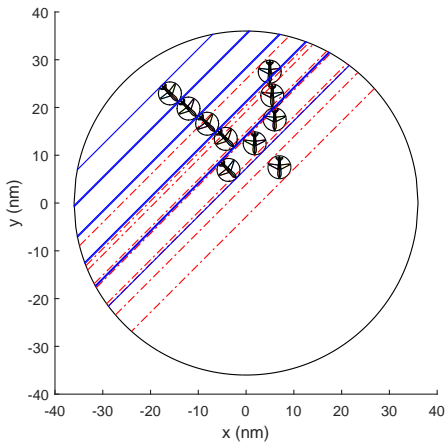
Figure 19: (cont.) Conflict resolution maneuver sequence with lateral maneuvers ( $\theta = 60^\circ$ ), at the 5th (e) – 8th (h) time steps. Solid (blue) lines represent the shadows of flow 1 aircraft, and dashed (red) lines represent the shadows of flow 2 aircraft.



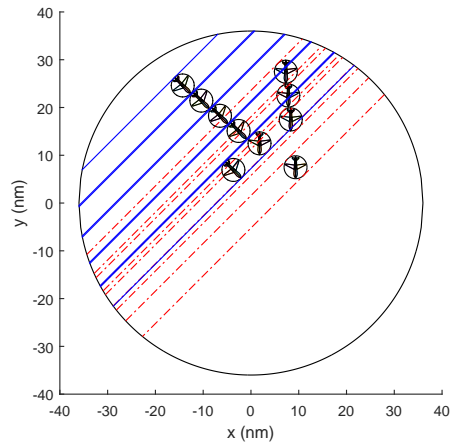
(a)



(b)

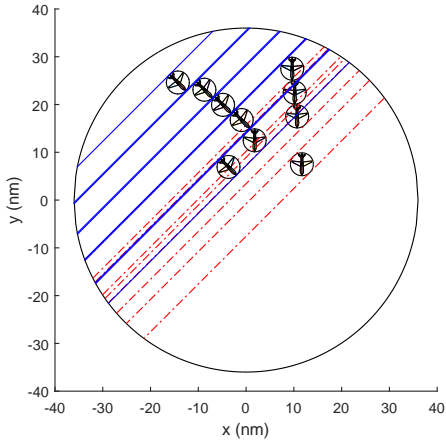


(c)

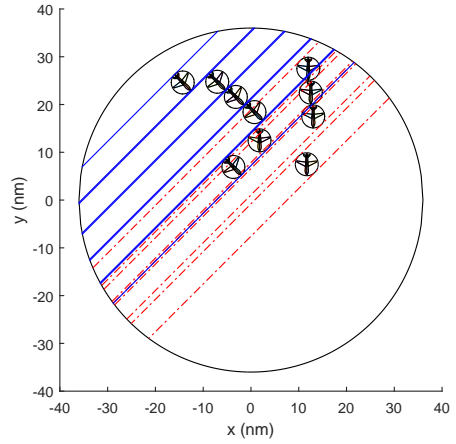


(d)

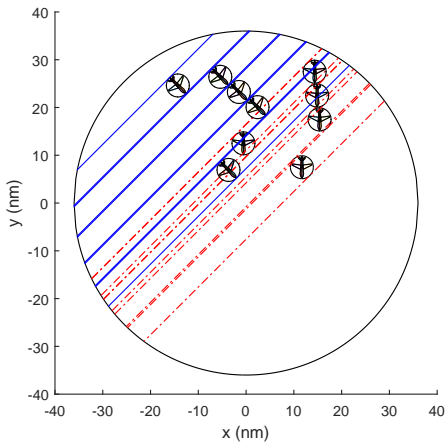
Figure 20: Conflict resolution maneuver sequence with lateral maneuvers ( $\theta = 45^\circ$ ), at the 1st (a) – 4th (d) time steps. Solid (blue) lines represent the shadows of flow 1 aircraft, and dashed (red) lines represent the shadows of flow 2 aircraft.



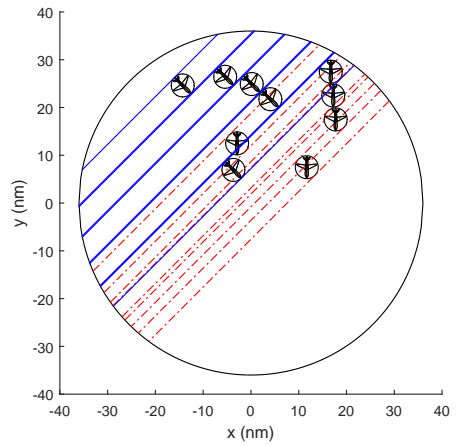
(e)



(f)



(g)



(h)

Figure 20: (cont.) Conflict resolution maneuver sequence with lateral maneuvers ( $\theta = 45^\circ$ ), at the 5th (e) – 8th (h) time steps. Solid (blue) lines represent the shadows of flow 1 aircraft, and dashed (red) lines represent the shadows of flow 2 aircraft.

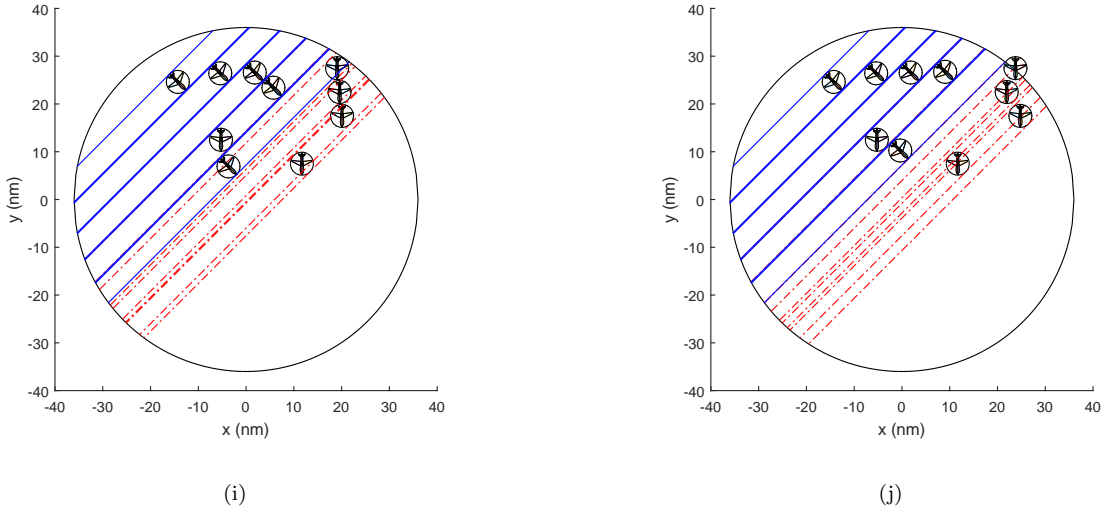
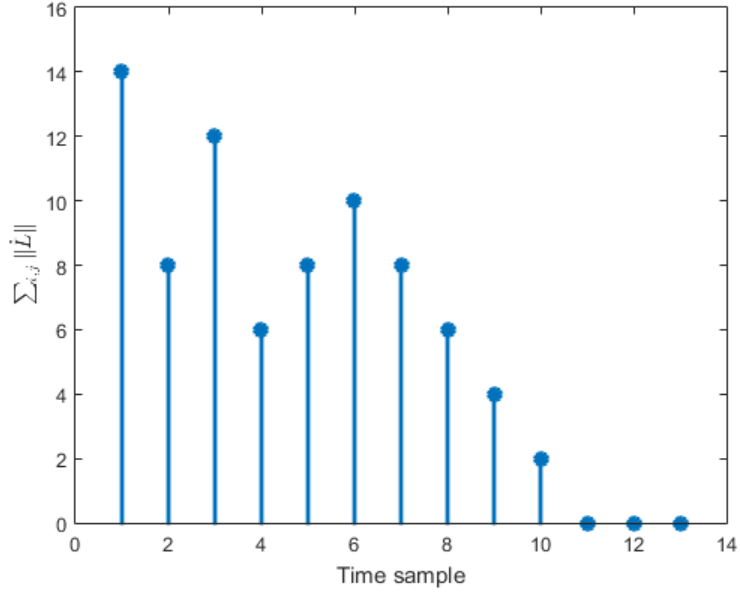


Figure 20: (cont.) Conflict resolution maneuver sequence with lateral maneuvers ( $\theta = 45^\circ$ ), at the 9th (i) and 10th (j) time steps. Solid (blue) lines represent the shadows of flow 1 aircraft, and dashed (red) lines represents the shadows of flow 2 aircraft.

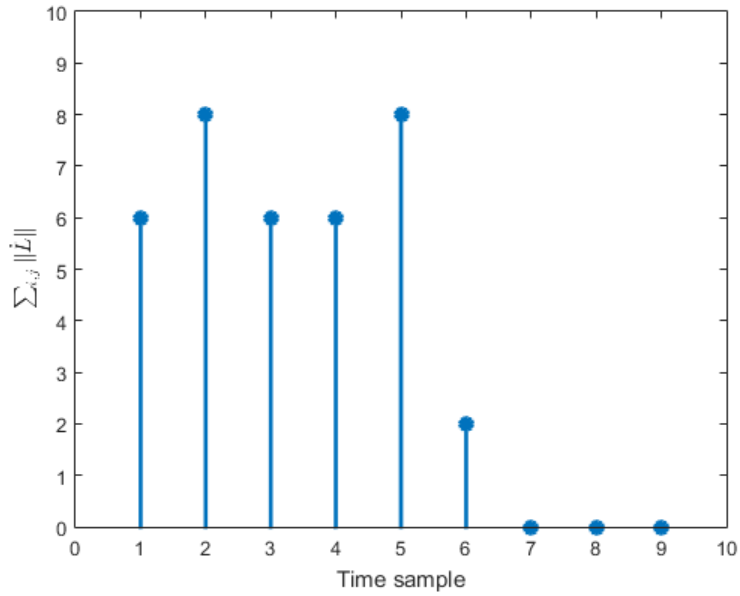
any newly born conflict is resolved collaboratively following the same rule. Aircraft finally can converge to an unoccupied corridor in the control volume or hide in the shadow of an aircraft belonging to the same flow. According to lemma 3.1.1 and the analyses in Section 3.2, convergence to safe trajectories ( $\dot{L} = 0$ ) is guaranteed as long as aircraft fly in flows regardless what the value of the encounter angle ( $\theta$ ) is.

## 4.2 MAGNITUDE OF LATERAL DEVIATIONS

In this section we study another aspect of the system. We study the bound of aircraft lateral deviation from their nominal trajectory as a result of following the conflict resolution rule to avoid any potential collisions. Since the system of intersecting aircraft flows is guaranteed to converge to safe trajectories within a bounded finite time, the magnitude of lateral deviations is also bounded. Figure. 22, Figure. 23, and Figure. 24 show three examples

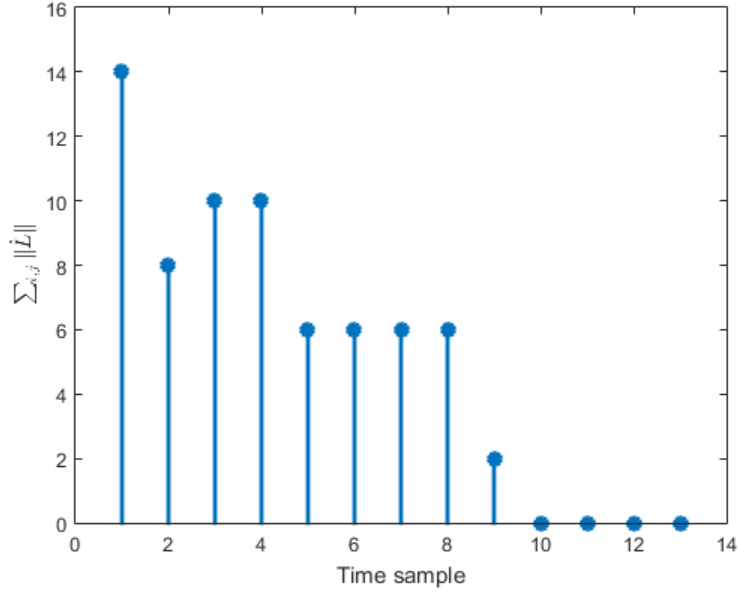


(a)



(b)

Figure 21: Summation of the magnitude of  $\dot{L}$  for all the aircraft in the control volume flying in flows with encounter angle is (a)  $90^\circ$ , (b)  $60^\circ$ , and (c)  $45^\circ$ ,  $c = 1$ .



(c)

Figure 21: (cont.) Summation of the magnitude of  $\dot{\mathbf{L}}$  for all the aircraft in the control volume flying in flows with encounter angle is (a)  $90^\circ$ , (b)  $60^\circ$ , and (c)  $45^\circ$ ,  $c = 1$ .

Table 2: Average convergence time. ( $\Delta t \equiv$  sampling time)

Encounter angle	Convergence time	
	$c = 0.5d_s \tan(\phi)$	$c = 0.75d_s \tan(\phi)$
$\theta = \pi/2$	$15.1\Delta t$	$11.8\Delta t$
$\theta = \pi/3$	$9.5\Delta t$	$6.2\Delta t$
$\theta = \pi/4$	$11\Delta t$	$7.5\Delta t$

of lateral deviations of two selected aircraft, one from each of the analyzed flow directions. The maximum deviation is 5.3 nm, 5.8 nm, and 2.35 nm for flows whose  $\theta = 90^\circ, 60^\circ,$  and  $45^\circ,$  respectively. The lateral deviations are bounded as time evolve, and in comparison to results presented in [3], these deviation magnitudes are less than the deviations resulted under their decentralized conflict resolution rule. This bound is expected since under the geometry and structure of the studied system, one aircraft can experience a maximum of two left or right touches. Hence, the rate of lateral maneuver at a given time instance is limited by  $2c,$  as previously described in Chapter 2. The net change of each aircraft lateral position is shown in Figures. 25, 26, and 27, for the three studied encounter angles  $\theta = 90^\circ, 60^\circ,$  and  $45^\circ,$  respectively. These deviations are still bonded and lie within the control volume. Therefore, the lateral maneuvers resulted from resolving conflicts do not have a severe effect on the nominal, originally planned, trajectories, and subsequently, the proposed conflict resolution rule does not affect the cost of operation severely to compromise for safety. In addition to aforementioned simulation analysis, we studied the lateral deviations maneuvered by 100 aircraft constituting flows with different encounter angles. Figure. 28 shows a histogram of the magnitude of lateral devotions taken by those 100 aircraft while resolving conflicts and avoiding potential collisions. It is shown than 96% of the lateral maneuver deviations have a magnitude that is less than 6 nm. These results prove that the conflict resolution control procedure (2.1) leads to safe trajectories using bounded lateral maneuvers for aircraft within the control volume, and this proves bounded convergence of the control system.

### 4.3 CONVERGENCE OF THE LYAPUNOV FUNCTION

Convergence of the Lyapunov function and its derivative over time give us more intuition about the convergence of system dynamics under the proposed conflict resolution control rule. Beside the mathematical analysis in Section 3.2, simulation analysis enables us to visualize the system convergence over time and the constraints and conditions imposed by Lyapunov theory and Lasalle’s stability principle. Figures. 29–31 show the change in Lyapunov function  $V$  over time, for the three simulation scenarios, on which intersecting flows have encounter

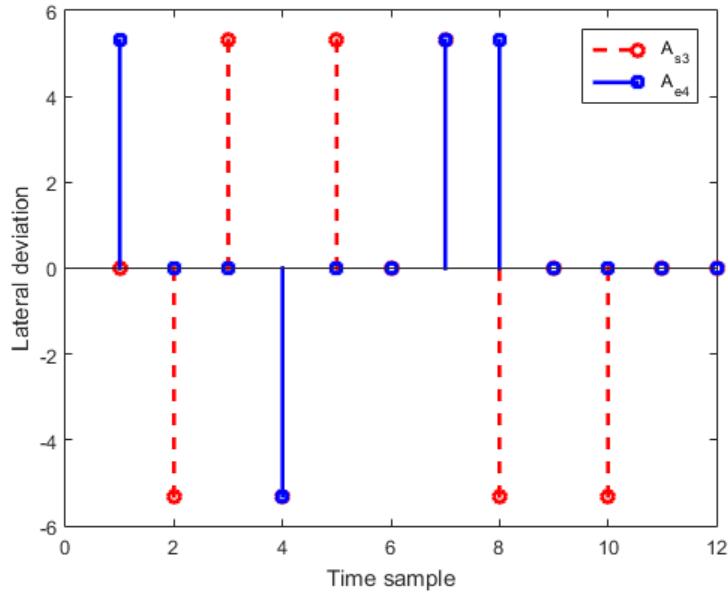


Figure 22: Example of aircraft lateral deviations for two perpendicular flows, eastbound (solid) and southbound (dashed).

angle  $\theta = 90^\circ, 60^\circ$ , and  $45^\circ$ , respectively. It is clear that, under all the studied encounter angles,  $\dot{V}$  is always less than or equal zero (i.e., it is negative along the trajectories of the system), and it converged to zero when the aircraft did the lateral maneuvers to resolve all the conflicts, and achieved safe, conflict free trajectories. This verifies the Lasalle's stability principle. Also, since  $\dot{V}$  is always negative,  $V$  is monotonically decreasing with time and it has converged to zero when all aircraft converged to safe trajectories, this is numerically verified in Figure. 29–31 as well as analytically proven in Section 3.2. This is in agreement with the stability conditions of the Lyapunov theory and our mathematical analysis and inferences in Section 3.2. These results numerically confirm the convergence of our conflict resolution model dynamics, and confirms that the proposed system is stable in the sense of Lyapunov.

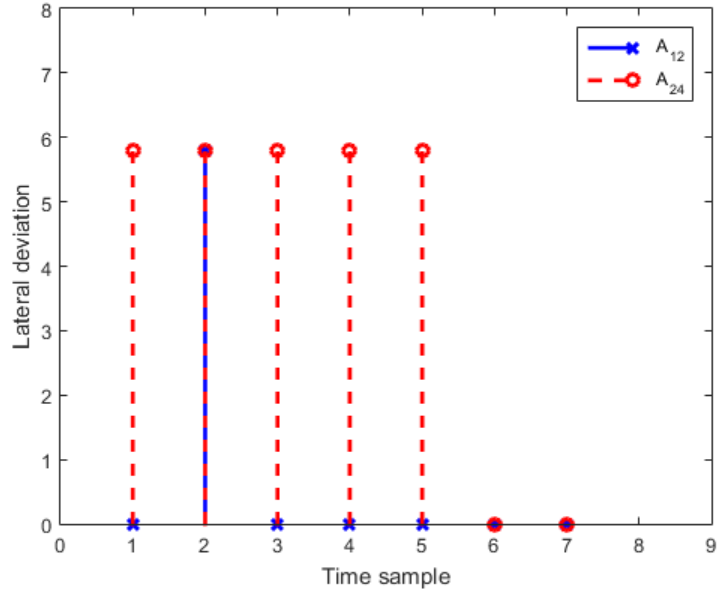


Figure 23: Magnitude of lateral deviation with time for two intersecting flows,  $\theta = 60^\circ$ .

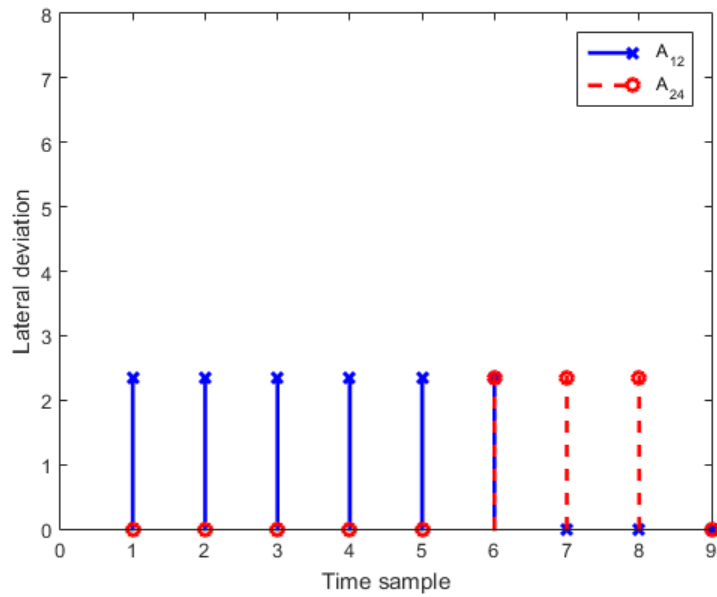


Figure 24: Magnitude of lateral deviation with time for two intersecting flows,  $\theta = 45^\circ$ .

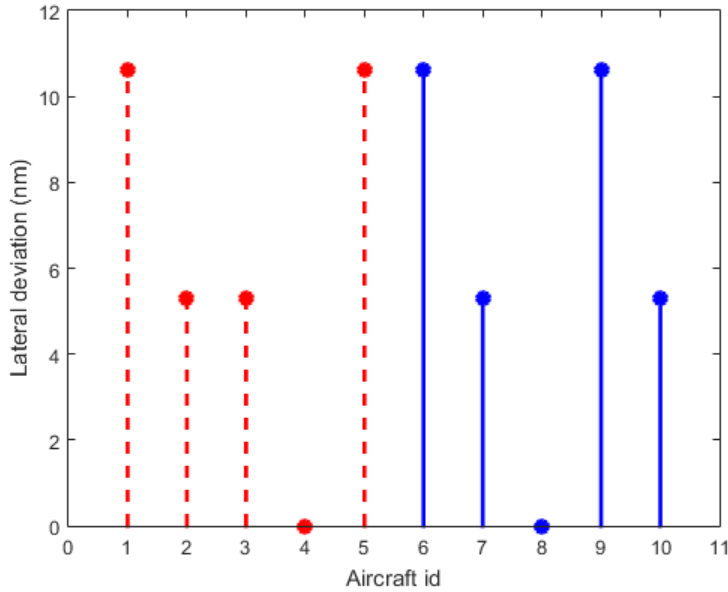


Figure 25: Net magnitude of lateral deviations of the aircraft forming flows with an encounter angle  $\theta = 90^\circ$ .

#### 4.4 SUMMARY

In this chapter, we have considered the simulation of aircraft conflict resolution in a specified control volume, under the proposed decentralized conflict resolution and collision avoidance rule. Simulations are important to gain more insight into the system dynamics and help to understand system behavior for situations that could be hard to analytically derived. This chapter simulated the lateral maneuvers of aircraft on intersecting flows at three different encounter angles to study the evolution of each aircraft trajectory over time. Simulations were provided to verify the validity of the proposed control rule and the convergence of the conflict resolution dynamics. This was visualized by tracking the change of aircraft trajectories when conflicts are detected and resolved, and by studying the numerical change of the Lyapunov function and its derivative with time. The simulated maneuvers were bounded. Additionally, the simulated aircraft reached safe trajectories that were close to their originally

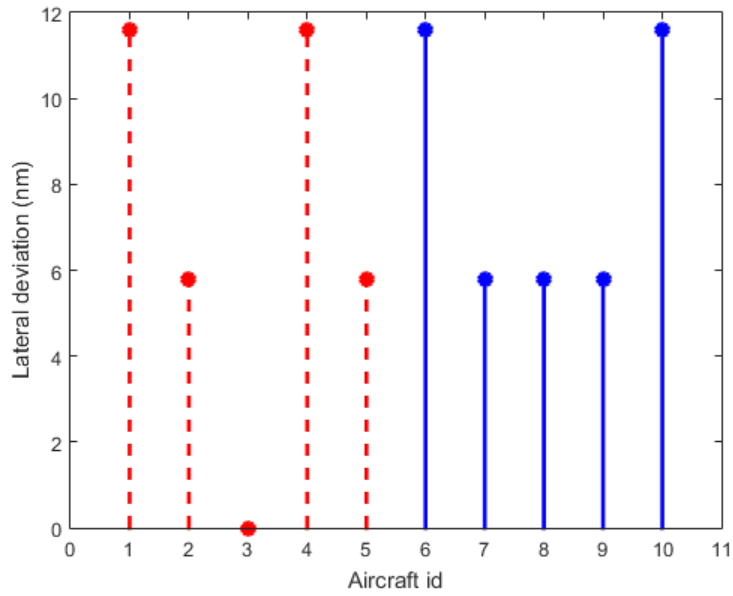


Figure 26: Net magnitude of lateral deviations of the aircraft forming flows with an encounter angle  $\theta = 60^\circ$ .

planned trajectory. Thus, the simulation results confirm the analytically derived conclusions and numerically proved the safety, and efficiency of the proposed collaborative decentralized conflict resolution rule.

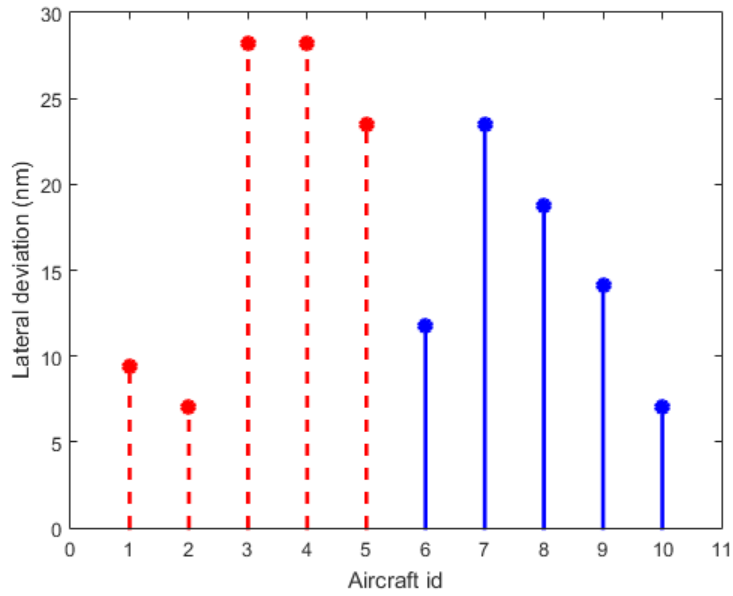


Figure 27: Net magnitude of lateral deviations of the aircraft forming flows with an encounter angle  $\theta = 45^\circ$ .

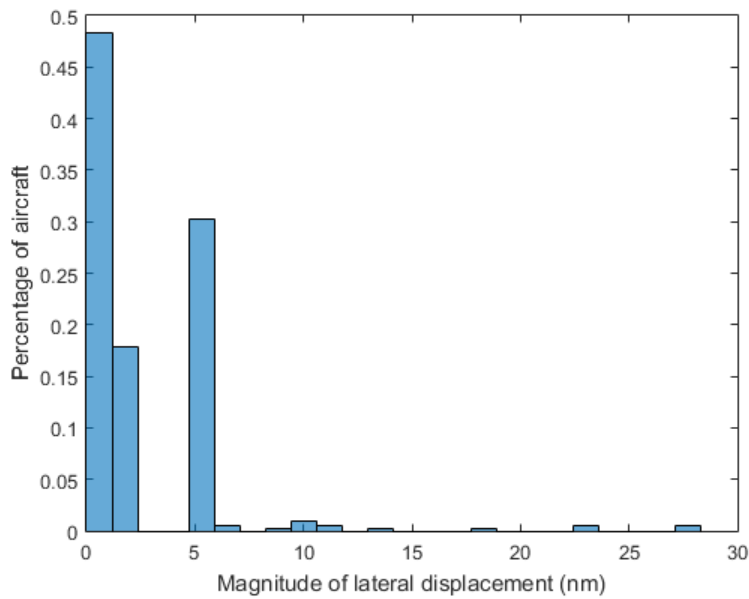
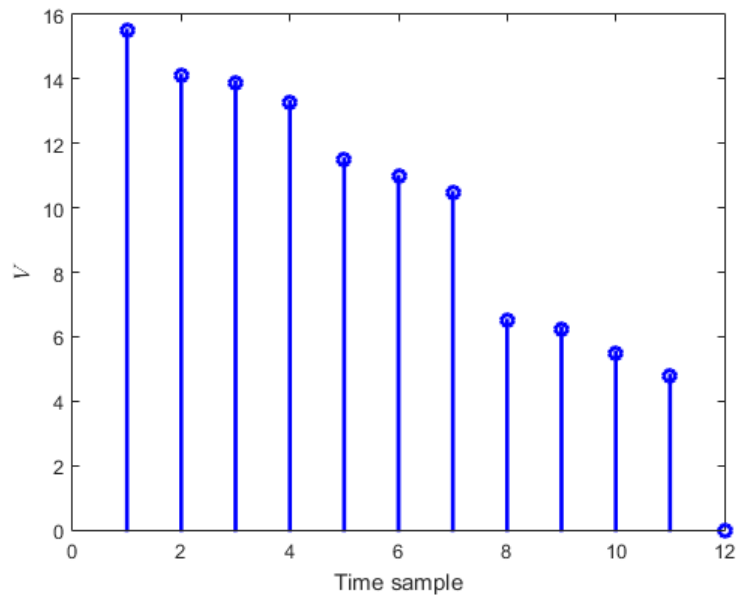
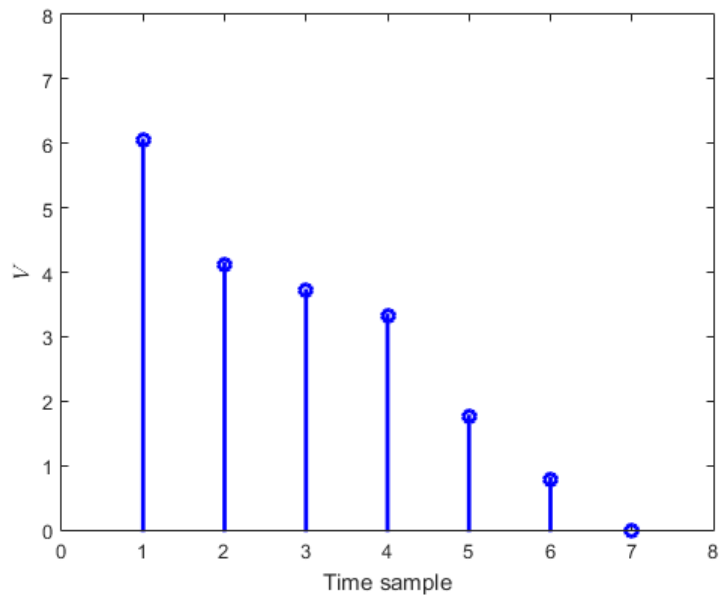


Figure 28: Histogram of lateral deviations for 100 aircraft.



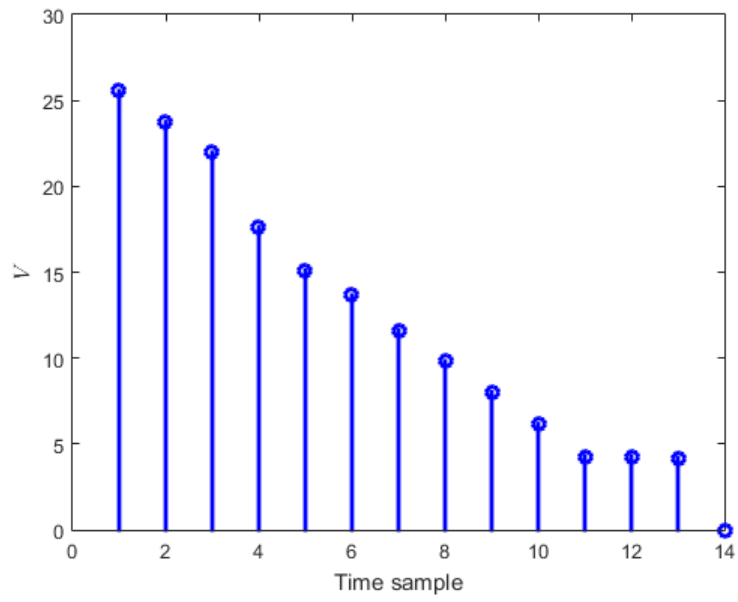
(a)

Figure 29: Lyapunov function  $V$  for two intersecting flows at  $\theta = 90^\circ$ .



(a)

Figure 30: Lyapunov function  $V$  for two intersecting flows at  $\theta = 60^\circ$ .



(a)

Figure 31: Lyapunov function  $V$  for two intersecting flows at  $\theta = 45^\circ$ .

## 5.0 HUMAN-MACHINE CO-LEARNING FOR CONFLICT RESOLUTION

Recent studies have shown that humans and machines are able to mutually adapt their behavior, intentions, and communications. In this cooperative scheme, machines are being partners, and not a tool, for humans. This collaboration can be modeled in a collaborative differential game framework. In this shared responsibility, authority, goals framework, the overall performance of the mission is increased.

In this chapter, we propose development of a conflict resolution controller that is based on the human-machine co-learning framework. Both human pilot and robot pilot are assumed to follow lateral maneuvers to collaboratively resolve an existing conflict between their aircraft. However, the rate of maneuver is not known in prior to the collaboration. The robot controller should adapt its output to human behavior in order to achieve the common goal of the collision avoidance. We introduce a model of human as an optimal controller, and propose an algorithm to estimate the human control criteria given his observed actions.

### 5.1 INTRODUCTION

Collaboration is essential in many situations of Human-Robot interaction (HRI) [72]. Most of the work on human-robot interaction take an approach focusing on interactive communications, such as providing cognitive support, personalized chats, or pet-like affective therapy. On the other hand, little research attention has been given to goal-oriented collaborative activities between human and robot. In this kind of human-robot interaction, human agent is actively involved in the joint task instead of just being a passive beneficiary of robot assistance.

Humans and robots have complementary advantages. Humans have excellent cognitive skills and are superior, over computers, in awareness and decision making. Therefore, robot controller can be designed to learn from humans and seek their help in unstructured environments [72]. On the other hand, robots are capable of performing repetitive, high-load tasks tirelessly and with high precision. This is because, robots are equipped with precise sensors, computers, and powerful actuators. Subsequently, an efficient human-robot collaboration (HRC) system should assign heavy loads to robots and achieve more robust performance in unstructured environments by maximizing the complementary capabilities of humans and robots [72]. In other words, varying the level of autonomy of a human-robot systems allow maximizing the strengths of both the robot and the human. This enables the system to optimize the problem solving skills of a human and effectively balance that with the speed and physical dexterity of a robotic system. An intelligent robot, in a collaborative environment, should be able to learn how to control a task from its human partner and later complete these tasks autonomously with human intervention only when requested by the robot [73].

Human-robot collaboration schemes have been studied in applications such as search and rescue, construction, space applications, and healthcare (e.g., [4, 73–80]). Moreover, the introduction of HRI operating systems has enabled teams of humans and robots to work collaboratively on missions that are well defined and narrow in scope. Generally, a team is defined as a small number of agents, with complementary skills, who share a common goal and approach for which they hold themselves mutually accountable. The same applies for human-robot teams collaborating to achieve a common goal. Efficient human-robot collaboration requires a common plan for all collaborating agents. To gain a joint intention, robot agents need to know the intentions of the other team members. Based on that knowledge a robot can plan its own control criteria that will eventually lead to satisfaction of the joint intention by reaching the shared goal for the collaborative agents. In human-robot collaboration it will be usually the human agent who sets that goal, while it is the mission of the robot agent to assist the human. Subsequently, to plan a control action, one agent needs information about the actions and intention of the other agent as well as knowledge about the abilities of all partners and about the current state of the system. If one of the partners acts in a manner

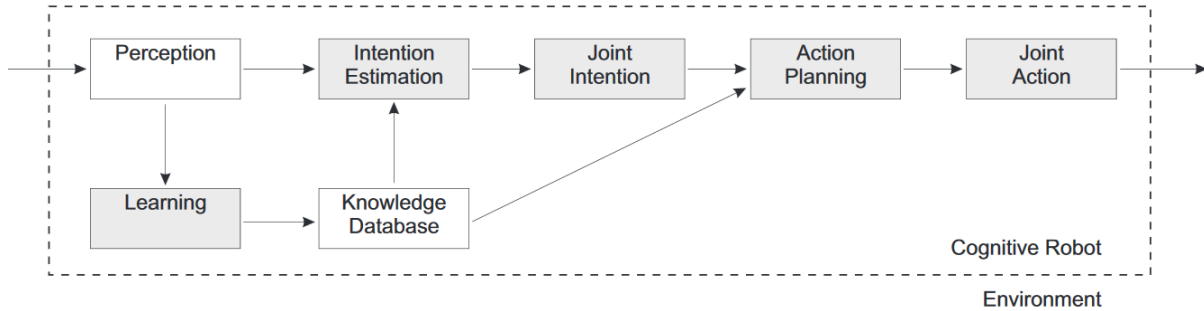


Figure 32: Robot mechanisms leading to joint action. (figure adopted from [4])

that was not predicted by the other agent, actions have to be re-planned. Accordingly intention needs to be re-estimated all the time as system states and intentions change over the time.

However, in many situations robots are still not “intelligent” enough to collaborate with human beings in a natural and effective way. Therefore, in order to attain successful collaboration, a good understanding of intrinsic properties and human intentions is required.

Figure 32 shows the internal mechanism of a robot that enables it to achieve a joint action in an HRC system. Robot uses sensors to observe the surrounding environment and its partner actions. The observed data are then used by the robot to learn and expand its own knowledge, then to gain an understanding of the current state of the environment and the partner, and to estimate the intention of the partner. The intention of the robot becomes to assist (or, cooperate with) the human to reach his or her intended goal. Then, a set of actions are taken to satisfy the perceived intention and according to an action plan. Of course, actions taken by either of the collaborating agents, or both, would lead to change in the system’s current state. This should not be a problem for the robot, since it has a closed-loop feedback system that enables it to observe the new states, and the actions of itself and others. Therefore, sensors and perception mechanisms have to be chosen and implemented individually depending on the purpose and desired functionality of the robot. Also, the knowledge database has to be programmed and trained, according to the desired functionality.

## 5.2 MODELING OF HUMAN-ROBOT INTERACTIONS FOR AIRCRAFT CONFLICT AVOIDANCE

When designing a human-machine interaction (HMI) system, the nature of the task and how it constrains the choice of possible actions for each agent and their interactions must be considered as design parameters. The control actions of each agent are then defined through a cost function that needs to be minimized. This enables the use of tools from Game Theory, optimal control and nonlinear adaptive control in order to derive control actions of the two interacting agents and their adaptation [81].

Neuroscience studies have shown that human interact with different situations by minimizing error ( $e$ ) and effort ( $u$ ) [82]. This can be modeled as an optimal controller that minimizes a cost function:

$$J(t) \equiv \alpha e^2(t) + \beta u^2(t), \quad \alpha, \beta > 0. \quad (5.1)$$

Moreover, when the dynamics states of the system change, the human is able to adapt his control criteria (e.g., force, trajectories, etc.) to minimize such cost function [83, 84].

In a collaboration tasks, there is a priori assignment of rule between agents, but spontaneous actions evolve based on the interactions history [81, 85]. However, an uneven distribution of subtasks or roles during the task may exist. Hence, synchronization between human and machine should be done to maintain the shared objective of the problem.

Generally, in collaboration games, both agents jointly try to develop a consensual solution to solve a problem or achieve a common goal [81, 86]. A cost function for each agent in such system could be given as

$$J_i(t) = \alpha_i e_i^2(t) + \beta_i u_i^2(t) + (\gamma_i \hat{e}_j^2(t) + \sigma_i \hat{u}_j^2(t)), \quad i \neq j; \quad i, j = 1, 2; \quad \text{and } \alpha, \beta, \gamma, \sigma \geq 0. \quad (5.2)$$

It is clear in (5.2) that each agent minimizes its own and the partner's error and control input. The value of the scaling parameters ( $\alpha, \beta, \gamma, \sigma$ ) defines the weight given by each agent to his and his partner's error and control input, and defines how much agents care about optimizing their control input. The challenge here is to learn the human's optimal control criteria in response to the current scenario.

In the collision avoidance problem, we assume that both human and machine controller will follow a lateral displacement control criteria to resolve a potential conflict between their aircraft. However, the rate of lateral deviation maneuvers is unknown, and must be negotiated and learned during the course of collaboration (i.e., human and robot should adapt their control to resolve the existing conflict). Mainly, the robot control should learn the rate from his human partner. We also assume that the human pilot and robot pilot are able to estimate the position of each other, and therefore can compute an accurate estimate of the miss distance ( $d_{ij}$ ) between their aircraft. Therefore, the common goal for both the human and robot agent is to do lateral maneuvers that maximizes the miss distance between their aircraft. In other words, for a successful collaboration, the following condition must be met, for two conflicting aircraft:

$$d_{ij} \geq d_s, \text{ for } i = 1, 2; j = 1, 2; i \neq j. \quad (5.3)$$

The lateral maneuver dynamics of one agent, who is collaboratively resolving a conflict, can be defined as

$$p_i(t + \Delta t) = p_i(t) + v_i(t)\Delta t \quad (5.4)$$

$$v_i(t + \Delta t) = v_i(t) + u_i(t)\Delta t \quad (5.5)$$

where  $i = 1, 2$ ,  $p_i(t)$  is the lateral position of aircraft  $i$ , at time  $t$ , relative to its position where the conflict was initially detected,  $v_i(t)$  is the velocity of aircraft  $i$  at time  $t$ , and  $u_i(t)$  is the pilot  $i$  acceleration control input at time  $t$ . Since the later maneuvers are taken to maximize the miss distance between the conflicting aircraft to satisfy the common goal of the developed HRC system, we can define the error to the target as

$$e_i(t) = p_i(t) - p_i^* \quad (5.6)$$

where  $p_i^*$  is a target position that satisfies the conflict resolution goal (5.3). From the definition in (5.6), we can use the change of lateral position dynamics (5.4) to define the error dynamics for each agent as

$$e_i(t + 1) = e_i(t) + v_i(t)\Delta t, \quad i = 1, 2. \quad (5.7)$$

Since both the human and robot pilots collaborate to solve a shared conflict, the coupled error dynamics for the whole conflict resolution systems with two aircraft can be defined as

$$e(t) = e_1(t) + e_2(t). \quad (5.8)$$

This definition of the coupled error function is equivalent to the following expression

$$e(t) = \begin{cases} d_{ij}(t) - d_s & \text{if } d_{ij}(t) < d_s \\ 0 & \text{if } d_{ij}(t) \geq d_s \end{cases} \quad (5.9)$$

where  $d_{ij}(t)$  is the miss-distance between the collaborating aircraft at time  $t$ . It is clear that the expressions in (5.6), (5.8) and (5.9) model the conflict between two aircraft as an error function that decreases with efforts that are trying to resolve the conflict. Minimizing that error would be done by maximizing the miss distance and, therefore, resolving the existing conflict.

The system dynamics equations in (5.4), (5.5), and (5.7) can be used to construct a state space dynamical model for each agent. The state vector associated with each agent can be defined as  $x_i(t) = [e_i(t), v_i(t)]^T$ ,  $i = 1, 2$ . Since both agents are working to collaboratively resolve a shared conflict, we can use a coupled system dynamics, whose state vector can be given as

$$x(t) = [e(t), v_1(t), v_2(t)]^T \quad (5.10)$$

where  $e(t)$  is the coupled error dynamics, as defined in (5.8). Therefore the dynamics equation for the coupled system can be given as:

$$x(t+1) = \begin{bmatrix} e(t+1) \\ v_1(t+1) \\ v_2(t+1) \end{bmatrix} = \begin{bmatrix} e(t) + v_1(t)\Delta t + v_2(t)\Delta t \\ v_1(t) + u_1(t)\Delta t \\ v_2(t) + u_2(t)\Delta t \end{bmatrix}. \quad (5.11)$$

The standard state space representation of system dynamics has the form

$$x(t+1) = Ax(t) + B_1u_1(t) + B_2u_2(t) \quad (5.12)$$

where  $A$  is the system dynamics matrix,  $B_i$  is the input matrix associated with agent  $i$ ,  $i = 1, 2$ , and  $u_1(t)$  and  $u_2(t)$  are the control input for agent 1 and agent 2, respectively. The coupled system dynamics (5.11) can be represented in the standard form as

$$x(t+1) = \begin{bmatrix} 1 & \Delta t & \Delta t \\ 0 & 1 & 0 \\ 0 & 0 & 1 \end{bmatrix} x(t) + \begin{bmatrix} 0 \\ \Delta t \\ 0 \end{bmatrix} u_1(t) + \begin{bmatrix} 0 \\ 0 \\ \Delta t \end{bmatrix} u_2(t). \quad (5.13)$$

Equation (5.13) models the coupled system dynamics of collaborative conflict resolution into a standard state space dynamical model. Theoretically, this model can be used into an optimal control framework to get the optimal control inputs that minimize the error. However, since one of the agents is a human, we cannot design his control criteria. Fortunately, this model matches with human control model given in (5.1), where we have an error function that needs to be minimized. Since human beings are superior in analysis and decision making, an efficient control criteria for the robot agent can be obtained by learning from the human agent while cooperating with him to maximize the miss-distance (minimize the error) under the proposed dynamical model (5.13). In the next section, we model the conflict resolution model as an optimal control problem under the presented dynamics (5.13), then we try to estimate the human agent control criteria (equivalently his/her intentions).

### 5.3 ESTIMATION OF HUMAN CONTROL CRITERIA

To resolve a potential conflict, both the human and robot controller are assumed to employ optimal control strategies with a quadratic cost function. Since human and machine collaboratively control the system, we can model the collaborative system using the linear quadratic regulator (LQR) framework [87]. A regulation problem with coupled system dynamics (e.q.(5.13)) can be formulated as

$$\begin{aligned} \{u^*, x^*\} &= \underset{u, x}{\operatorname{argmin}} \sum_{n=1}^{\infty} x_n^T Q x_n + u_n^T R u_n \\ \text{s.t.} \quad &x_{n+1} = A x_n + B_h u_{hn} + B_r u_{rn}, \end{aligned} \quad (5.14)$$

where  $Q \geq 0$  and  $R > 0$  are the weight matrices associated with the states  $x_n$  and control inputs  $u_n = [u_{hn}^T, u_{rn}^T]^T$  respectively,  $u_{hn}$  and  $u_{rn}$  are the human and robot controller control inputs respectively,  $A$  is the coupled system dynamics matrix, and  $B_h$  and  $B_r$  are the input matrices associated with the human and robot inputs, respectively. The optimal human control that minimizes (5.14) is obtained as:

$$u_{hn} = -Kx_n, \quad (5.15)$$

where  $K$  is the optimal state feedback (Kalman) gain, and is given by:

$$K = (B^T P B + R)^{-1} B^T P A, \quad (5.16)$$

with  $P$  being the unique positive-semidefinite solution to the discrete-time algebraic Riccati equation (ARE)

$$A^T P A - P - (A^T P B) (B^T P B + R)^{-1} B^T P A + Q = 0. \quad (5.17)$$

Equations (5.15)–(5.17) give the optimal control criteria of human that minimize the LQR problem (5.14). However, to be able to simulate this control response, either  $K$ , or  $Q$  and  $R$  should be known. Unfortunately, this human control process is done internally in the human’s brain and these parameters are inaccessible, only the actions can be measured. Given the human control actions, few studies have been proposed to determine a cost function that would generate that control in some optimal sense. For example, Priess *et. al.* [88] used the measured control and formulated an inverse LQR problem to estimate the weighting matrices,  $Q$  and  $R$ , that would reproduce that control output, and applied the results on a seated-balance model of the human subject.

In this section, we propose an algorithm to directly estimate the human control parameters by directly estimating the Kalman gain  $K$  instead of estimating  $Q$  and  $R$  and solving the ARE equation, as previously developed in [88]. We continue this section, by first reviewing the inverse LQR solution, and then present our algorithm for direct estimation of the Kalman gain.

### 5.3.1 The Inverse LQR Problem

The objective of the inverse LQR problem is that, given an estimate of  $K_h$ , the Kalman gain of the human agent, an updated estimate of  $Q$  and  $R$  such that  $Q > 0$ ,  $R > 0$  and  $K_h$  satisfies:

$$K_h = (B^T P B + R)^{-1} B^T P A \quad (5.18)$$

where  $P$  is the unique positive-semidefinite solution to the discrete-time ARE (5.17). This problem can be formulated as a convex optimization problem, subject to linear matrix inequality (LMI):

$$\begin{aligned} (\hat{Q}, \hat{R}, \hat{P}, \hat{\delta}) &= \underset{Q, R, P, \delta}{\operatorname{argmin}} \delta^2, \text{ such that} & (5.19) \\ P &\geq 0 \\ A^T P A - P - A^T P B K_e + Q &= 0 \\ B^T P A - (B^T P B + R) K_e &= 0 \\ I &\leq \begin{bmatrix} Q & 0 \\ 0 & R \end{bmatrix} \leq \delta I \end{aligned}$$

where  $K_e$  is the full-state feedback gain matrix determined via a system identification method from the experimental data [88], and  $\delta$  is the condition number to ensure numerical stability [88, 89]. Equation (5.19) is a convex optimization problem with strictly convex objectives [90]. Therefore, if a feasible solution exists that minimizes the objective function, it will be unique [88, 90]. However, if no exact solution exists, then an approximation  $\hat{K}$  minimizing the residual error between  $\hat{K}$  and  $K_e$  can be found via a gradient descent algorithm [88].

This formulation can be used to get an estimate of the system weighing matrices  $Q$ , and  $R$ . However, solving the optimization problem (5.19) either under the LMI constraints or using gradient descent, may not be computationally efficient, and is not suitable for online estimation of the human control criteria during a critical, time sensitive task, such as aircraft conflict resolution. Therefore, we propose a direct estimate of the human's feedback gain  $K$  through an online least-square minimization framework.

### 5.3.2 Least-Squares Estimation of Human Feedback Gain

This section presents our main contribution in this chapter. We use a least-squares framework to estimate the human's feedback gain  $K$  given an observed measurements of his/her control criteria. Having a good estimate of  $K$  means that we can estimate humans control behavior. Therefore, a robot agent can use this gain,  $K$ , to learn and predict its human partner actions.

Assuming that we have a sensory measurement of humans input for  $N$  time samples, we can combine state estimation with the human input in a least square formulation to get an estimate of the Kalman gain as follows:

$$K = -\mathbf{u}_h (\mathbf{x}^T \mathbf{x})^{-1} \mathbf{x} \quad (5.20)$$

where  $\mathbf{x} = [x_1^T, \dots, x_N^T]^T$  is the state history,  $\mathbf{u}_h = [u_1, \dots, u_N]^T$  is the human agent control history, and  $N$  is the total number of observed time samples. The estimate of the  $K$  can be updated online whenever a new observations of the system states and human agent control input are available by just updating the parameters in (5.20).

Due to the time variance nature of the human's actions, the control criteria of the human agent could be non-stationary with time. This may affect the learned robot, because as time evolves, the estimate of the human agent feedback gain may no longer be valid if we used all the actions history to get an updated gain  $K$ . To overcome this issue, we divide the observed response period into short segments of length  $w$ . Then, we obtain an estimate  $K$  for each segment. Under this windowing approach, an estimate of  $K$  can be obtained by:

$$K(N+1, w) = -\mathbf{u}_h(N, w) (\mathbf{x}^T(N, w) \mathbf{x}(N, w))^{-1} \mathbf{x}(N, w) \quad (5.21)$$

where  $\mathbf{x}(N, w) = [x_{N-w}^T, \dots, x_N^T]^T$  is the state history for the most recent segment of length  $w$ ,  $\mathbf{u}_h(N, w) = [u_{N-w}, \dots, u_N]^T$  is the human agent control history for the most recent segment of length  $w$ , and  $N$  is the total number of observed time samples. It is also clear that, the Kalman gain can be estimated at every time step or every few time samples periods. The algorithm uses the most recent state and human action observations to get an updated estimate of the human's control criteria  $K$ . Knowing the state feedback of the human, will therefore enable us to estimate his action and train a robot controller that is able to collaborate with him in resolving airborne conflicts.

Equations (5.20) and (5.21) provide a direct method to estimate the human feedback without the need of prior knowledge of the weighing matrices  $Q$  and  $R$ . Unlike the inverse LQR formulation, this estimation criteria can be applied online to estimate the human actions and directly train a robot controller. Moreover, the proposed algorithm does not require solution of a constrained optimization problem. Beside these advantages, the proposed algorithm in (5.21) accounts for the possible non-stationarity in the human control criteria without increasing the cost of computation.

We conducted a human experiment to test out human-in-the-loop conflict resolution algorithm. To train a robot controller, we used the estimate of human feedback gain using (5.20) and (5.21). Thus, the robot pilot can collaboratively assist the human pilot to resolve an existing conflict between their aircraft. The experimental setup and results for robot learning and conflict resolution is presented in the next section.

## 5.4 EXPERIMENTAL RESULTS

To test the proposed Human-Machine collaborative framework, we conducted human experiment to simulate the human-in-the-loop actions. The experiment in this section use the proposed rules (5.20) and (5.21) to train a robot-pilot based on the observations from the human partner. The shared goal between the collaborating agents (human and robot) is to resolve an existing conflict between their aircraft by means of lateral maneuvers. The lateral maneuvers should be in effect until both aircraft reach a target position, where the conflict is completely resolved. The rate of maneuvering action should learned as the agents collaborate together. Primarily, since the decision making capabilities of the human agent are superior to that of the robot pilot, the human pilot should take the initiative and then the robot pilot would learn from the human actions. Both agents then adapt their control criteria, based on their combined actions, to meet the common goal of conflict resolution and collision avoidance.



Figure 33: Computer simulation framework for aircraft conflict resolution HRC system. Human can cooperate with the computer controller by using joystick to control the acceleration of the lateral maneuver.

#### 5.4.1 Experimental Setup

In order to observe the human control actions and train a robot-pilot, seven subjects were recruited to conduct a human-in-the-loop experiment for HRC on aircraft conflict resolution. We built a flight simulator with two aircraft in conflict. The human subject was assigned the control of one aircraft, while the other aircraft was controlled by a computer based controller. The human subject can control his aircraft lateral position via a control stick connected to the simulation computer (Figure 33). However, (s)he does not have a control over the speed of aircraft on its nominal direction of flow, since we use a constant speed model for both aircraft. In other words, human agent can only control the rate of lateral maneuvering. To make the system easier for the participants, we restricted the simulations to only horizontal and vertical lateral maneuvers. Meaning that the human agent was controlling an aircraft heading in one of the cardinal directions (i.e., eastbound/westbound and northbound/southbound).

The objective of the experiment is to train the computer controller using estimates of the human control plan by applying the estimation algorithm in (5.20) and (5.21). A successful collaboration would result in a complete resolution of the existing conflict using bounded lateral maneuvers within a bounded period of time.

Each human subject was informed with the system operation and the shared goal of efficient conflict resolution. To get comfortable with the system and the control stick, each subject was allowed a training session to explore the system and how to control it. This training session would allow the human agent to understand how to control the acceleration of the aircraft later maneuver, and how to precisely control his/her aircraft lateral position. The training session can be done with or without a computer controller being involved. When the participant is ready, the experiment starts to train the computer-pilot that collaboratively interact with the human participant during the experiment.

#### 5.4.2 Results

Figure 34 shows the estimated control behavior of the human agent. The figure compares between the actual human control and the estimated control, and displays the resultant error function for each input. It is clear that the change in the error function,  $e(t)$  in response to the control input is exactly the same for the actual human input and the estimated control input. On the other hand, the estimated control input appears to be smoother than the actual control input. This is because both equations (5.20) and (5.21) use historical data, from previous time samples, to estimate the current control signal. The human input, in Figure 34, appears to be a little bit discretized because the joystick is not easy to control, and we divided a distance of 6 nm onto 120 discrete steps. This estimated control behavior is then used for online training of the computer controller.

Figures 35 and 36 show the results of Human-Robot collaboration for aircraft conflict resolution at two different levels of collaboration. Initially, the shadows of both aircraft was completely overlapping. Therefore, the miss-distance between the two aircraft  $d_{ij}(0) = 0$  nm, and the error function  $e(0) = d_s$  nm (we used a safety distance of 5 nm in this experiment). Figure 35 shows the control inputs where both the human and robot pilots was contributing

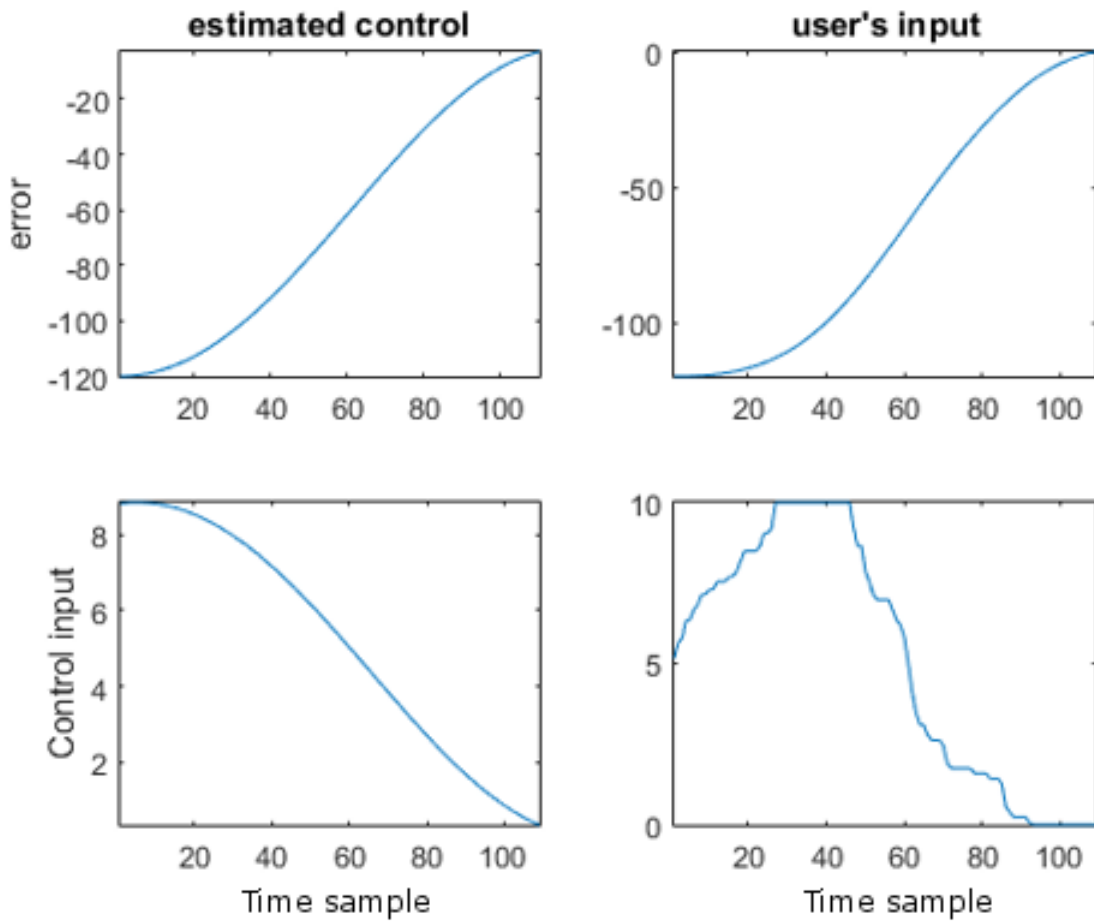


Figure 34: Human participant control criteria (right) and his estimated criteria (left), measured for the error function  $e(t)$  (top), and the acceleration control input  $u(t)$  (bottom).

equally to resolve the existing situation. On the other hand, Figure 36 show the control inputs where the robot controller was designed to minimize the human efforts (input) and do most of the job based on the estimated human intentions. Therefore, it is shown that the robot's control input is larger than the human input at this case. Both figures show the convergence of the error function over time. We can see that the system converged to safe trajectories within a finite period of time. Moreover, the control input at both cases was bounded. Thus, both the collaborating agents were able to successfully collaborate to fulfill the shared goal. Therefore, we can conclude the stability of the proposed human-machine co-learning system for aircraft conflict resolution.

The results obtained in this section show that we was able to successfully train a robot pilot to learn and adapt its control input according to its human partner criteria. Both human and robot pilots were able to adapt their actions and successfully collaborate to minimize the error function, while keeping their inputs bounded, and achieve their common goal of resolving the existing conflict.

## 5.5 SUMMARY

In this chapter, we proposed a human-machine collaboration framework to solve the problem of aircraft conflict resolution. First, we modeled the system dynamics using the state-space representation. To comply with the neuroscience studies which suggested human optimal control strategies, we defined an error function that measure how successful an agent manage to resolve the conflict. The value of the error function decreases with lateral maneuvers that aim to resolve the conflict. Second, we formulated the collaboration between the human and robot agents as an linear regulation optimal control problem. Then, to learn the human intentions and estimate his/her control criteria, we proposed a least-squares based algorithm to estimate the human feedback gain using observations of the current system state and the human actions. Once, we obtain an estimate for the human feedback gain, we then train a robot controller based on human behavior. The trained robot controller can then collaborate with human and update its control actions in real time. The proposed framework

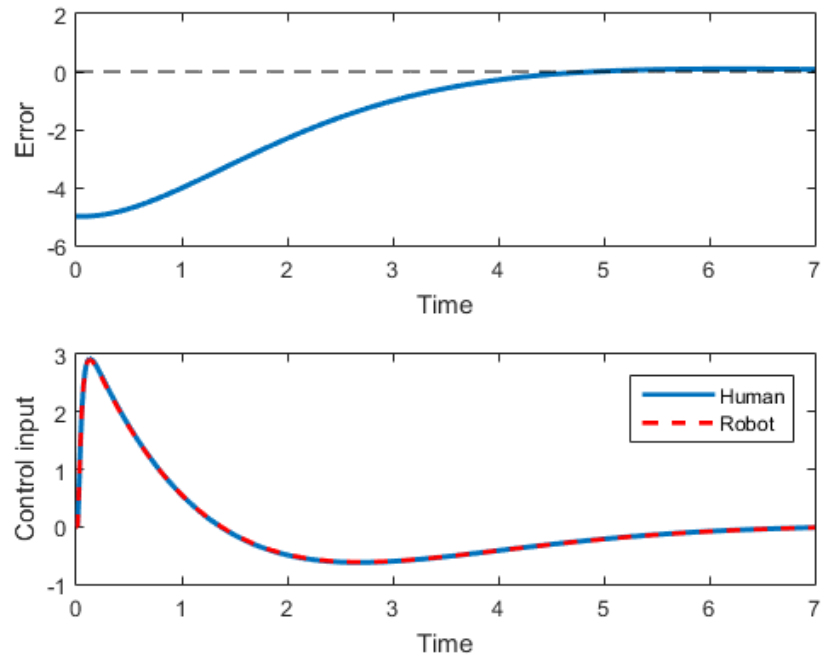


Figure 35: Human-Robot collaboration to resolve a complete overlap of aircraft shadows, at equal contribution level. (top) The error function in nm, (bottom) each agent control input.

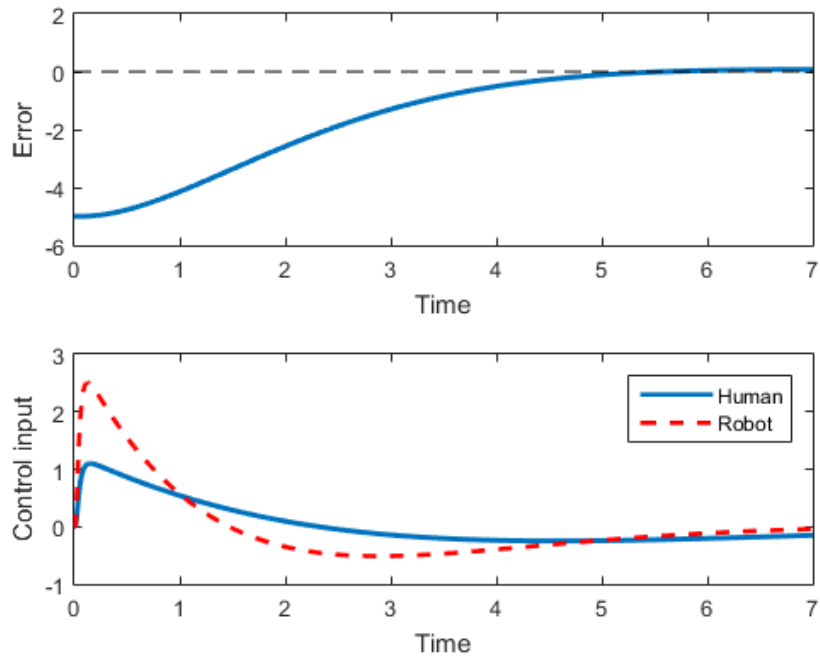


Figure 36: Human-Robot collaboration to resolve a complete overlap of aircraft shadows, with the robot seeking to minimize the human input. (top) The error function in nm, (bottom) each agent control input.

is considered a reverse-engineering of black-box controllers, and offers a new dimension of information (control design cost function) beyond that available using traditional system identification techniques.

We conducted a human experiment to study the human control action and test our collaborative framework for aircraft conflict resolution. The experimental results showed that we were able to accurately estimate the human control criteria and train a robot controller that can collaborate with that human agent. The collaboration experiment to resolve an existing conflict, shows that both human and robot agents were able to adapt and co-learn their control criteria to achieve the common goal of conflict resolution. Both agents were able to derive the aircraft system to safe trajectories with a finite time, using bounded control inputs.

## 6.0 CONCLUSIONS

In this dissertation, we have considered the problem of conflict resolution of intersecting aircraft flows in a specified control volume. To approach this problem, we proposed to decentralized collaborative frameworks. The first one is an automatic conflict resolution rule, and the second is based on a human-robot co-learning framework. Based on the model geometry, we defined an automatic decentralized collaborative conflict resolution rule, where each aircraft involved in a conflict should make a lateral maneuver, that satisfies the defined resolution rule, to resolve this conflict, and other conflicts that may be created via the domino effect. The lateral deviations were taken in the direction that reduce congestion, and thus increase the number of resolved conflict situations. Conflict resolution procedure not only deals with finding maneuvers for each aircraft to avoid potential collisions at any time instant, but also concerns with maintaining the whole system safe as the system dynamics evolve over time, i.e., to ensure that all aircraft will always be able to find feasible conflict free trajectories. The main focus was given to both analytical approaches and simulations to evaluate the evolution of aircraft trajectories, within a control volume, over time. For the analytical part, we defined a Lyapunov function to study the convergence of conflict resolution dynamics under the proposed decentralized conflict resolution maneuvers, and we analytically proved that the system will converge to safe, conflict free, trajectories in a finite bounded time. Simulations of aircraft flows at different intersecting angles were provided to verify the validity of the proposed control rule. The simulated maneuvers were bounded, satisfying one of the ATM routing requirements. Additionally, the simulated aircraft reached safe trajectories that were close to their original trajectories. Besides that, simulations verified our analytically derived conclusions about dynamics convergence, obtained by using the Lyapunov stability theorem. Thus, the simulation results proved the convergence, safety,

and efficiency of the proposed collaborative decentralized conflict resolution rule. Therefore, the proposed decentralized conflict resolution rule can be used for safe and efficient Free Flight operations.

The human-machine co-learning based aircraft conflict resolution depends on the collaboration between human and robot pilots to resolve an existing conflict. The conflict resolution was also based on a lateral maneuver model. However, the maneuver rate is not known and should be learned during collaboration. To achieve a successful, the robot pilot should be designed based on the human pilot control criteria. We modeled the system as an optimal control problem, where both collaborating agents aim to minimize the conflict while maintaining a bounded control input. Then, the human control criteria and feedback gain was estimated using a least-squares based solution. Knowing the state feedback gain of the human agent, will therefore enable us to estimate his action and train a machine controller that is able to collaborate with him in resolving airborne conflicts. We then conducted a human experiment to test our state feedback estimation algorithm and to test the human-machine co-learning collaborative framework at different levels of collaboration. The experimental results showed that we can accurately estimate the human control criteria and train a robot pilot for the task of aircraft conflict resolution. The performance of the two collaborating agents was measured at two different collaboration levels, and the results showed that both agents were able to collaborate and adapt their control criteria to completely resolve the existing conflict within a finite time. This suggests that the proposed human-machine co-learning framework can be used for air traffic applications, when an autonomous aircraft can collaborate with a human pilot to resolve potential conflicts and avoid collisions.

## APPENDIX A

### ACRONYMS

ARE	Algebraic Riccati Equation
ARTCC	Air Route Traffic Control Center
ATC	Air Traffic Control
ATCs	Air Traffic Controllers
ATM	Air Traffic Management
ERASMUS	EN Route Air Traffic Soft Management Ultimate System project
Eurocontrol	The European Organisation for the Safety of Air Navigation
FAA	Federal Aviation Administration
HMI	Human-Machine Interaction
HRC	Human-Robot Collaboration
HRI	Human-Robot Interaction
LMI	Linear Matrix Inequality
LQR	Linear Quadratic Regulator
MILP	Mixed Integer Linear Programming
MSP	Minneapolis - St. Paul International Airport
NAS	National Airspace System
NextGen	Next Generation Air Transportation System
nm	Nautical Mile
SESAR	Sky Air Traffic Management Research Program

TCAS	Traffic Alert and Collision Avoidance System
TFM	Traffic Flow Management
TRACON	Terminal Radar Approach Control
ZMP	Minneapolis Air Route Traffic Control Center

## APPENDIX B

### NOTATION

#### Flow and Conflict Geometry

$\theta$	Encounter angle between two intersecting flows
$\phi$	Angle of the relative velocity vector (Aircraft shadow angle)
$A_i$	Aircraft $i$
$A_{ki}$	Aircraft $i$ that belong to flow $k$
$d_{ij}$	Miss-distance between aircraft $i$ and aircraft $j$
$d_s, D_{sep}^{min}$	Safety (separation) distance
$v_1$	Velocity vector of aircraft in flow 1
$v_2$	Velocity vector of aircraft in flow 2

#### Conflict Resolution Rule

$c$	Positive constant
$\dot{L}$	Rate of lateral maneuvering
$\dot{L}_i$	Rate of change of the lateral position of aircraft $i$
$N_{Li}$	Number of left touches currently experienced by aircraft $i$
$N_{Ri}$	Number of right touches currently experienced by aircraft $i$
$\mathbf{u}_i^\perp$	The unit vector normal to the direction of flow of aircraft $i$

## Aircraft Flow Safty and Conflict Resolution Convergence

$\delta_{ij}$	The touch function between aircraft $i$ and aircraft $j$
$\dot{d}_{ij}$	The rate of change of the miss-distance between aircraft $i$ and aircraft $j$
$N_c$	The initial number of conflicts within the control volume before any lateral maneuver is taken
$N_e$	Number of eastbound aircraft
$N_s$	Number of southbound aircraft
$t_{conv}$	Convergence time
$V$	Lyapunov function
$\dot{V}$	Dervative of Lyapunove function with time

## Human-Robot Collaboration

$\alpha, \gamma$	Weighting coefficients associated with the error function
$\beta, \sigma$	Weighting coefficients associated with the control input
$\Delta t$	Sampling time
$A$	System dynamics matrix
$B$	Input matrix
$e(t)$	Error function
$J(t)$	Cost function
$K$	State-feedback (Kalman) gain matrix
$N$	Number of time samples
$p_i(t)$	Position of aircraft $i$ at time $t$
$p^*$	Target position
$P$	The unique positive-semidefinite solution to the discrete-time ARE
$Q$	Weight matrix associated with the states
$R$	Weight matrix associated with the control input
$u(t)$	Control input
$u_h$	Human control input

$\mathbf{u}_h$	The human agent control history vector
$u_r$	Robot control input
$v_i(t)$	Velocity of aircraft $i$ at time $t$
$w$	Window length
$x_i(t)$	State vector of agent $i$
$x(t), x_n$	State vector of the coupled system dynamics
$\mathbf{x}$	The state history vector

## APPENDIX C

### LYAPUNOV THEORY AND LASALLE'S STABILITY PRINCIPLE

Lyapunov stability theory is a standard tool and one of the most important tools in the analysis of nonlinear systems [71]. The idea of Lyapunov theory is to define an energy-like function, called Lyapunov function. Then, by studying the change of this function over time, the stability condition of the system under study can be concluded, without solving its differential equation.

Consider the nonlinear autonomous system

$$\dot{x} = f(x), \tag{C.1}$$

where  $f$  is a locally Lipschitz function. Suppose the system (C.1) has an equilibrium point  $\bar{x}$ , i.e.  $f(\bar{x}) = 0$ . We would like to characterize if the equilibrium point  $\bar{x}$  is stable or not. Lyapunov theory defines a continuously differentiable function,  $V$ , that contains the origin. The rate of change of  $V$  along the trajectories of (C.1) is given by

$$\dot{V}(x) \triangleq \frac{d}{dt}V(x) = \frac{\partial V}{\partial x}f(x) \tag{C.2}$$

The main idea of Lyapunov's theory is that if  $\dot{V}(x)$  is negative along the trajectories of the system, then  $V(x)$  will decrease as time advances. Moreover, we do not really need to solve the nonlinear ODE (C.1) for every initial condition. Stability conditions for Lyapunov theory are listed in theorem C.0.1.

**Theorem C.0.1.** *Let  $x = \bar{x} \in D \subset \mathbb{R}^n$  be an equilibrium point for  $\dot{x} = f(x)$ . Let  $V : D \rightarrow \mathbb{R}$  be a continuously differentiable function such that*

$$\begin{aligned} V(\bar{x}) &= 0, \\ V(x) &> 0, \forall x \in D \\ \dot{V}(x) &\leq 0, \forall x \in D \end{aligned} \tag{C.3}$$

*Then,  $x = \bar{x}$  is stable. Moreover, if*

$$\dot{V}(x) < 0, \forall x \in D \tag{C.4}$$

*then  $x = \bar{x}$  is asymptotically stable.*

According to Lyapunov theory, condition C.4 is necessary for asymptotic stability. However, for some instances we can conclude asymptotic stability without that condition. LaSalle's theorem allows us to conclude asymptotic stability with only  $\dot{V}(x) \leq 0$ , along with an observability type condition. Theorem C.0.2 states LaSalle's Invariance Principle.

**Theorem C.0.2.** (LaSalle's Invariance Principle) *Let  $\Omega \subset D$  be a compact set that is positively invariant with respect to  $\dot{x} = f(x)$ . Let  $V : D \rightarrow \mathbb{R}$  be a continuously differentiable function such that  $\dot{V}(x) \leq 0$ , in  $\Omega$ . Let  $E$  be the set of all points in  $\Omega$  where  $\dot{V}(x) = 0$ . Let  $M$  be the largest invariant set in  $E$ . Then every solution starting in  $\Omega$  approaches  $M$  as  $t \rightarrow \infty$ .*

Figure. 37 displays Theorem C.0.2 graphically. An important result that follows from Theorem C.0.2 is the following corollary.

**Corollary C.0.3.** *Let  $x = 0 \in D$  be an equilibrium point of the system  $\dot{x} = f(x)$ . Let  $V : D \rightarrow \mathbb{R}$  be a continuously differentiable positive definite function on the domain  $D$ , such that  $\dot{V}(x) = 0, \forall x \in D$ . Let  $S \triangleq \{x \in D | \dot{V}(x) = 0\}$  and suppose that no solution can stay identically in  $S$ , other than the trivial solution  $x \equiv 0$ . Then, the origin is asymptotically stable.*

Thus, four conditions are required to prove asymptotic stability of a system according to LaSalle's principle. These conditions are:

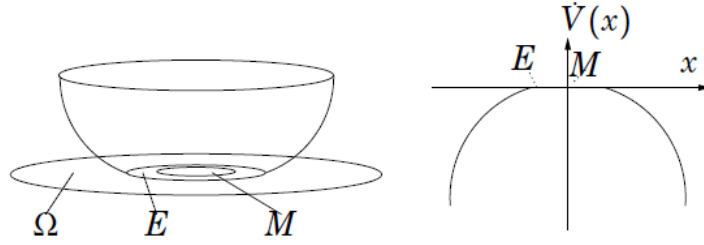


Figure 37: LaSalle's Invariance Principle. Every solution starting in  $\Omega$  approaches  $M$  as  $t \rightarrow \infty$ .

1.  $V(0) = 0, V(x) > 0 \forall x \neq 0$
2.  $\dot{V}(x) \leq 0, \forall x$
3.  $V(x) \rightarrow \infty$  as  $\|x\| \rightarrow \infty$
4. The only solution of  $\dot{x} = f(x), \dot{V}(x) = 0$  is  $x = 0$ .

We use the result of theorem [C.0.1](#) and Corollary [C.0.3](#) to prove the convergence of the system dynamics under proposed the conflict resolution system [\(2.1\)](#).

## BIBLIOGRAPHY

- [1] A. E. Vela, “Understanding conflict-resolution taskload: implementing advisory conflict-detection and resolution algorithms in an airspace,” Ph.D. dissertation, Georgia Institute of Technology, 2011.
- [2] J. Kuchar and L. Yang, “A review of conflict detection and resolution modeling methods,” *IEEE Transactions on Intelligent Transportation Systems*, vol. 1, no. 4, pp. 179–189, 2000.
- [3] Z.-H. Mao, E. Feron, and K. Bilimoria, “Stability and performance of intersecting aircraft flows under decentralized conflict avoidance rules,” *IEEE Transactions on Intelligent Transportation Systems*, vol. 2, no. 2, pp. 101–109, Jun 2001.
- [4] A. Bauer, D. Wollherr, and M. Buss, “Human–robot collaboration: a survey,” *International Journal of Humanoid Robotics*, vol. 5, no. 01, pp. 47–66, 2008.
- [5] B. Elder, “Free Flight: The Future of Air Transportation Entering the Twenty-First Century,” *Journal of Air Law and Commerce*, vol. 62, 1996.
- [6] N. Pujet and E. Feron, “Flight plan optimization in flexible air traffic environments,” in *Guidance, Navigation, and Control Conference*, 1996, p. 3765.
- [7] P. K. Menon, G. D. Sweriduk, and B. Sridhar, “Optimal Strategies for Free-Flight Air Traffic Conflict Resolution,” *Journal of Guidance, Control, and Dynamics*, vol. 22, no. 2, pp. 202–211, Mar 1999.
- [8] R. C. Ruigrok and J. M. Hoekstra, “Human factors evaluations of free flight: Issues solved and issues remaining,” *Applied ergonomics*, vol. 38, no. 4, pp. 437–455, 2007.
- [9] H. Swenson, R. Barhydt, and M. Landis, “Next generation air transportation system (ngats) air traffic management (atm)-airspace project,” Technical report, National Aeronautics and Space Administration, Tech. Rep., 2006.
- [10] Z.-H. Mao, D. Dugail, and E. Feron, “Space partition for conflict resolution of intersecting flows of mobile agents,” *IEEE Transactions on Intelligent Transportation Systems*, vol. 8, no. 3, pp. 512–527, 2007.

- [11] K. Bilimoria, H. Lee, Z.-H. Mao, and E. Feron, "Comparison of centralized and decentralized conflict resolution strategies for multiple-aircraft problems," in *18th Applied Aerodynamics Conference*, 2000, p. 4268.
- [12] I. Hwang and C. E. Seah, "Intent-based probabilistic conflict detection for the next generation air transportation system," *Proceedings of the IEEE*, vol. 96, no. 12, pp. 2040–2059, 2008.
- [13] L. Pallottino, E. Feron, and A. Bicchi, "Conflict resolution problems for air traffic management systems solved with mixed integer programming," *IEEE Transactions on Intelligent Transportation Systems*, vol. 3, no. 1, pp. 3–11, Mar 2002.
- [14] P. Ky and B. Miaillier, "Sesar: towards the new generation of air traffic management systems in europe," *Journal of Air Traffic Control*, vol. 48, no. 1, 2006.
- [15] M. Nolan, *Fundamentals of air traffic control*, 5th ed. Cengage learning, 2010.
- [16] C. Manning, E. Stein, B. Kirwan, M. Rodgers, and D. Schafer, "Measuring air traffic controller performance in the 21st century," *Human factors impacts in air traffic management*, pp. 283–316, 2005.
- [17] R. Fewings, "Air traffic management," *Encyclopedia of Aerospace Engineering*, 2010.
- [18] B. Sridhar, K. S. Sheth, and S. Grabbe, "Airspace complexity and its application in air traffic management," in *2nd USA/Europe Air Traffic Management R&D Seminar*, 1998, pp. 1–6.
- [19] K. Dalamagkidis, K. Valavanis, and L. Piegler, "On unmanned aircraft systems issues, challenges and operational restrictions preventing integration into the National Airspace System," *Progress in Aerospace Sciences*, vol. 44, no. 7-8, pp. 503–519, Oct 2008.
- [20] D. Bertsimas and S. S. Patterson, "The air traffic flow management problem with en-route capacities," *Operations research*, vol. 46, no. 3, pp. 406–422, 1998.
- [21] P. B. Vranas, D. Bertsimas, and A. R. Odoni, "Dynamic ground-holding policies for a network of airports," *Transportation Science*, vol. 28, no. 4, pp. 275–291, 1994.
- [22] J. Krozel, M. Peters, K. D. Bilimoria, C. Lee, and J. Mitchell, "System performance characteristics of centralized and decentralized air traffic separation strategies," in *Fourth USA/Europe air traffic management research and development seminar*, 2001.
- [23] D. Rey, C. Rapine, V. V. Dixit, and S. T. Waller, "Equity-Oriented Aircraft Collision Avoidance Model," *IEEE Transactions on Intelligent Transportation Systems*, vol. 16, no. 1, pp. 172–183, Feb 2015.
- [24] E. Statfor, "Eurocontrol long-term forecast: ifr flight movements 2013-2035," 2013.

- [25] K. Treleaven and Z.-H. Mao, "Conflict resolution and traffic complexity of multiple intersecting flows of aircraft," *IEEE Transactions on Intelligent Transportation Systems*, vol. 9, no. 4, pp. 633–643, 2008.
- [26] E. S. Stein, "Human operator workload in air traffic control." *Human factors in air traffic control*, 1998.
- [27] S. Loft, P. Sanderson, A. Neal, and M. Mooij, "Modeling and predicting mental workload in en route air traffic control: Critical review and broader implications," *Human Factors*, vol. 49, no. 3, pp. 376–399, 2007.
- [28] R. H. Mogford, J. Guttman, S. Morrow, and P. Kopardekar, "The complexity construct in air traffic control: A review and synthesis of the literature." DTIC Document, Tech. Rep., 1995.
- [29] M. Rodgers, *Human Factors Impacts in Air Traffic Management*. Routledge, 2017.
- [30] P. J. Smith, C. E. McCoy, and C. Layton, "Brittleness in the design of cooperative problem-solving systems: The effects on user performance," *IEEE Transactions on Systems, Man, and Cybernetics-Part A: Systems and Humans*, vol. 27, no. 3, pp. 360–371, 1997.
- [31] R. Parasuraman and V. Riley, "Humans and automation: Use, misuse, disuse, abuse," *Human Factors: The Journal of the Human Factors and Ergonomics Society*, vol. 39, no. 2, pp. 230–253, 1997.
- [32] G. Gawinowski, J.-L. Garcia, R. Guerreau, R. Weber, and M. Brochard, "Erasmus: a new path for 4d trajectory-based enablers to reduce the traffic complexity," in *Digital Avionics Systems Conference, 2007. DASC'07. IEEE/AIAA 26th*. IEEE, 2007, pp. 1–A.
- [33] E. Cruck and J. Lygeros, "Subliminal air traffic control: Human friendly control of a multi-agent system," in *American Control Conference, 2007. ACC'07*. IEEE, 2007, pp. 462–467.
- [34] C. E. Billings and D. D. Woods, "Concerns about adaptive automation in aviation systems," *Human performance in automated systems: Current research and trends*, pp. 264–269, 1994.
- [35] N. Barnier and C. Allignol, "4d-trajectory deconfliction through departure time adjustment," in *ATM 2009, 8th USA/Europe Air Traffic Management Research and Development Seminar*, 2009.
- [36] N. R. C. U. C. for a Review of the En Route Air Traffic Control Complexity and W. Model, *Air Traffic Controller Staffing in the en Route Domain: A Review of the Federal Aviation Administration's Task Load Model*. Transportation Research Board, 2010, vol. 301.

- [37] G. Chaloulos, G. Roussos, J. Lygeros, and K. Kyriakopoulos, “Ground assisted conflict resolution in self-separation airspace,” in *AIAA Guidance, Navigation and Control Conference and Exhibit*, 2008, p. 6967.
- [38] N. E. Dougui, D. Delahaye, S. Puechmorel, and M. Mongeau, “A new method for generating optimal conflict free 4d trajectory,” in *ICRAT 2010, 4th International Conference on Research in Air Transportation*, 2010, pp. pp–185.
- [39] C. Tomlin, G. J. Pappas, and S. Sastry, “Conflict resolution for air traffic management: A study in multiagent hybrid systems,” *IEEE Transactions on automatic control*, vol. 43, no. 4, pp. 509–521, 1998.
- [40] S. Pettersson and B. Lennartson, “Controller design of hybrid systems,” in *Hybrid and Real-Time Systems*. Springer, 1997, pp. 240–254.
- [41] M. Prandini, J. Hu, J. Lygeros, and S. Sastry, “A probabilistic approach to aircraft conflict detection,” *IEEE Transactions on intelligent transportation systems*, vol. 1, no. 4, pp. 199–220, 2000.
- [42] R. A. Paielli and H. Erzberger, “Conflict probability estimation for free flight,” *Journal of Guidance, Control, and Dynamics*, vol. 20, no. 3, pp. 588–596, 1997.
- [43] L. Yang and J. Kuchar, “Using intent information in probabilistic conflict analysis,” in *Guidance, Navigation, and Control Conference and Exhibit*, 1998, p. 4237.
- [44] —, “Prototype conflict alerting logic for free flight (aiaa 97-0220),” *Reston, VA: American Institute of Aeronautics and Astronautics. GLOSSARY OF TERMS*, 1997.
- [45] A. Bicchi and L. Pallottino, “On optimal cooperative conflict resolution for air traffic management systems,” *IEEE Transactions on Intelligent Transportation Systems*, vol. 1, no. 4, pp. 221–231, 2000.
- [46] J. Yoo and S. Devasia, “Provably safe conflict resolution with bounded turn rate for air traffic control,” *IEEE Transactions on Control Systems Technology*, vol. 21, no. 6, pp. 2280–2289, 2013.
- [47] M. Christodoulou and S. Kodaxakis, “Automatic Commercial Aircraft-Collision Avoidance in Free Flight: The Three-Dimensional Problem,” *IEEE Transactions on Intelligent Transportation Systems*, vol. 7, no. 2, pp. 242–249, Jun 2006.
- [48] A. Alonso-Ayuso, L. F. Escudero, and F. J. Martín-Campo, “Collision avoidance in air traffic management: a mixed-integer linear optimization approach,” *IEEE Transactions on Intelligent Transportation Systems*, vol. 12, no. 1, pp. 47–57, 2011.
- [49] D. Alejo, J. M. Díaz-Báñez, J. A. Cobano, P. Pérez-Lantero, and A. Ollero, “The Velocity Assignment Problem for Conflict Resolution with Multiple Aerial Vehicles Sharing Airspace,” *Journal of Intelligent & Robotic Systems*, vol. 69, no. 1-4, pp. 331–346, Aug 2013.

- [50] K. D. Bilimoria, “A geometric optimization approach to aircraft conflict resolution,” in *AIAA guidance, navigation, and control conference and exhibit*. AIAA Reston, VA, 2000, pp. 14–17.
- [51] D. Rey, C. Rapine, R. Fondacci, and N.-E. El Faouzi, “Minimization of Potential Air Conflicts Through Speed Regulation,” *Transportation Research Record: Journal of the Transportation Research Board*, vol. 2300, pp. 59–67, Dec 2012.
- [52] S. Cafieri and N. Durand, “Aircraft deconfliction with speed regulation: new models from mixed-integer optimization,” *Journal of Global Optimization*, vol. 58, no. 4, pp. 613–629, Apr 2014.
- [53] J. Omer, “A space-discretized mixed-integer linear model for air-conflict resolution with speed and heading maneuvers,” *Computers & Operations Research*, vol. 58, pp. 75–86, Jun 2015.
- [54] J. Omer and J.-L. Farges, “Hybridization of nonlinear and mixed-integer linear programming for aircraft separation with trajectory recovery,” *IEEE Transactions on Intelligent Transportation Systems*, vol. 14, no. 3, pp. 1218–1230, 2013.
- [55] N. Durand and J.-M. Alliot, “Ant colony optimization for air traffic conflict resolution,” in *ATM Seminar 2009, 8th USA/Europe Air Traffic Management Research and Development Seminar*, 2009.
- [56] E. Frazzoli, Z.-H. Mao, J.-H. Oh, and E. Feron, “Resolution of conflicts involving many aircraft via semidefinite programming,” *Journal of Guidance, Control, and Dynamics*, vol. 24, no. 1, pp. 79–86, 2001.
- [57] Z.-H. Mao, D. Dugail, E. Feron, and K. Bilimoria, “Stability of intersecting aircraft flows using heading-change maneuvers for conflict avoidance,” *IEEE Transactions on Intelligent Transportation Systems*, vol. 6, no. 4, pp. 357–369, 2005.
- [58] M. Heymann and G. Meyer, “An agent based framework for control of merging air-traffic,” *IFAC Proceedings Volumes*, vol. 37, no. 6, pp. 493–498, 2004.
- [59] S. Resmerita and M. Heymann, “Conflict resolution in multi-agent systems,” in *Decision and Control, 2003. Proceedings. 42nd IEEE Conference on*, vol. 3. IEEE, 2003, pp. 2537–2542.
- [60] S. Resmerita, M. Heymann, and G. Meyer, “A framework for conflict resolution in air traffic management,” in *Decision and Control, 2003. Proceedings. 42nd IEEE Conference on*, vol. 2. IEEE, 2003, pp. 2035–2040.
- [61] M. S. Refai and R. Windhorst, “Impact of tactical and strategic weather avoidance on separation assurance,” in *11th AIAA Aviation Technology, Integration, and Operations (ATIO) Conference, September 20-22, Virginia Beach, VA*, 2011.

- [62] T. A. Lauderdale, “The effects of speed uncertainty on a separation assurance algorithm,” in *Proceedings of the 10th AIAA Aviation Technology, Integration, and Operations (ATIO) Conference*, 2010.
- [63] K. Lee, E. Feron, and A. Pritchett, “Describing airspace complexity: Airspace response to disturbances,” *Journal of Guidance, Control, and Dynamics*, vol. 32, no. 1, pp. 210–222, 2009.
- [64] J. Kuchar and L. Yang, “Survey of conflict detection and resolution modeling methods,” in *AIAA Guidance, Navigation, and Control Conf*, 1997, pp. 1388–1397.
- [65] T. Williamson and N. A. Spencer, “Development and operation of the traffic alert and collision avoidance system (tcas),” *Proceedings of the IEEE*, vol. 77, no. 11, pp. 1735–1744, 1989.
- [66] J. M. Histon, R. J. Hansman, B. Gottlieb, H. Kleinwaks, S. Yenson, D. Delahaye, and S. Puechmorel, “Structural considerations and cognitive complexity in air traffic control,” in *Digital Avionics Systems Conference, 2002. Proceedings. The 21st*, vol. 1. IEEE, 2002, pp. 1C2–1.
- [67] J. Krozel, J. S. Mitchell, V. Polishchuk, and J. Prete, “Maximum flow rates for capacity estimation in level flight with convective weather constraints,” *Air Traffic Control Quarterly*, vol. 15, no. 3, pp. 209–238, 2007.
- [68] S. Devasia, D. Iamratanakul, G. Chatterji, and G. Meyer, “Decoupled conflict-resolution procedures for decentralized air traffic control,” *IEEE Transactions on Intelligent Transportation Systems*, vol. 12, no. 2, pp. 422–437, 2011.
- [69] D. Iamratanakul, G. Meyer, G. Chatterji, and S. Devasia, “Quantification of airspace sector capacity using decentralized conflict resolution procedures,” in *IEEE Conference on Decision and Control*, 2004.
- [70] W. Niedringhaus, “Stream Option Manager (SOM): automated integration of aircraft separation, merging, stream management, and other air traffic control functions,” *IEEE Transactions on Systems, Man, and Cybernetics*, vol. 25, no. 9, pp. 1269–1280, 1995.
- [71] H. K. Khalil, *Nonlinear systems*, 3rd ed. Prentice Hall, 2002.
- [72] Y. Li, K. P. Tee, S. S. Ge, and H. Li, “Building companionship through human-robot collaboration,” in *International Conference on Social Robotics*. Springer, 2013, pp. 1–7.
- [73] S. A. Green, M. Billingham, X. Chen, and J. G. Chase, “Human-robot collaboration: A literature review and augmented reality approach in design,” *International journal of advanced robotic systems*, vol. 5, no. 1, p. 1, 2008.
- [74] R. R. Murphy, D. Riddle, and E. Rasmussen, “Robot-assisted medical reachback: a survey of how medical personnel expect to interact with rescue robots,” in *Robot and Human*

- Interactive Communication, 2004. ROMAN 2004. 13th IEEE International Workshop on.* IEEE, 2004, pp. 301–306.
- [75] R. R. Murphy, S. Tadokoro, D. Nardi, A. Jacoff, P. Fiorini, H. Choset, and A. M. Erkmen, “Search and rescue robotics,” in *Springer Handbook of Robotics*. Springer, 2008, pp. 1151–1173.
- [76] K. Kosuge, M. Sato, and N. Kazamura, “Mobile robot helper,” in *Robotics and Automation, 2000. Proceedings. ICRA’00. IEEE International Conference on*, vol. 1. IEEE, 2000, pp. 583–588.
- [77] W. Bluethmann, R. Ambrose, M. Diftler, S. Askew, E. Huber, M. Goza, F. Rehnmark, C. Lovchik, and D. Magruder, “Robonaut: A robot designed to work with humans in space,” *Autonomous robots*, vol. 14, no. 2, pp. 179–197, 2003.
- [78] M. A. Diftler, J. Mehling, M. E. Abdallah, N. A. Radford, L. B. Bridgwater, A. M. Sanders, R. S. Askew, D. M. Linn, J. D. Yamokoski, F. Permenter *et al.*, “Robonaut 2—the first humanoid robot in space,” in *Robotics and Automation (ICRA), 2011 IEEE International Conference on*. IEEE, 2011, pp. 2178–2183.
- [79] A. H. Dallal, A. S. Derbala, and M. F. Taher, “A mobile robot for hospitals controlled using wlan,” in *Biomedical Engineering Conference (CIBEC), 2012 Cairo International*. IEEE, 2012, pp. 100–103.
- [80] K. Wada and T. Shibata, “Robot therapy in a care house—its sociopsychological and physiological effects on the residents,” in *Robotics and Automation, 2006. ICRA 2006. Proceedings 2006 IEEE International Conference on*. IEEE, 2006, pp. 3966–3971.
- [81] N. Jarrassé, T. Charalambous, and E. Burdet, “A framework to describe, analyze and generate interactive motor behaviors,” *PloS one*, vol. 7, no. 11, p. e49945, 2012.
- [82] D. W. Franklin, E. Burdet, K. P. Tee, R. Osu, C.-M. Chew, T. E. Milner, and M. Kawato, “Cns learns stable, accurate, and efficient movements using a simple algorithm,” *Journal of neuroscience*, vol. 28, no. 44, pp. 11 165–11 173, 2008.
- [83] E. Burdet, G. Ganesh, C. Yang, and A. Albu-Schäffer, “Interaction force, impedance and trajectory adaptation: by humans, for robots,” in *Experimental Robotics*. Springer, 2014, pp. 331–345.
- [84] C. Yang, G. Ganesh, S. Haddadin, S. Parusel, A. Albu-Schaeffer, and E. Burdet, “Human-like adaptation of force and impedance in stable and unstable interactions,” *IEEE transactions on robotics*, vol. 27, no. 5, pp. 918–930, 2011.
- [85] N. Jarrassé, V. Sanguineti, and E. Burdet, “Slaves no longer: review on role assignment for human–robot joint motor action,” *Adaptive Behavior*, vol. 22, no. 1, pp. 70–82, 2014.

- [86] P. Dillenbourg, M. J. Baker, A. Blaye, and C. O'Malley, "The evolution of research on collaborative learning," *Learning in Humans and Machine: Towards an interdisciplinary learning science.*, pp. 189–211, 1995.
- [87] P. Antsaklis and A. N. Michel, *Linear systems.* Springer Science & Business Media, 2006.
- [88] M. C. Priess, R. Conway, J. Choi, J. M. Popovich, and C. Radcliffe, "Solutions to the inverse lqr problem with application to biological systems analysis," *IEEE Transactions on Control Systems Technology*, vol. 23, no. 2, pp. 770–777, 2015.
- [89] E. Cheney and D. Kincaid, *Numerical mathematics and computing.* Nelson Education, 2012.
- [90] S. Boyd and L. Vandenberghe, *Convex optimization.* Cambridge university press, 2004.